Molecular Mechanisms Underlying the Unprecedented Liver Regeneration Induced by ALPPS Surgery

---

Dissertation

zur

Erlangung der naturwissenschaftlichen Doktorwürde

(Dr. sc. nat.)

vorgelegt der

Mathematisch-naturwissenschaftlichen Fakultät

der

Universität Zürich

von

Magda Langiewicz

aus

Polen

Promotionskommission

Prof. Dr. Pierre-Alain Clavien (Vorsitz)

PD Dr. Bostjan Humar

Prof. Dr. Rolf Graf

Prof. Dr. Bernd Bodenmiller

Zürich, 2018

Table of Contents

Summaries

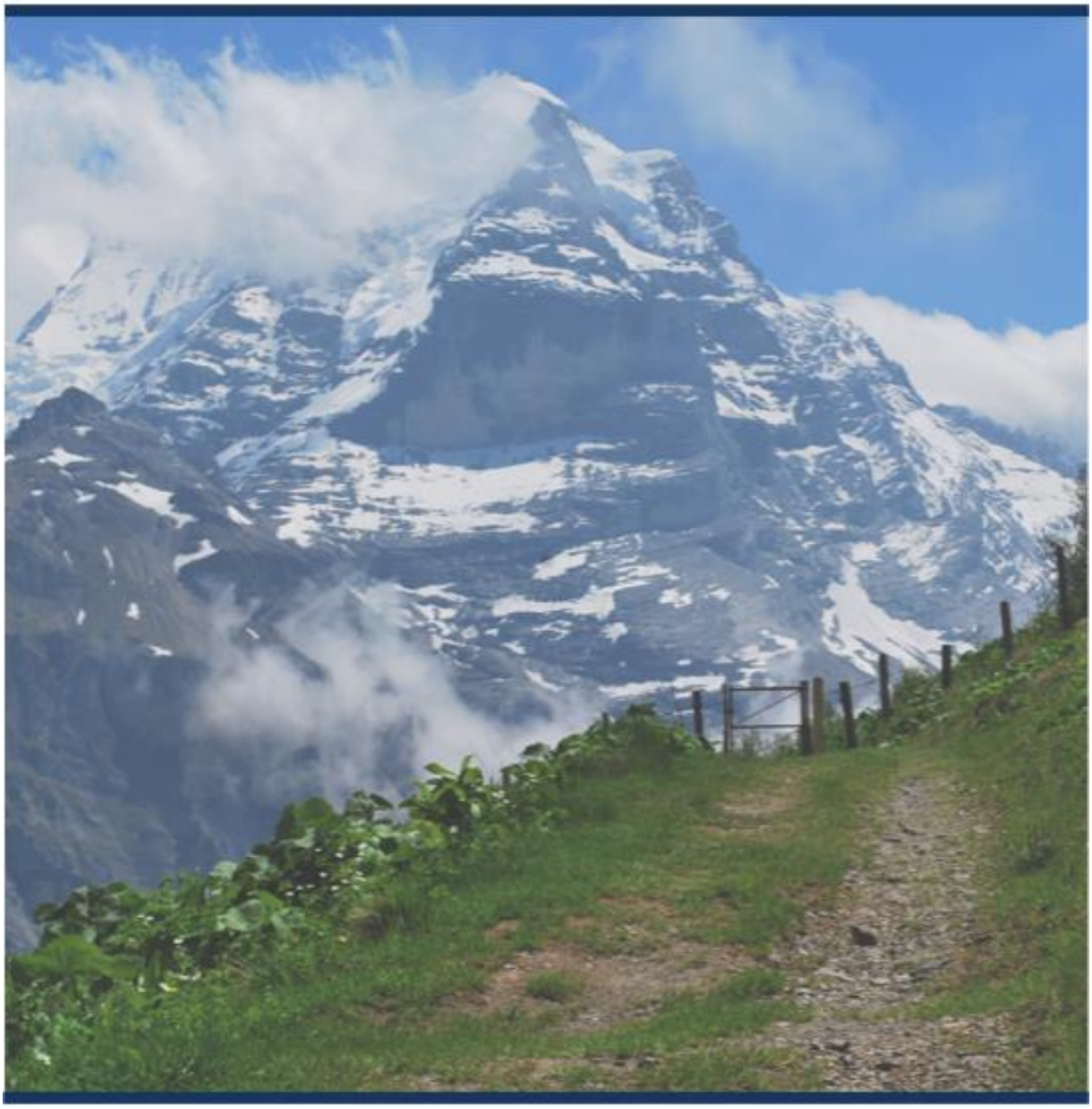

1. Summary

Surgery for the treatment of liver tumors relies on the unique ability of liver to regenerate after tissue loss. Although surgery is the most curative treatment for extensive tumor loads, limitations to the extent of resections exist, with resection-induced liver failure (known as small-for-size syndrome, SFSS) remaining the primary cause of postoperative death. Therefore, there is a need for innovative approaches to push the boundaries of resection in liver surgery.

ALPPS - *A*ssociated *L*iver *P*artition and Portal vein ligation for *S*taged hepatectomy - is the most recent advancement in the treatment of extensive liver tumors. ALPPS is a modified two-staged hepatectomy that allows for a more extensive tumor removal than usual approaches. In conventional two-stage hepatectomies, the diseased liver part is occluded in the first stage to induce growth of the contralateral healthy liver part, enabling the resection of the diseased part at the second stage. Unlike in conventional approaches, ALPPS combines occlusion with parenchymal transection, which induces liver regeneration at an unprecedented rate. In patients, ALPPS stage 1 enables resection (i.e. stage 2) in just ten days compared to 2-13 months after conventional two-staged hepatectomies, while in mice, regeneration doubles or triples in speed. The molecular pathways behind this accelerated regeneration remain uncharacterized. The aim of my PhD thesis was to explore unique molecular mechanisms underlying the accelerated regeneration induced by ALPPS surgery.

RNA deep sequencing on ALPPS regenerative tissue revealed unique gene expression changes as early as 4 hours after operation. Further analyses identified Indian hedgehog (IHH) as a primary candidate in mediating ALPPS regeneration. Through functional *in-vivo* assays, the necessity of IHH in accelerated regeneration was confirmed. When recombinant IHH protein was injected into the slower regenerating PVL (portal vein ligation only) mice, regeneration was accelerated to ALPPS levels. On the contrary, neutralizing IHH antibody injected prior to ALPPS surgery slowed regenerative speed to levels seen in PVL only mice. Furthermore, ALPPS induced IHH secretion from stellate cells, which led to paracrine activation of the hedgehog effector GLI1 and its target cyclin D1 in hepatocytes accompanied by increases in hepatocellular proliferation. All these events were replicated by recombinant IHH injected into PVL mice, and abrogated in ALPPS mice by neutralizing IHH antibody.

To establish the important of IHH in ALPPS, IHH upstream regulators were explored through *in-silico* mining of transcriptomics data, which identified *Mapk8* (JNK1) as a potential candidate. JNK1 activation was validated at the protein level to occur 1 hour after ALPPS surgery (preceding IHH secretion at 4 hours). Immunofluorescence indicated JNK1-

IHH co-localization in stellate cells. Pharmacological inhibition of JNK1 through SP600125 prior to ALPPS surgery reduced the regenerative pace to PVL levels, abrogated IHH secretion, counteracted the subsequent induction of GLI1-cyclin D in hepatocytes, and reduced hepatocellular proliferation. When recombinant IHH was injected into ALPPS mice with inhibited JNK1, GLI1-cyclin D upregulation was restored, as was hepatocellular proliferation and accelerated regeneration. Intriguingly, recombinant IHH also re-elevated JNK1 activity, suggesting a feed forward loop, which to establish will require further research.

Finally, a proteomics approach was used to investigate additional plasma proteins that may trigger acceleration of regeneration after ALPPS. Previous experiments with plasma injections indicated the presence of accelerating proteins present in circulation as early as 30 minutes after surgery. While several candidates were detected through proteomics, their validation proved difficult. Nevertheless, novel plasma proteins displaying unique upregulation after ALPPS were identified, however without a clear association with the JNK1-IHH axis but feeding future research.

In conclusion, the experimental work for my PhD thesis has identified the first molecular mechanism that drives the acceleration of regeneration after ALPPS surgery. ALPPS triggers early activation of JNK1 in stellate cells to promote subsequent release of IHH, which then accelerates hepatocyte proliferation via GLI1-cyclinD in a paracrine fashion. Mechanistically, regenerative acceleration may result from a positive feedback between IHH and JNK1. If confirmed in patients, the JNK1-IHH-GLI1-cyclin D axis may be therapeutically exploited for patients at risk of SFSS, a currently untreatable entity.

2. Zusammenfassung

Die chirurgische Enfernung von Lebertumoren beruht auf der einzigartigen Fähigkeit der Leber, sich nach Gewebeverlust vollständig zu regenerieren. Obwohl die Chirurgie die erfolgreichste Option bei starkem Tumorbefall darstellt, sind ihr Grenzen gesetzt. Wird zu viel Lebergewebe entfernt, kann Leberversagen eintreten. Dieses sogenannte 'Small-For-Size Syndrom' (SFSS) ist nach wie vor die häufigste postoperative Todesursache in der Leberchirurgie. Deshalb besteht der Bedarf nach innovativen Ansätzen, welche die Grenzen der Resektibilät weiter ausdehnen.

ALPPS - 'Associated Liver Partition and Portal vein ligation for Staged hepatectomy' - ist eine Abwandlung sogenannter 2-Stufen-Resektionen und die neueste chirurgische Strategie zur extensiven Entfernung von grossen oder multiplen Lebertumoren. Bei 2-Stufen-Resektionen wird im ersten Schritt der erkrankte Leberteil ligiert ('portal vein ligation', PVL), um kompensierendes Wachstum im gesunden Leberteil zu induzieren. Wenn dieser genügend gewachsen ist, kann in einem zweiten Schritt der kranke Leberteil reseziert werden. Im Gegensatz zu den üblichen 2-Stufen-Resektionen, wird bei ALPPS die Schritt 1-Ligation zusätzlich mit einer parenchymalen Transektion kombiniert, was das Wachstum des gesunden Leberteiles massiv beschleunigt. Dadurch kann die Resektion (Schritt 2) bereits nach etwa 10 Tagen statt der üblichen 2-13 Monate durchgeführt werden, während die ALPPS Operation in Mäusen die Regenerationsrate um das zwei- bis dreifache beschleunigt.

Die molekularen Prozesse, welche der ALPPS-induzierten Beschleunigung der Leberregeneration zugrunde liegen, sind noch ungeklärt. Das Ziel meiner Dissertation war, die für die regenerative Beschleunigung wesentlichen Signalwege zu identifizieren, um eine mechanistische Erklärung für das ALPPS-Phänomen zu ermöglichen.

Mittels 'RNA deep sequencing' konnte ich 4 Stunden nach der Operation ALPPS-spezifische Expressionsmuster beobachten. Weitere Analysen identifizierten Indian Hedgehog (IHH) als das primäre Kandidatenmolekül in der ALPPS Regeneration. Durch funktionelle *in vivo* Experimente konnte dir Rolle von IHH als Regenerationsbeschleuniger in ALPPS bestätigt werden. Wenn rekombinantes IHH nur mit PVL-behandelten (also langsam regenerierenden) Mäusen injiziert wurde, beschleunigte sich die Regeneration auf ALPPS Niveau. Umgekehrt, die Regeneration wurde auf PVL Niveau verlangsamt, wenn Mäusen vor der ALPPS Operation neutralisierender Antikörper gegen IHH verabreicht wurde. Weiter konnten wir zeigen, dass IHH von Sternzellen sekretiert wurde, um parakrin den hedgehog Effektor GLI1 und sein Zielgen cyclin D1 in Hepatozyten zu aktivieren und dadurch deren

Proliferation zu verstärken. All diese Effekte wurden durch rekombinantes IHH in PVL Mäusen repliziert, und durch neutralisierenden IHH Antikörper in ALPPS Mäusen unterbunden.

Um die zentrale Rolle von IHH in ALPPS zu bestätigen, haben wir nach vorgelagerten IHH Regulatoren gesucht. Mittels *in silico* Analyse der Transkriptom Daten identifizierten wir *Mapk8* (JNK1) als möglichen Kandidaten. Tatsächlich konnten wir eine Stunde nach ALPPS die Aktivierung der JNK1 Kinase bestätigen (also bevor IHH induziert wird) und weiter mittels Immunfluoreszenz feststellen, dass JNK1 mit IHH in Sternzellen ko-lokalisiert. Die pharmakologische Inhibierung der JNK1 vor der ALPPS Operation verlangsamte die Regenerationsgeschwindigkeit auf PVL Niveau, unterdrückte die IHH Sekretion sowie die Aktivierung von GLI1-cyclin D1 in Hepatozyten, und vermiderte die hepatozelluläre Proliferation. Wenn Mäusen mit inhibierter JNK1 vor der ALPPS Operation auch rekombinantes IHH injiziert wurde, wurde die GLI-cyclin D1 Induktion wiederhergestellt, die Heptozytenproliferation angekurbelt, und die Regeneration wieder beschleunigt. Interessanterweise konnte rekombinantes IHH auch die JNK1 Aktivität erhöhen, was auf eine wechselseitige Verstärkung zwischen diesen Proteinen hindeutet, aber eine Bestätigung in weiteren Studien erfordert.

Schliesslich haben wir auch einen Proteomics Ansatz verfolgt, um zusätzliche Plasmaproteine, welche die Beschleunigung der ALPPS-Regeneration auslösen könnten, zu beschreiben. Vorgängige Experimente mit Plasmainjektionen wiesen auf die Präsenz von beschleunigenden Proteinen in der Zirkulation schon 30 min. nach der ALPPS Operation hin. Während mehrere Kandidaten durch Proteomics detektiert wurden, erwies sich deren Validierung im Plasma als schwierig. Nichtsdestotrotz, wir konnten neue Plasmaproteine mit spezifischer Aufregulierung durch ALPPS nachweisen - leider ohne eine Assoziation mit der JNK1-IHH Achse, dafür mit neuen Hinweisen für zukünftige Projekte.

Zusammenfassend konnte ich in meiner Dissertation den ersten molekularen Mechanismus, welcher die ALPPS-induzierte Beschleunigung der Leberregeneration antreibt, identifizieren. ALPPS stimuliert die Aktivierung der JNK1 in Sternzellen, um die Sekretion des 'hedgehog' Liganden IHH zu fördern, welcher dann parakrin auf Hepatozyten wirkt, um dort mittels der GLI1-cyclin D1 Achse deren Proliferation zu beschleunigen. Die positive Wechselwirkung zwischen IHH und JNK1 könnte dabei eine mechanistische Erklärung für die Beschleunigung liefern. Falls diese Befunde im Patientenmaterial bestätigt werden, könnte die JNK1-IHH-GLI1-cyclin D1 Achse möglicherweise therapeutisch genutzt werden, um die Regeneration bei Patienten mit erhöhtem Risiko für das SFSS zu stimulieren.

Introduction

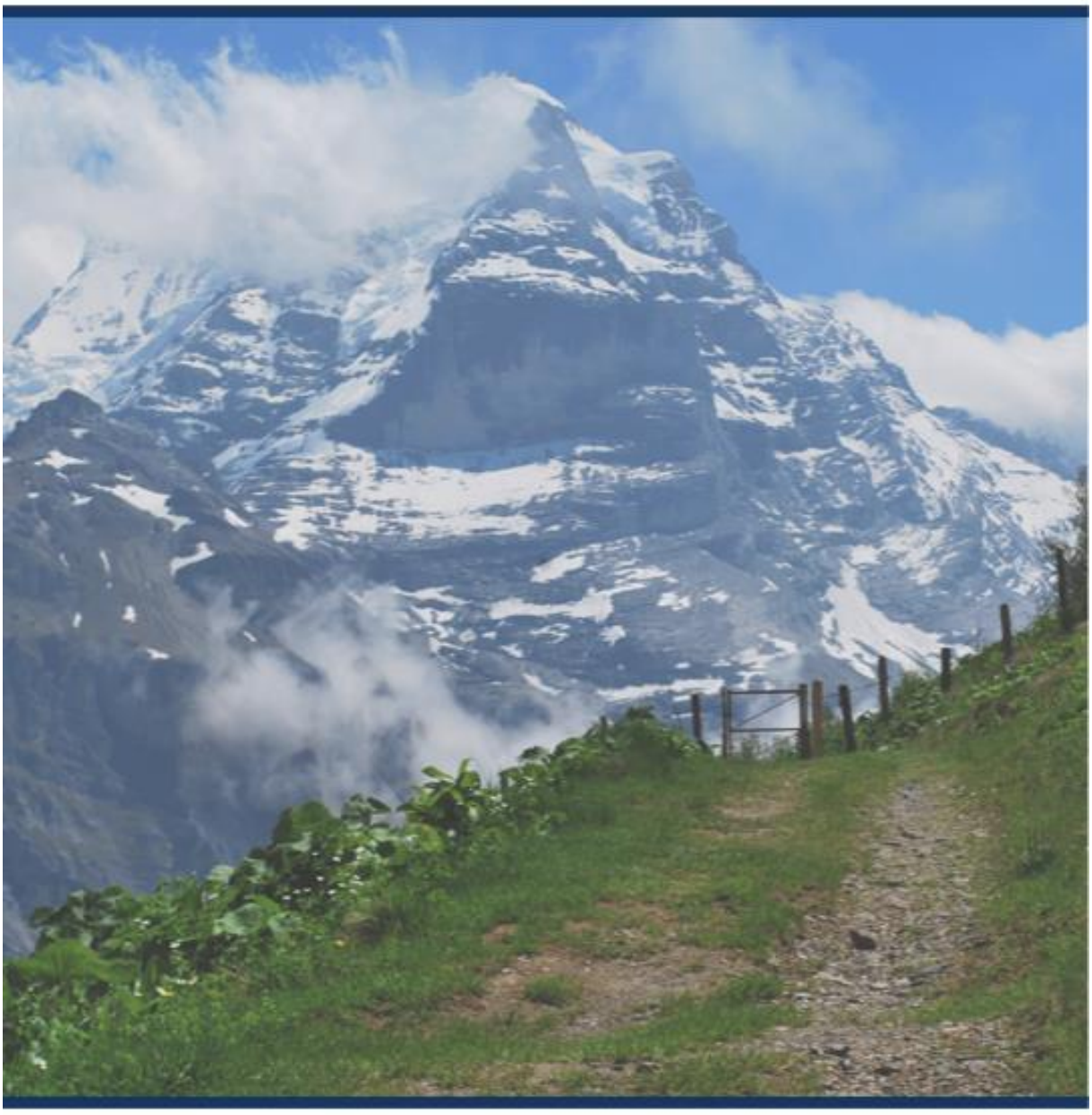

3. Introduction

3.1 The liver

Triangular in shape, the liver is the largest gland in the body and accounts for about 2.5% of the human body weight. The human liver is composed of four lobules and is anatomically located to serve its dual role as a metabolic and biochemical transformation factory [1]. Indeed, the liver is the central metabolic organ; accordingly, its functions are many but that can be divided into three categories: resorption and storage, synthesis and secretion, and detoxification and excretion [2]. The intricate architecture and cellular components of the liver complement and contribute to these varied functions.

Liver architecture

The hepatic lobule, the basic architectural unit of the liver, is composed of hepatocytes arranged in single-cell thick cords lined by sinusoidal capillaries that extend from the portal triad to the central vein. The liver receives 75% of its blood supply from the portal vein and the rest from the hepatic artery. The portal veins and hepatic arteries terminate in the intrahepatic portal tracts, which contain bile ducts that transport bile from the canaliculus through the extrahepatic biliary system. The terminal portal veins, or channels of Herring, give rise to septal branches that drain blood into the sinusoids that then take blood through the acinus to the central vein. The hepatic artery terminates in axial branches that run parallel to the portal vein and likewise terminate in sinusoids. Bile canaliculi are located on the lateral surfaces of adjoining hepatocytes (Fig 1). The blood from the portal triad is rich in oxygen (from the artery) and nutrients (from the portal vein, the terminal outflow of the mesenteric system), and as blood flows to the central vein, nutrients and oxygen are consumed creating three zones that differ in oxygenation and metabolic functions in the most metabolically relevant unit, the liver acinus [2]. Therefore, hepatocytes line up along the porto-central axis leading to a structural and functional heterogeneity known as metabolic zonation, allowing for maintenance of metabolic homeostasis in the body [1] and contributing to the varied vital functions of the liver.

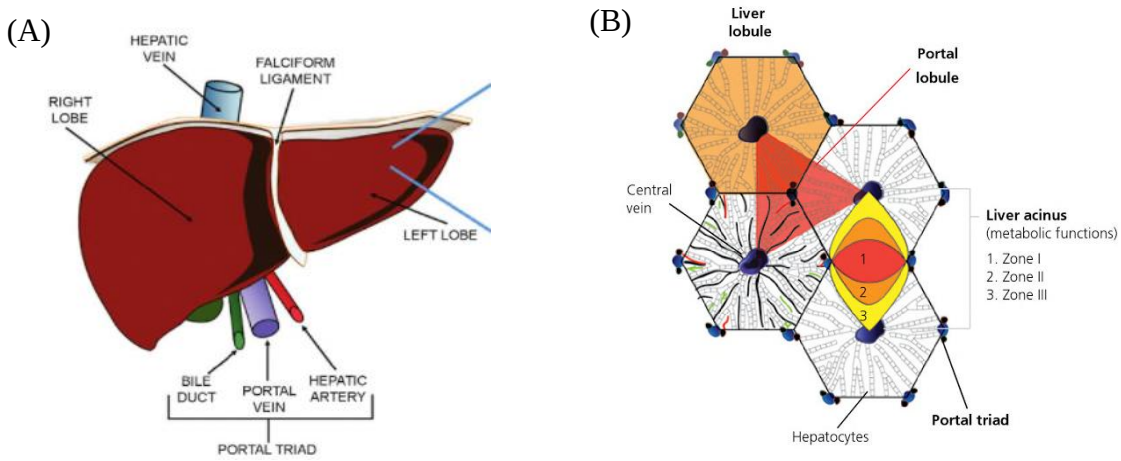

Figure 1. (A) The physiology of the liver. Adapted from [1]. (B) Functional units of the liver parenchyma. Adapted from [2].

The parenchyma is composed of a network of cell plates made of hepatocytes that have di- or polyploid nuclei. The sinusoids are lined by highly specialized fenestrated endothelial cells characterized by the absence of tight junctions and lack of basement membrane. The sinusoidal endothelium is interspersed with Kupffer cells as well as the space of Disse, a specialized extracellular matrix containing stellate cells and occupying he space between LSECs and hepatocytes. Kupffer cells and NK cells may also bulge into the sinusoidal lumen [2,3] (Fig 2). Each cell type plays a specific role in maintaining liver homeostasis.

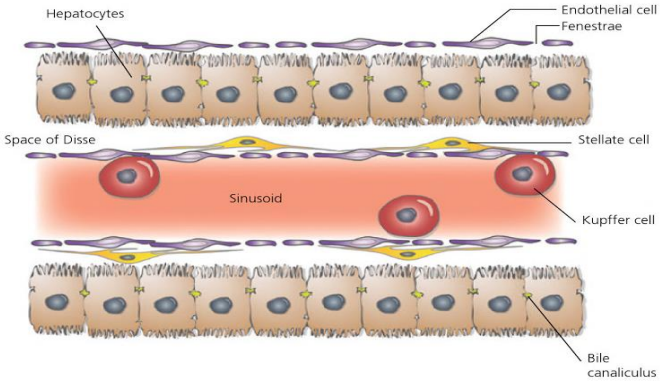

Figure 2. The structural integration of hepatocytes and non-parenchymal cells in the liver. Adapted from [2].

Parenchymal and non-parenchymal cell types

Hepatocytes are the most numerous cells in the liver (60-70% of all cells and composing 80% of its mass/volume) and are responsible for most of the synthetic and metabolic functions. To fulfill their numerous metabolic functions, hepatocytes contain a complex array of mitochondria, peroxisomes, lysosomes, Golgi complexes, rough and smooth endoplasmic reticulum, microtubules and microfilaments [1].

Nonparenchymal cells include endothelial cells, Kupffer cells, stellate cells, cholangiocytes, and natural killer cells. Endothelial cells, the second largest cell population (about 20% of all cells), form the lining of the sinusoidal wall and contain fenestrae. The endothelial cells form cylindrical structures in single cells in a row to form the typical liver capillary, the sinusoid. Free access of fluid, solutes, droplets, and particles from the lumen toward the space of Disse (and vice versa) occurs solely through the fenestrae. Hence, the fenestrated phenotype enables the blood-hepatocyte exchange and is a prerequisite for normal liver function. Kupffer cells, the macrophages of the liver, comprise about 2% of the liver volume/mass and are located within the lumen of sinusoids. Kupffer cells are phagocytic and when activated produce a large number of chemokines and cytokines for the liver's acute phase response. Stellate cells comprise about 1.5% of the liver volume and are located in the space of Disse. They are multifunctional and metabolize vitamin A, synthesize, secrete, and degrade components of the perisinusoidal extracellular matrix. In response to cytokines, stellate cells acquire a myofibroblast phenotype, become migratory, and have a major role in the fibrotic response of the liver injury. Cholangiocytes, the only other type of epithelial cell, account for 3-5% of the liver cell population. Albeit small in population, they have an important pathophysiological role in the modification of the composition of bile during transit in the bile ducts. Cholangiocytes form the bile canaliculi and line the channels of Hering as bile flows to the periphery [4,5]. Lastly, liver-associated natural killer cells, or pit cells, are localized in the lumen of the sinusoid and closely adhere to the endothelial and Kupffer cells. They are important components of the liver-centered immune system involved in antigen presenting, removal, or neutralization of numerous foreign materials [1,6]. Therefore, the composition of the liver is varied albeit specific in its contribution to maintaining proper liver function.

3.2 Liver regeneration

The Greek myth of Prometheus recalls an eagle devouring a titans liver during the day (a symbolic consumption of the physical manifestation of his soul), resulting in eternal torture for the titan as his liver regenerated back every night [7]. Today, we know that the liver is not necessarily the seat of the soul as the ancient Greeks believed, but rather an organ that provides a number of fundamental functions, such as detoxification and bodily provision of nutrients. Due to its diverse and vital functions, it is only reasonable that the liver is the only

organ in the body that is able to reach 100% re-adjustment to its original size after tissue loss or liver injury.

In humans, up to 70% of the liver can be resected with a recovery of the original mass within 2-3 weeks [8]. The term 'hepatostat' has been coined to describe the livers ability to recover its original mass by proper initiation and termination of regeneration to recover its full functions after a massive loss of hepatocytes. However, only the mass and not the lobular composition of the liver is restored and therefore, 'compensatory hyperplasia' is a term most often used to describe regeneration. To be precise: first liver mass is reconstituted, followed by a long (i.e. several months) remodeling period that eventually restores the livers original architecture [9].

General concepts of liver regeneration

There are two models describing how the liver may regenerate: (i) replacement of tissue loss with phenotypic fidelity of cell types, or (ii) replacement of tissue by activation of transdifferentiation pathways originating from facultative stem cells [9]. These processes are not mutually exclusive and can occur at different proportions depending on the size of tissue loss and impairment of cellular compartments. Vaguely speaking, regeneration after partial hepatectomy occurs from the proliferation of differenitated hepatocytes, while regeneration after injury tends to be initiated from stem cells. To study these concepts of regeneration, various experimental animal models have been developed throughout the years; although we will focus on the standard model of regeneration after partial hepatectomy.

Higgins and Anderson first presented a murine standard hepatectomy model (sHx) in 1931; whereby 70% of the liver is resected and liver regeneration mass is regained after 5-7 days [8,10,11]. sHx has been established as a reliable model to study regeneration due to minimal liver injury, a synchronized cell cycle, and very high reproducibility. The lobular structure of murine livers allows the 'clean' removal of tissue without inducing massive necrosis. sHx stimulates quiescent G0 hepatocytes to enter the cell cycle, replicate their genome, undergo cytokinesis, and exit the cell cycle back to the resting state once the original liver mass has been restored [7]. At 32-48h after operation in mice, DNA synthesis peaks in hepatocytes, followed by initiation of DNA synthesis in nonparenchymal cells such as biliary epithelial cells, liver sinusoidal epithelial cells (LSECs), and stellate cells [1,12,13,14]. Liver regeneration may also be evaluated by models using chemicals to induce liver injury, such as CCl_4 and APAP (acetyl-para-aminophenol; commonly known as acetaminophen); however, these regenerative responses differ in that they initiate from stem cells and are overlayed with

the pathogenesis of fibrosis and acute inflammation of necrotic zones [7,11,15]. Therefore, we will only focus on those mechanisms instigated by sHx.

The phases of liver regeneration

The kinetics of liver regeneration can be divided into three phases characterized by timely mechanisms, whereby hepatocytes are *primed* and prepared to enter the cell cycle (*initiation*) and then proceed through replication and mitosis (*progression*) to re-establish the original liver volume (*termination*). These processes are briefly described below and represented in Figure 3.

Priming. It is a common belief that a cytokine-mediated priming process is essential for the quiescent hepatocytes to enter cell cycle during initiation of regeneration. Once primed, these hepatocytes respond to other mitogenic stimuli [9,16]. There is not a single signaling pathway associated with the complete success of the regenerative response, but based on the mode of action, extracellular signals are characterized as (i) complete mitogens and (ii) auxiliary mitogens [9]. HGF and EGF receptor ligands are complete mitogens as they are considered core drivers of parenchymal regeneration [1]. After sHx, HGF acts in an endocrine and paracrine manner on hepatocytes. The first round of HGF signaling is derived from the matrix, while stellate cells and endothelial cells produce new HGF after sHx. Although inactive HGF is available for use by hepatocytes already bound in the ECM, 3h after sHx stellate and endothelial cells start producing new HGF mRNA [17]. EGFR ligands that are important for survival after sHx are amphiregulatin and TGF-α that act in an autocrine manner on hepatocytes, as well as heparin-binding EGF-like growth factor (HB-EGF) synthesized by Kupffer cells and LSECs that acts in a paracrine manner. HB-EGF is also available from endothelial cells and macrophages [18]. Auxiliary mitogens include norepinephrine, Notch and Jagged, PDGF, VEGF, insulin, bile acids, serotonin, leptin, estrogens, triodothronine, TNF, FGF1 and FGF2 [1]. However, these classifications may remain somewhat artificial, as for example interruption of VEGF signaling can lead to a severe, long-lasting halt in regeneration [19]. Anyway, the combination of these signals results in hepatocyte cell cycle progression that leads to DNA synthesis and proliferation of hepatocytes. However, the liver employs effective redundancy to secure proper regeneration. Deregulation of either the HGF and EGF pathways delay the cell cycle by reducing G1 entry, and diminishing G1 to S phase and G2 to M phase transitions. Only depletion of both signaling pathways leads to complete failure of regeneration [20].

Initiation. The immediate consequence of sHx is an increase in the entire flow of the portal vein to 1/3 of the remaining liver. Furthermore, several genes are initiated very shortly after sHx, also characterized as 'immediate early genes' (changes occurring within minutes to hours), that are thought to induce cells for cell cycle entry but are likewise induced in hypertrophic regeneration [21].

The early mechanistic changes begin with a huge increase in the activity of urokinase within 5 minutes (perhaps activated through shear stress), followed by a cascade by which urokinase activates plasminogen into plasmin, and proceeds to activate metalloproteinases (MMPs). This protease cascade degrades specific components of the extracellular matrix (ECM) and is associated with the release of bound HGF. An early event is the nuclear translocation of β-catenin, occurring as early as 5 min. after resection, followed by a peak at 60 minutes, and continuous activity for at least 24 hours. LSECs are important inducers of β-catenin, as they provide mitogenic WNT2 to activate β-catenin in the hepatocytes [19,22]. In the nucleus, β-catenin dimerizes with TCF family transcription factors and initiates transcription of genes associated with the cell cycle. WNT, MET, and EGFR protect β--catenin by specific tyrosine phosphorylation to enhance its migration to the nucleus [9]. Furthermore, 15 minutes after sHx, Notch migrates into hepatocyte nuclei and initiates transcription of Notch-dependent genes, such as HES1 that promotes cyclin E to prepare for proliferation and inhibition of apoptosis. [9,23]. Early remodeling of the ECM induced by urokinase results in HGF release and activation as well as release and inactivation of TGF-β by alpha-2-macroglobulin. This creates an imbalance that triggers entry of hepatocytes from G0 to G1 phase of the cell cycle. Furthermore, EGF has an enhancing effect as its concentrations rise according to the increased portal flow towards a reduced liver volume after sHx. EGFR and MET receptor stimulation leads to the activation of NFkB, STAT3, PI3K, and eventually Akt [11]. NFkB activation occurs 30 minutes after sHx, which migrates into the nucleus to enhance transcription of multiple target genes involved in proliferation [24]. STAT3 activation occurs within 1 hour after sHx and lasts up to 8h [25,26], and is triggered by EGFR-ligands, HGF binding to the MET receptor, as well as IL6 and TNF-α cytokines derived from Kupffer cells [27-30]. STAT3 migrates to the nucleus and triggers expression of genes associated with cell cycle regulation including components of the AP1 transcription factor, marking the activation of STAT3 crucial for G1 entry. STAT3 is thought to collaborate with NFkB for G0 entry, and both can be activated via IL6 signaling from Kupffer cells. This culmination of signals results in the activation of cyclin D1 and its migration to the nucleus, committing hepatocytes to enter into S phase. [31-33].

Although, hyperplasia is considered the core mechanism behind regeneration, upon 30% hepatectomy, the liver also recovers its original mass via hypertrophy, i.e. the growth of cell size in the absence of mitoses [21,34]. Hypertrophy and the immediate gene response occur after both 30% and 70% hepatectomy, but only the latter loss is extensive enough to push hepatocytes into mitosis.

Progression. Hepatocytes receive multiple signals from diverse mitogenic pathways not only to move through G1 and enter into S phase, but also to complete G2 and M phases (characterized as 'delayed activation genes', gene changes occurring from 1 hour until longer). It appears the cell cycle progression through S and M is driven by the same mitogens as the cell cycle entry, however without the activity of certain molecules considered key drivers of G0 entry (e.g. NFKB, STAT3). The transcription factor FOXM1 is a central mediator of these mitogenic pathways. FOXM1 is required for efficient S and particularly M phase progression during regeneration, through not only its virtue to activate S and M phase genes but also through repression of the cell cycle inhibitor p21 [35].

Termination. Termination of regeneration is the least understood phase. Near the end of regeneration, the ECM is being reconstructed leading to the engagement of integrins, such as ILK, that activate complex signaling pathways [8]. ILK pathways overall foster polarization and suppress hepatocyte growth [36], as seen in ILK-deficient mice subjected to sHx where the final liver weight substantially exceeds the pre-operative liver weight [37]. TGF-β1 and activin are the best known to selectively inhibit hepatocyte proliferation in the termination of liver regeneration. Early after sHx, TGF-β is removed from the environment of the hepatocyte, but is later resynthesized and restored by binding to decorin at the end of regeneration [38]. Decorin itself has direct inhibitory effects on both MET and EGFR [39,40] and the balance between binding TGF-β and acting on MET and EGFR are important in termination. Glypican-3 (GPC3), a protein bound to the plasma membrane of hepatocytes, also partakes in the growth suppressing signaling system [41]. GPC3 binds to hedgehog family members and may prevent them from stimulating growth in many liver cell types [42]. Furthermore, activins are members of the TGF-β superfamily and share similar signaling pathways. Activin A suppresses hepatocyte growth and is produced by hepatocytes, suggesting an autocrine effect [9]. Interestingly, there is a greater number of hepatocytes at the end of regeneration than that of the original liver and this is corrected by a small wave of apoptosis that occurs in the final stages [43]. Overall, termination of regeneration is based on

the balance between the effects of growth stimulators and mitoinhibitors, which are integrated into the matrix remodeling occurring after sHx.

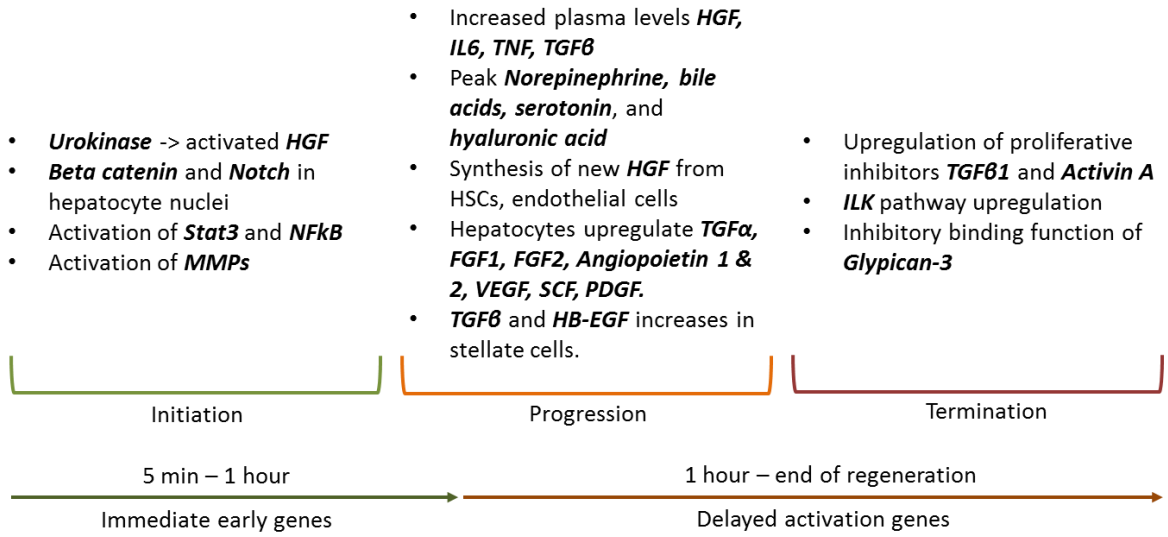

Figure 3. Simplified representation of mechanisms involved in the three phases of liver regeneration.

Interactive mechanisms during liver regeneration

Complex crosstalks. Liver regeneration is a complex process that is precisely orchestrated by autocrine, paracrine, and endocrine signaling, many of which are highly redundant [7]. These pathways are very complex and are interplayed throughout the various types of cells within the liver. Hepatocytes are the first cells to respond to regenerative stimuli, followed by biliary cells, and later by endothelial and stellate cells [9]. On the other hand, non-parenchymal cells produce early signals (i.e. Kupffer cells induce TNFα, IL6; while stellate cells produce HGF, hedgehog ligands, and LSECS produce WNT2 and HGF) to push hepatocytes into proliferation. Proliferating hepatocytes in turn synthesize growth factors effective towards adjacent cells, such as TGF-α, FGF1, FGF2, VEGF, angiopoietins, and PDGF. Most of these factors have angiogenic activity and are important for the vascular remodeling that occurs in later stages of regeneration. Proliferating endothelial cells and hepatocytes interact to form vascular channels, eventually acquiring the structure of sinusoids and restoring intact histology of the liver [9]. Biliary epithelial cells proliferate almost as early as hepatocytes and respond to the same proliferative signals (Fig 4). Lastly, there are no new portal triads and lobules generated in regeneration, and rather the size of the lobules of the regenerated liver are overall larger.

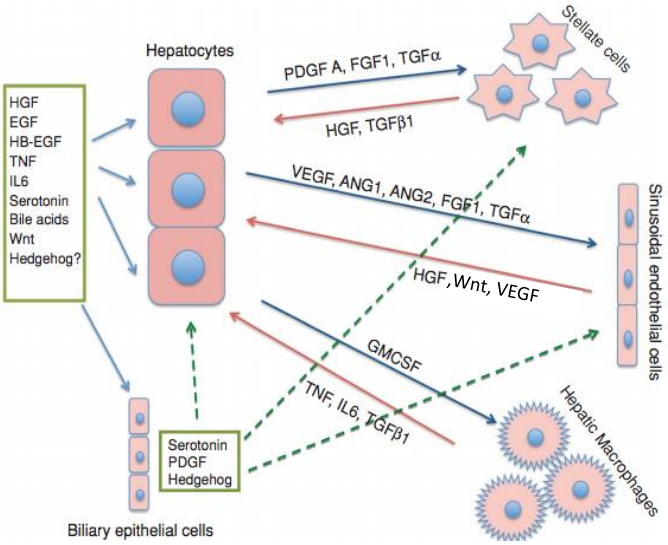

Figure 4. Coordination of liver cells during regeneration. Adapted from [9] with modifications.

Other players in regeneration. Several mechanisms are continuously being studied for their roles in regeneration. Bile acids have been found to play a role in the progression of regeneration by activating the proliferative properties of the nuclear factor FXR [9,44]. The neurotransmitter serotonin likewise has been implicated in regeneration; however, the underlying mechanisms remain unclear. Recent evidence indicates it may be involved in an autocrine or paracrine manner in the proliferation of cholangiocytes [9,45,46]. Hypoxia has been shown to be an important driver of normal hepatocyte mitosis through HIF2α, which in parallel induces enforced VEGF production to instigate the subsequent angiogenic phase [47]. Lastly, regeneration is an energy-consuming process, and recently it has been shown that fat import from the periphery (in response to the dropping blood sugar levels following liver tissue loss) is required to provide regenerative fuel via β-oxidation, a process fostered by PTEN downregulation [48].

Through this mechanistic summary, we can see that many studies throughout the decades have sought to elucidate the pathways and gene expression changes underlying liver regeneration after sHx; however, it still remains a complex and highly relevant topic of investigation (Fig 5).

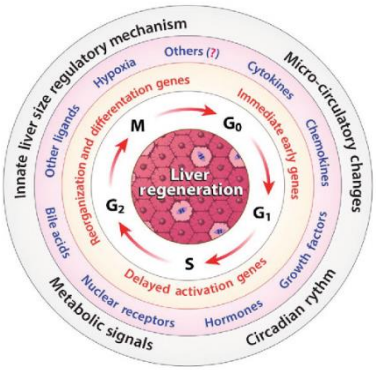

Figure 5. Overview of mechanisms involved in liver regeneration. Adapted from [7].

3.3 The role of hepatic stellate cells role in the liver and in regeneration

Hepatic stellate cells (HSCs), identified by von Kupffer in 1876, are liver-specific mesenchymal cells that are located in the space of Disse interposed between liver sinusoidal endothelial cells (LSECs) and hepatocytes [49]. They are often considered a substitute for pericytes, which support endothelial function but are absent in sinusoids. HSCs have roles in differentiation, proliferation, and morphogenesis of other hepatic cell types during liver development and regeneration. Their exact origin remains unclear as they express both neuroectodermal and mesodermal cystoskeletal markers [50].

In healthy livers, stellate cells are quiescent and contain vitamin A lipid droplets (comprising the largest reservoir of bodily vitamin A), regulating vitamin A homeostasis in the body [51]. Most of the vitamin A stored in HSCs is in the form of retinyl esters, which account for half of the content of lipid droplets. HSCs are also sites of β-carotene storage and release, which is used for retinoic acid production and maintenance of homeostasis of circulating carotenoids [52]. Therefore, the functions of HSCs are predominantly regulated by retinoic acid receptors (RARs) and peroxisome proliferator-activated receptors (PPARs). RARs meditate most physiological functions of vitamin A, and PPARγ is the master gene for adipose cell differentiation [51].

In liver injury, however, the natural wound healing responses are activated (in acute liver damage) and deregulation of these responses can result in fibrosis (resulting in chronic liver damage). Upon injury, hepatic stellate cells differentiate to myofibroblasts (MF). MFs produce increased amounts of ECM components such as collagen I and become proliferative, contractile, inflammatory, and chemotactic [49,53]. The expression of the cytoskeletal protein alpha-smooth muscle actin (αSMA) is recognized as a marker of activated HSCs [54].

Nevertheless, in regeneration after partial hepatectomy, a form of acute injury, TNF-α and IL6 secretion occurs early, primarily from Kupffer cells and to a lesser extent from HSCs. Matrix remodeling becomes critical and HSCs produce a number of matrix metalloproteinases (MMPs) to degrade the ECM and promote the release of growth factors, such as HGF [53]. This facilitation of forming new blood vessels is further supported by HSC-secreted angiopoietin 1 (ANG1), which binds to Tie-2 on LSECs to promote their close association and to stabilize the new vascular system [55]. HSCs also play a role in the termination of liver regeneration by the secretion of TGF-β1 [56]. This gives HSCs control of the balance between liver fibrosis and regeneration. Hedgehog signaling promotes the transition of quiescent

hepatic stellate cells to fibrogenic myofibroblasts, which can contribute to the epithelial compartment and support the regeneration of parenchyma [57]. Therefore, HSC-derived factors facilitate regeneration independent of direct mitogenic effects on hepatocytes (Fig 6).

Lastly, HSCs are also known to play a role in hepatocellular carcinoma (HCC), although the associations between HCC and fibrosis are incompletely understood [58,59]. Nevertheless, inflammatory cells, integrin signaling, growth factor interactions with the ECM, and communication between activated HSCs and tumor cells all play a role [60]. For example, activated HSCs increased proliferation and migration of human HCC cells in culture [61], suggesting that fibrosis promotes HCC, although not in all cases, as fibrosis and HCC could occur due to the same underlying factors.

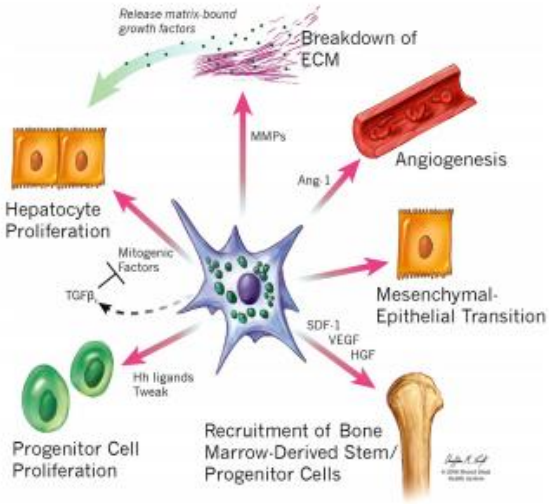

Figure 6. The role of hepatic stellate cells in regeneration. Adapted from [53].

3.4 Liver surgery and its limitations

The fact that liver can regrow after tissue loss has enabled the surgical management of liver diseases, such as tumors. The progression of surgical treatment for safe removal of extensive tumor loads in the liver has been steadily improving since the first introduction of portal vein embolization (PVE) in the 1980's [62]. The goal in surgical removal of liver tumors is to remove the diseased parts of the liver while maintaining enough healthy tissue to allow for regeneration of the organ back to its original size. However, there are many limitations to the removal of multiple/large tumor loads as extensive resection can lead to liver failure leading to small-for-size syndrome (SFSS, see below), the most frequent cause of death due to liver surgery.

The introduction of PVE was rapidly adopted through its integration into two-staged hepatectomies as a measure to prevent liver failure after extensive right-sided hepatectomies [63]. The introduction of two-staged hepatectomies was the first step-wise procedure to remove liver tumors where - in the first stage - PVE or portal vein ligation (PVL) prevented blood flow to the tumor-laden section of the liver, while smaller tumors were removed from the healthy non-occluded liver. The occlusion of the diseased lobe, however, led to a compensatory growth of the un-occluded contralateral lobe. A few weeks later, when the healthy contralateral lobe gained sufficient volume to sustain the patient, the second stage was performed, that is the resection of the atrophied tumor-laden lobe [64] (Fig 7). These developments led to the successful removal of multiple liver lesions that were previously unresectable.

One disadvantage to this procedure is the requirement for long intervals between the two stages – from 2 to 13 months – in order to attain a future liver remnant large enough to enable stage 2. This interval presents opportunity for undesirable disease progression. Furthermore, insufficient hypertrophy of the healthy future liver remnant would often occur, preventing the feasibility of a stage 2 resection in order to avoid liver failure and the SFSS [65].

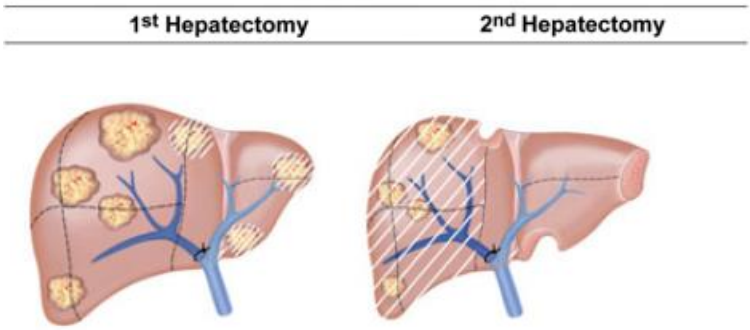

Figure 7. Pictorial example of a two-staged hepatectomy in a liver with extensive tumor load. Adapted from [66].

Small-for-size syndrome (SFSS)

SFSS is a clinical syndrome described following liver transplantation and extended hepatectomy. Although its pathophysiology is ill-defined, it is characterized by liver dysfunction (postoperative coagulopathy, persisting steatosis, hypoalbuminemia, hyperbilirubinemia) and regenerative deficiency due to insufficient functional liver mass. As already mentioned, the SFSS remains the most common cause of postoperative death, but is currently untreatable. It is particularly unclear whether the impaired liver function is a result of disproportional tissue damage after resection or secondary to a primary failure in

regeneration of the small remnant. At least in mice, it could be demonstrated that a transient cell cycle arrest is sufficient to cause classic SFSS symptoms [67], albeit in humans – unlike in the multilobular mouse liver- resection usually is associated with direct parenchymal injury. Regardless, the minimal functional future liver remnant required to avoid SFSS is ≥ 25% in a normal liver and ≥ 40% with preoperative liver dysfunction [68]. PVE and two-staged hepatectomies allow for volume manipulation by increasing the functional capacity of the liver remnant before complete resection as a preventative measure against the SFSS. Furthermore, many characteristics should be monitored after extended hepatectomy to help manage developing SFSS, such as the size of the future liver remnant, the portal blood flow and pressure, and assessments of serum bilirubin, albumin, and liver enzymes [69]. The most recent strategy to avoid SFSS and propel successful regeneration has been introduced as ALPPS (*A*ssociated *L*iver *P*artition and *P*ortal vein ligation for *S*taged hepatectomy).

3.5 ALPPS

This innovative development in surgical treatment of extensive tumor-laden livers was the by-chance finding of combining portal vein ligation (PVL) with parenchymal transection in stage 1 of a two-staged hepatectomy. The combination of these two surgical procedures resulted in an enormous growth of the future liver remnant in just 8 days (compared to 2-13 months after standard two-stage hepatectomy), allowing swift resection of the occluded segments in stage 2 of the procedure [70,71] (Fig 8). Since this discovery, ALPPS has been performed in patients with extensive liver tumor loads, although the molecular mechanisms behind the accelerated regeneration remain unknown.

ALPPS in patients

Since ALPPS was first performed in patients in the clinic before any experimental models came to fruition, most publications on ALPPS are clinical observations. As already mentioned, portal vein ligation and parenchymal transection are performed in stage 1 with the diseased liver segment left in place. The ligated diseased liver acts as an auxiliary liver to assist the future liver remnant for the first critical week after ligation [66], and maintains some function, representing up to 60% of the total liver function 6 days after stage 1 of surgery [70]. Meanwhile, the metabolic capacity of the liver is significantly compromised after removal of the diseased lobe in the second stage of surgery.

The hypertrophy induced by ALPPS is superior to other procedures as there is an average 74% volume increase of the future liver remnant in a mean of 9 days [71]. Due to the short interval between surgical stages, tumor progression is unlikely and the second stage of surgery is less demanding as there are fewer adhesions allowing faster recovery for the patient and earlier restoration of chemotherapy [66]. The novelty of this technique is the *in-situ* split, but this surgical aspect has already been altered in the few years since the introduction of ALPPS in the clinic. ALPPS stage 1 was initially performed with a 100% parenchymal transection; however, with results eliciting a high mortality rate [72], as little as a 50% parenchymal transection has been determined necessary to induce the accelerated regeneration of ALPPS [73].

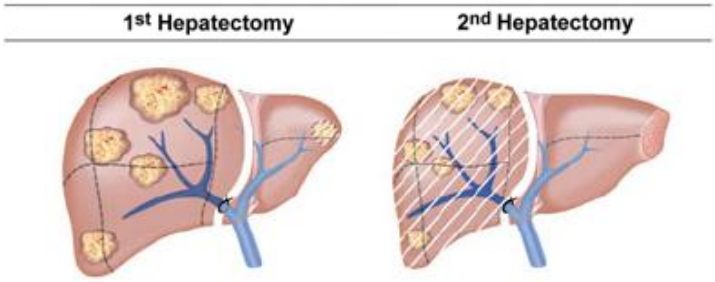

Figure 8. The ALPPS procedure in human livers. Adapted from [66]

ALPPS experimental models

Various animal models have been reported in an attempt to further understand the phenomenon of this accelerated liver regeneration on a molecular level. Models exist in mouse, rat, rabbit, swine, although there seems to be no consensus as to which lobe to assign as the future liver remnant. Nevertheless, amongst all these models, the common finding is that ALPPS-like procedures in experimental models induce similarly accelerated regeneration compared to portal vein occlusion alone. Primary research reveals that several pathways known to be involved in regeneration after partial hepatectomy have also been validated in ALPPS animal models. IL6, TNF-α, pSTAT3, nuclear NFkBp65, and YAP were all upregulated after ALPPS stage 1; whereby IL6 and TNF-α were the only molecules further validated in human ALPPS tissue [74-76].

We presented the first ALPPS mouse model in 2014 [76] to study this regenerative phenomenon on the molecular level. Although, the liver anatomy is different in mouse, the ALPPS procedure was adapted to fit mouse physiology and to convey similar results (Fig 9A). In stage 1 of murine ALPPS, 90% of the liver is ligated (with resection of the left lateral lobe, LLL, to mimic the ‘cleaning’ of the liver from smaller tumors) and an 80% parenchymal

transection is performed (Fig 9B). Just 48 hours after stage 1, the future liver remnant (the median left lobe, FLR), restores a volume large enough to sustain the mouse, allowing stage 2 to be performed by resecting the atrophied ligated lobes (Fig 9C-D). Using this model throughout my PhD studies, I sought to complete the aims stated in the next section.

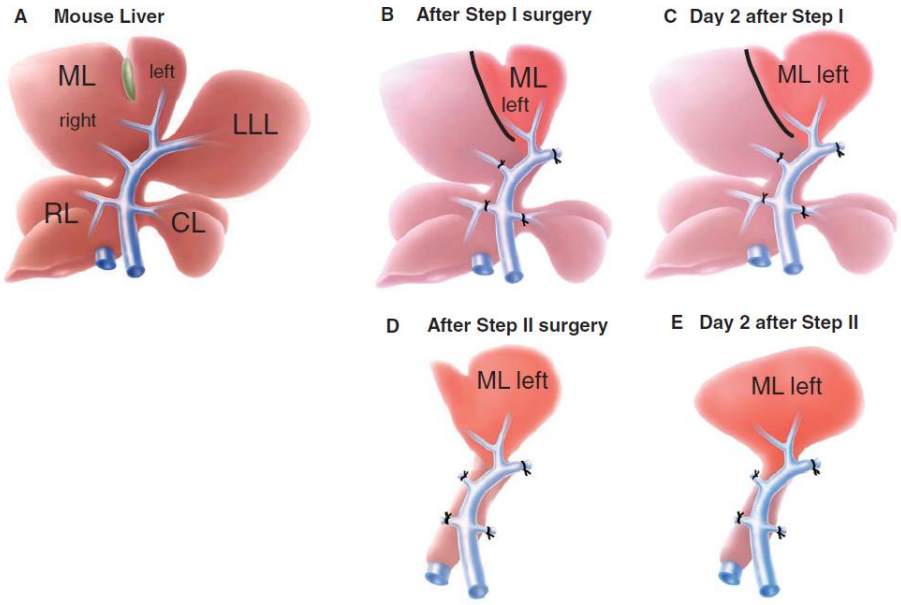

Figure 9. Surgical procedure of ALPPS in mice. Adapted from [76].

3.6 Goal and aims of the PhD thesis

The above introduction portrays the complexity and incomplete understanding of the molecular changes incurred during liver regeneration after partial hepatectomy. Furthermore, the limits imposed on two-stage hepatectomies propelled the innovation of ALPPS, whose driving mechanisms have not been investigated. There exists a necessity to further understand these processes of regeneration with the intention of improving patient care. Indeed, the introduction of ALPPS has revealed that simple surgical additions can unleash an unprecedented acceleration of liver regeneration beyond the expected physiological limits. Therefore, the understanding of the molecular mechanisms underlying the acceleration of regeneration is not only of obvious biological interest, but might identify molecular processes the modulation of which could aid regeneration in the clinic. Liver regeneration after sHx activates molecules as early as 5 minutes after surgery. In ALPPS, we hypothesize that some pathways may be similar to regeneration after sHx, albeit occurring at a much faster rate, while others are unique and necessary to induce this accelerated regeneration.

This PhD thesis set out to explore the pathways dysregulated in accelerated regeneration induced by ALPPS surgery and to assess their impact on regenerative speed. More specifically, after an explorative RNA deep sequencing approach, the focus prevailed to the following:

1) *The role of the Indian hedgehog (IHH) pathway as a unique component in the early induction of accelerated regeneration as well as its mechanism of action;*
2) *The identification of the upstream regulators of IHH as essential inducers of accelerated regeneration in ALPPS, here with a focus on JNK1.*

The following paragraphs provide a more detailed background on the two central pathways investigated in this thesis, IHH and JNK1.

3.7 The Hedgehog pathway

Hedgehog signaling involves the three ligands Sonic Hedgehog (SHH), Indian Hedgehog (IHH), and Desert Hedgehog (DHH). All three are thought to have the same affinity for the receptor Patched (PTCH1); SHH and IHH are widely expressed, while DHH expression is limited to nervous tissue and testis [2,77]. Hedgehog ligands are lipid-modified proteins, meaning they can diffuse through the hydrophilic extracellular matrix and can form complexes with lipoproteins facilitated by glypicans. Therefore, hedgehog ligands can activate downstream signaling to hedgehog-responsive cells via autocrine, paracrine, or endocrine mechanisms [78].

Canonical hedgehog signaling involves ligands binding to *Patched* (PTCH), which blocks its inhibitory effect on the co-receptor *Smoothened* (SMO), allowing SMO, a G protein-coupled receptor, to transduce hedgehog-initiated signals intracellularly. Active SMO releases GLI from its suppressor complex (Fused kinase and Suppressor of Fused), where it can translocate into the nucleus to promote transcription of its target genes. There are three GLI family members: GLI1, GLI2, and GLI3; where GLI1 is a transcription activator and is transcriptionally regulated by hedgehog signals, GLI2 also functions as a transcription activator, while GLI3 functions as a transcription repressor [2,79] (Fig 10). However, hedgehog signaling is also associated with non-canonical pathways. These are categorized as ligand-independent activation of the downstream hedgehog pathway, signaling through the ligand independently of GLI, and cross-talk of hedgehog components with other pathways. For example, TGF-β can activate GLI2 directly, independently of SMO. PTCH can also directly interact with cyclin B1 and caspases, omitting interaction with GLI to inhibit cell proliferation and promote apoptosis [80].

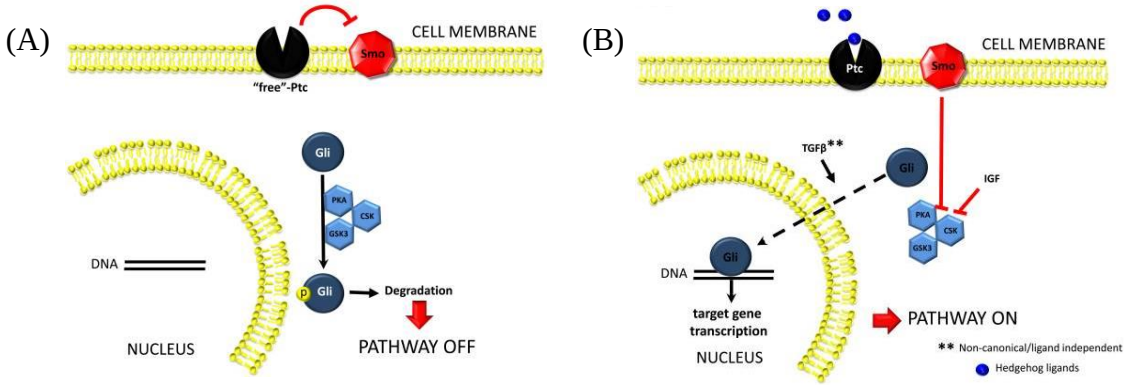

Figure 10. Hedgehog signaling in the (A) absence (B) or presence of Hedgehog ligands. Adapted from [78].

During development, the hedgehog ligands are essential morphogens. They are secreted by various cells, diffuse throughout the embryo, and modulate cell fate as a function of ligand concentration [81]. Hedgehog regulates several key cell functions, namely proliferation, survival, migration, and differentiation [78]. Inhibition of the hedgehog pathway during development leads to many defects including failure of brain development and skeletal defects [82]. However, in the healthy, resting adult liver, there is minimal hedgehog activity.

Chronic liver injury or tissue loss reactivate the hedgehog pathway to modulate liver repair. Upon injury, hepatocytes, LSECs, myofibroblastic HSCs, NKT cells, and Kupffer cells induce expression of SHH and IHH. Therefore, most stromal cells that accumulate in injured livers are capable of activating the canonical hedgehog pathway, promoting viability, growth, activation, and transition towards a more mesenchymal phenotype [2]. HSCs are particularly responsive to hedgehog ligands, and hedgehog enhances HSC survival by inhibiting apoptosis, promoting HSC proliferation, and stimulating HSCs to acquire a myofibroblastic phenotype [83]. HSC activation can also be induced by mitogens again in a hedgehog-dependent way [84].

During regeneration following tissue loss such as after sHx, hedgehog pathway activation is required for a normal healing response. The expression of hedgehog ligands and GLI2 increases 24-48 hours after sHx in mice, paralleling maximal hepatocyte proliferative activity. Furthermore, inhibition of the hedgehog pathway by the SMO-specific inhibitor cyclopamine reduced hepatocyte proliferation, blocked restoration of liver mass, and reduced posthepatectomy survival [85]. Currently, it is not known whether one or all hedgehog ligands are contributing to the regenerative process. Interestingly, the binding of IHH to GPC3 decreases dramatically during the proliferative phase post hepatectomy, while IHH is re-sequestered by GPC3 towards the end of regeneration, perhaps suggesting IHH is transiently freed to support regeneration after tissue loss [86].

On the other hand, prolonged overactivation of the hedgehog pathway appears to promote chronic liver disease and carcinogenesis. For example, pharmacological inhibition of the hedgehog pathway by cyclopamine protects mice from developing chronic liver disease [87]. Hedgehog pathway activity has been consistently identified in about two-thirds of HCC tumors, while the physiological inhibitor of hedgehog, HHIP, is epigenetically silenced in liver cancer [88]. Hedgehog activation correlates with tumor size, capsular invasion, vascular invasion, higher tumor stage, intrahepatic metastasis, decreased survival, and recurrence after

curative resection [2]. Furthermore, preclinical studies in mice show that inhibiting the hedgehog pathway via SMO reduces tumor size and regresses HCC [89].

Overall, the hedgehog pathway is a master regulator of the repair response after adult liver injury, but also determines the extent of chronic liver damage. Therefore, appropriate control of hedgehog signaling is essential for normal liver function to orchestrate hepatic wound-healing, inflammation, vascular remodeling, fibrogenesis, and epithelial regeneration.

The Hedgehog pathway in ALPPS

Our aim was to explore dysregulated pathways in ALPPS compared to surgical controls at early time points after operation through RNA deep sequencing of liver tissue. We identified *Ihh* as a top upregulated gene unique in ALPPS at 4 hours after operation. We explored the role of hedgehog signaling in the context of accelerated liver regeneration through western blots, immunohistochemistry, and PCR. Our findings show that IHH secretion from stellate cells peaks at 4 hours after ALPPS to activate the translocation of GLI1 into the nucleus, leading to the subsequent upregulation of GLI1's key proliferative target gene, *Ccnd1,* along with increased hepatocyte proliferation. The necessity of IHH in the ALPPS regenerative response was confirmed by the *in vivo* inhibition of IHH through a neutralizing antibody, as well as the replication of its accelerating effects with recombinant IHH protein.

3.8 The JNK pathway

c-Jun NH2-terminal kinases (JNKs) are members of the mitogen-activated kinase (MAPK) family. In the context of tissue regeneration, JNKs have been shown to regulate processes to ensure (i) proper repair of cells sustaining minor damage and (ii) elimination of cells sustaining irreversible damage, including their proper replacement [2]. Three genes, *Mapk8*, *Mapk9*, and *Mapk10* encode JNK proteins JNK1, JNK2, and JNK3 respectively. JNK1 and JNK2 are ubiquitously expressed, while JNK3 is largely restricted to neuronal cells [90]. A wide range of stimuli including UV- and γ-radiation, cytokines, bacterial products, and endoplasmic reticulum stress activate JNKs. Activation of JNKs occurs through a three-tier phosphorylation cascade involving MAPK kinase kinases (MKKKs) and two mitogen-activated protein kinase kinases (MKKs) that dually phosphorylate JNK1 at threonine and tyrosine residues to unfold their activity [91]. JNKs then target c-Jun that dimerizes to form the activating protein-1 (AP-1) transcription factor complex. JNKs additionally phosphorylate

other transcription factors, nuclear hormone receptors, scaffold proteins, ubiquitin ligases, kinases, cytoskeletal proteins, and BCL2 family members, likely contributing to JNKs varying functions [92]. Furthermore, JNK1 and JNK2 share some downstream genes leading to redundant function, although many gene targets differ [93,94].

The JNK signaling cascade promotes proliferation in several ways [2]:

(i) activation of cyclin D1, cyclin E-dependent kinases (CDKs) and transcription factor E2F,

(ii) repression of the tumor suppressor gene p53 and its target gene, p21, and

(iii) direct phosphorylation of Cdc25C to negatively regulate its phosphatase activity and to activate Cdk1 enabling timely control of mitosis onset.

JNK1 seems to mediate the majority of proliferation as with only JNK1- but not JNK2-deficient fibroblasts do proliferation rates decrease [95].

In liver regeneration after sHx, JNK – notably JNK1 - is strongly upregulated, leading to AP-1 activation, the promotion of cyclin D1 expression, and G0 to G1 transition. Inhibiting JNK activity by SP600125, a specific JNK inhibitor, not only impairs liver regeneration but also decreases the expression of cyclin D1 along with reduced hepatocyte proliferation [96].

However, in liver injury, JNK activation prolonged by sustained TNF-α stimulation induces a c-Jun-dependent mitochondrial death pathway, a process involved in the pathophysiology of many types of liver injury such as viral hepatitis or alcoholic liver disease, resulting in cell death-promoting effects [97]. Examples of prolonged JNK expression in liver disease states include increased JNK activity in acetaminophen-induced liver failure in both mice and humans [98], JNK upregulation following ischemia-reperfusion during transplantation that contributes to hepatic reperfusion injury [2], and JNK1's role in fibrosis with the activation of HSCs and the promotion of ASMA expression [99]. Furthermore, chronic activation of JNK has been associated with the development and progression of hepatocellular carcinoma (HCC). Consistent JNK1 activity has been reported to predict a bad outcome in HCC, an aspect that perhaps relates to JNK1 activation secondary to chronic liver injury, an accepted cause of HCC. Although the proapoptotic function of JNK1 has been related to anti-cancerous actions [100], recent evidence indicates a more complex situation, as JNK1 may directly promote the repair of DNA breaks [101]. These observations suggest a disturbed balance between the removal or repair of damaged hepatocytes that underlies JNK1's association with a bad HCC outcome [101]. There is evidence that JNK acts as a key

mediator by promoting an inflammatory environment, although the underlying mechanisms are unclear [102]. Lastly, JNK1 promotes the development of nonalcoholic steatohepatitis (NASH) through various mechanisms including promotion of adiposity and steatosis, increased cell death and increased inflammation, whereas JNK2 exerts cytoprotective effects in fatty liver disease [2].

Therefore, the biological role of JNK can be contradictory and complex depending on the molecular environment. Overall, it seems that short-term activation of JNK exerts cytoprotective effects in the liver, while prolonged JNK activity is associated with cell death and disease.

The JNK pathway in ALPPS

By *in-silico* analysis of possible upstream regulators of IHH, we identified *Mapk8* (JNK1) to be upregulated in stellate cells 1 hour after ALPPS, preceding the 4 hour IHH peak we previously identified. Through specific JNK inhibition with SP600125, we established that JNK1 induces the IHH-GLI1-cyclin D peak after ALPPS as an essential pathway in accelerated regeneration. Furthermore, the use of recombinant IHH after JNK-inhibition rescued the regenerative effects of ALPPS, indicating JNK1 acts through IHH, a hitherto undescribed interaction in a regenerative model.

Manuscripts

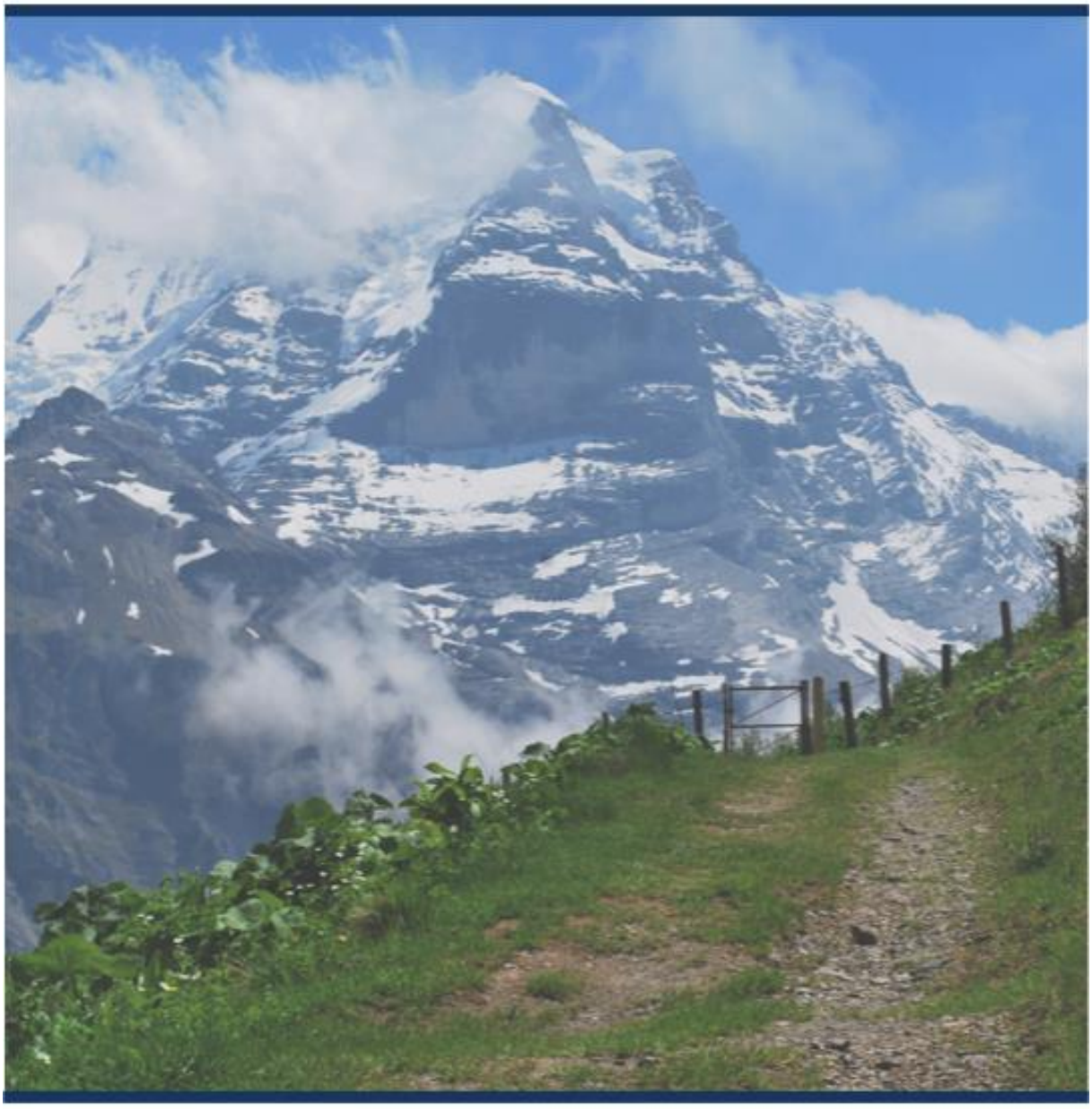

4. Manuscript A

Hedgehog pathway mediates early acceleration of liver regeneration induced by a novel two-staged hepatectomy in mice

Magda Langiewicz[1], Andrea Schlegel[1], Enrica Saponara[1], Michael Linecker[1], Pieter Borger[1], Rolf Graf[1], Bostjan Humar[1]±, Pierre A. Clavien[1]±

± shared senior authorship

[1]Laboratory of the Swiss Hepato-Pancreato-Biliary (HPB) and Transplantation Center, Department of Surgery, University Hospital Zurich, Switzerland.

Published in *Journal of Hepatology*, 2017

Contribution: The first publication of my PhD project. I have conducted most experiments, data acquisition, and analyses with a few exceptions in the revision of the paper. I contributed to experimental design under the supervision of Dr. Humar, the data interpretation, and in writing the manuscript.

Hedgehog pathway mediates early acceleration of liver regeneration induced by a novel two-staged hepatectomy in mice

Authors: Magda Langiewicz[1], Andrea Schlegel[1], Enrica Saponara[1], Michael Linecker[1], Pieter Borger[1], Rolf Graf[1], Bostjan Humar[1*], and Pierre A. Clavien[1*].

*shared senior authorship

[1]Laboratory of the Swiss Hepato-Pancreato-Biliary (HPB) and Transplantation Center, Department of Surgery, University Hospital Zurich, Raemistrasse 100, Zurich, CH-8091, Switzerland.

Corresponding author: Pierre-Alain Clavien, Department of Surgery & Transplantation, University Hospital Zurich, Raemistrasse 100, CH-8091 Zurich, Phone: +41 44 255 3300, email: clavien@access.uzh.ch

Abbreviations: ALPPS: Associating Liver Partition and Portal Vein Ligation Surgery, PVL: Portal Vein Ligation, Ts: Transection, LLLx: Left lateral lobe resection, Ihh: Indian hedgehog, pH3: phosphohistone 3, SFSS: small-for-size-syndrome, TSH: two-stage hepatectomy, FLR: functional liver remnant.

Abstract

Background & Aims: ALPPS, a novel two-staged approach for the surgical removal of large/multiple liver tumors, combines portal vein ligation (PVL) with parenchymal transection. This causes acceleration of compensatory liver growth, enabling faster and more extensive tumor removal. We sought to identify the plasma factors thought to mediate the regenerative acceleration following ALPPS.

Methods: We compared a mouse model of ALPPS against PVL and additional control surgeries (n=6 per group). RNA deep sequencing was performed to identify candidate molecules unique to ALPPS liver (n=3 per group). Recombinant protein and a neutralizing antibody combined with appropriate surgeries were used to explore candidate function in ALPPS (n=6 per group). Indian hedgehog (IHH/Ihh) levels were assessed in human ALPPS patient plasma (n=6).

Results: ALPPS in mouse confirmed significant acceleration of liver regeneration relative to PVL ($p<0.001$). *Ihh* mRNA, coding for a secreted ligand inducing hedgehog signaling, was uniquely upregulated in ALPPS liver ($p<0.001$). Ihh plasma levels rose 4h after surgery ($p<0.01$), along with hedgehog pathway activation and subsequent cyclin D1 induction in the liver. When combined with PVL, Ihh alone was sufficient to induce ALPPS-like acceleration of liver growth. Conversely, blocking Ihh markedly inhibited the accelerating effects of ALPPS. In the small cohort of ALPPS patients, IHH tended to be elevated early after surgery.

Conclusions: Ihh and hedgehog pathway activation provide the first mechanistic insight into the acceleration of liver regeneration triggered by ALPPS surgery. The accelerating potency of recombinant Ihh, and its potential effect in human ALPPS may lead to a clinical role for this protein.

Lay Summary: ALPPS, a novel two-staged hepatectomy, massively accelerates liver regeneration, thereby helping treat patients with otherwise unresectable liver tumors. The molecular mechanisms behind this accelerated regeneration are unknown. Here, we elucidate that Indian hedgehog, a secreted ligand important for fetal development, is a crucial mediator of the regenerative acceleration triggered by ALPPS surgery

Keywords: associating liver partition and portal vein ligation for staged hepatectomy, compensatory hypertrophy, contralateral growth, accelerator, morphogenic ligand

Introduction

The liver is unique with regards to its regenerative capacity. Its ability to regrow after tissue loss has permitted the surgical removal of large or multiple liver tumors with curative intent. Physiological limits to liver regeneration nevertheless exist. When the functional liver remnant is too small, the liver cannot recover vital function due to deficient hepatocyte proliferation [1, 2]. In the clinic, resection-induced liver failure is known as the small-for-size syndrome (SFSS) and represents the most frequent cause of death due to liver surgery [3, 4].

To reduce the risk of SFSS and to expand the application of surgery, two-staged hepatectomies (TSHs) have been developed. In a first step, the portal veins of one (i.e. the diseased) liver section are occluded, causing compensatory growth of the non-occluded (i.e. healthy) part. The thereby increased liver volume enables extended liver resection in a second step. While the combination of portal vein ligation (PVL) with later resection have become standard strategies [4,5], liver growth after PVL is slow and sometimes insufficient to enable TSH completion or prevent SFSS [6]. Even if successful, several months can pass until resection can be performed, increasing the likelihood of disease progression and complicating surgery due to developing tissue adhesion [7].

In the past few years, a novel two-staged approach, associating liver partition and portal vein ligation for staged hepatectomy (ALPPS), has been designed. This procedure has the potential to avoid most of the drawbacks associated with conventional TSHs [8, 9]. ALPPS differs from conventional TSHs in that step one combines PVL with the additional transection (an *in situ* split) along the demarcation between the occluded and non-occluded liver. Intriguingly, the PVL-transection combination causes an unprecedented acceleration of compensatory liver growth [8, 9]. Within 9 days after PVL-transection, an average 74% volume increase of the non-occluded lobe has initially been reported [9], greatly reducing the time interval to resection. Extrapolated liver growth rates after ALPPS may be up to 11 times higher than after PVL [7]. In other words, ALPPS enables surgery in patients otherwise deemed as unresectable due to marginal liver remnants with high SFSS risk [9, 7]. Whereas optimal conditions for the application of ALPPS are still being defined, a marginal size of the liver remnant appears to be of small concern for ALPPS [10].

The acceleration of liver regeneration observed after ALPPS inquires for the nature of underlying mechanisms. Consequently, we have developed the first animal model of ALPPS that is based on the adaptation of human surgery to mouse liver architecture [11]. Akin to the human operation, PVL plus transection in mice massively accelerates the regenerative speed compared to PVL alone. When PVL-transection is completed as a first step, the second step (i.e. extended resection) is performed 48h later, leading to completed regeneration within 4 days despite starting from a remnant with only 10% of the original liver volume [11]. In comparison, regeneration after standard 70%-hepatectomy (leaving a 30% remnant) needs about a week for completion in mice, while a 90%-hepatectomy is lethal [1, 2]. Intriguingly, plasma obtained from mice subjected to ALPPS step 1 comparably accelerates regeneration when injected into mice subjected to PVL only [11]. Therefore, ALPPS in mice seems to trigger unknown circulating factors that mediate regenerative acceleration and hence might be of therapeutic interest.

This study was set out to obtain a first insight into the molecular mechanisms underlying ALPPS-triggered acceleration of liver regeneration. We sought to uncover a plasma factor that is induced by ALPPS step 1 to accelerate PVL-mediated liver regeneration. By using an unbiased expression profiling approach in comparing ALPPS step 1 with PVL, transection, and control surgery, we identified Indian hedgehog (Ihh) as a plausible candidate. We then explored the role of Ihh in the acceleration of PVL-induced regeneration and tested the dependency of ALPPS on circulating Ihh. Altogether, we describe circulating Ihh as a key component mediating early acceleration of liver regeneration following ALPPS surgery.

Materials and Methods

Animals

All animal experiments were performed in accordance with Swiss Federal Animal Regulations and approved by the Veterinary Office of Zurich. Male C57Bl/6 mice (Envigo, Horst, NL) aged 10-12 weeks kept on a 12-hour day/night cycle with free access to food and water were used.

Animal surgery and treatment

To mimic human ALPPS surgery in mice, 90% PVL was performed leaving a 10% functional remnant consisting of the left and a part of the right middle lobe. Then, a partial 80% transection was done through the middle lobe along the demarcation line of the occluded/non-occluded parenchyme. The left lateral lobe (LLL, 25% of liver volume) was also resected to simulate the cleaning of the liver from smaller tumors as often done in human ALPPS (Fig. 1A). Left lateral lobe resection (LLLx) does not induce significant regeneration in mouse and is comparable to sham. Details on isoflurane anesthesia, buprenorphine analgesia, ALPPS procedures, and the control operations (90% PVL, 80% transection, LLLx, and sham laparotomy) have been described [11]. After surgery, animals were allowed to recover on a warming pad in a separate cage until completely conscious. Standard (68%) hepatectomy was performed as described [1]. Animals were weighed before surgery and at sacrifice, where weight of resected and remnant liver was recorded. Tissue was formalin fixed or snap frozen, while plasma was stored at -80°C for analysis.

Recombinant Ihh (200 ng/kg, 160µl final volume; R&D, 1705-HH-025/CF Minneapolis, MN) or PBS was injected into the vena cava right after PVL. Ihh antibody (4ug/kg, 160µl final volume; R&D MAB8048) or PBS was injected via tail vein one hour before operation.

Liver regeneration

Liver regeneration was assessed by the percentage of functional-liver-remnant-to-the-body weight ratio (FLR/BW) derived from six animals per group and time point.

Quantitative real-time PCR

Total RNA was extracted from 50 mg of tissue using Trizol reagent following provided instructions (Invitrogen, Basel, Switzerland). RNA quality/quantity was assessed using a spectrophotometer and converted to cDNA briefly as follows: a reaction was prepared with the Taqman Fast Universal PCR Master Mix, no AmpErase UNG (ThermoFischer Scientific, cataloque number 4352042), (4µl in a 20 µl reaction with 1 µg RNA). A 5 min incubation at room temperature was performed, followed by an incubation at 42°C for 30 min, and lastly an incubation at 85°C for 5 min. qPCR was performed with two replicates/sample on cDNA (Thermo Script reverse transcription PCR System, Invitrogen) using an ABI Prism 7500 Sequence Detector system (PE Applied Biosystems Rotkreuz, Switzerland). Taqman gene expression assays (Applied Biosystems) are listed in Supplementary Table 1. Results represent

mean fold induction ($2^{-\Delta Ct}$) ±SD relative to the normalization control *18S rRNA* [1].

Immunohistochemistry

Archived liver sections (3 μm) were stained (antibodies in Supplementary Table 2) using the Dako Autostainer Link48 Instrument and the iView 3,3-diaminobenzidine (DAB) kit (Dako Denmark A/S). Antibodies are listed in Supplementary Table 2. Quantification of Ki67- and pH3-positive hepatocytes was done by blinded manual counting in ten random visual fields (20x).

RNA deep sequencing

Total liver RNA prepared by DNA Column Clean-up (Qiagen, Basel, CH) was deep sequenced by the Functional Genomics Center Zurich using poly-A selection on the Illumina Hiseq 2500. A QC report was generated and two-group analyses (comparing all procedures normalized to sham) were performed to retrieve differential gene expression data. Data were analyzed for pathways and genes unique to ALPPS through Metacore (filter criteria, $p<0.05$ and $\log_2$ratio>4). All data have been deposited to the European Nucleotide Archive (ENA) under the accession number PRJEB15593.

Western blotting

Blotting was performed as described [1]. Antibodies are listed in Supplementary Table 2. NE-PER Nuclear and Cytoplasmatic Extraction reagents (Thermo Fisher Scientific, Waltham, MA, PK207589) were used to isolate subcellular fractions, with their separation ascertained through β-tubulin (cytoplasmic) and lamin B1 (nuclear) blotting.

Hedgehog ligand levels

Ihh/IHH and sonic hedgehog (Shh) protein levels were measured by ELISA (mouse Ihh: Cusabio, CSB-E16517m; human IHH: CSB-E12007h; mouse Shh: R&D, MSH00).

Human samples

EDTA-blood was obtained from ALPPS patients (n=6) directly (t=0, baseline) or 2h, 24h, and 48h after transection (step 1). Plasma was stored at -80°C. The use of human samples was approved by the cantonal ethics committee Zürich (KEK-ZH-Nr. 2015-057). Informed consent was obtained from all patients. See Supplementary Table 3 for patient description.

Statistical Analysis

Data are expressed as mean ±SD. Differences between groups (n=6/group unless for expression profiling where n=3/group) were determined using unpaired, two-tailed t tests assuming unequal variance via GraphPad Prism v4.0 (GraphPad, San Diego CA), with significance set at $P<0.05$. Analyses were blinded.

Results

The ALPPS model of accelerated liver regeneration

To study mechanisms underlying the ALPPS-associated acceleration of liver regeneration, we used our recently developed mouse model of ALPPS [11]. Liver weight gain induced by ALPPS (here specifically referred to PVL-transection-LLLx, see Fig. 1A and Methods for explanation) was compared to appropriate control surgeries (PVL, transection, LLLx, sham laparotomy) in order to ascertain acceleration of regeneration (see Supplementary Fig 1. for a comparison with hepatectomy). All procedures similarly affected body weight (Fig. 1A). LLLx alone did not induce significant liver weight regain, akin to transection only. As expected, PVL led to a steady weight gain, while ALPPS markedly accelerated regeneration relative to PVL (Fig. 1B). Acceleration was particularly evident during the first 12-24h, and ALPPS elevated the number of hepatocytes positive for Ki67 (cycling cells) and bold pH3 (marking mitotic cells [1]) at 4h and particularly 8h compared to PVL (Fig 1B). Next, we assessed the expression of key cell cycle molecules, the cyclins, most of which were elevated at 8h after ALPPS. *Ccnd1* mRNA (encoding cyclin D1, a crucial promoter of the hepatocyte cell cycle [12]) displayed an ALPPS-specific peak at 8h (Fig. 1C) akin to pH3 counts, while the cell cycle inhibitor p21 [1] was downregulated (Fig. 1D, see Supplementary Fig. 2 for immunoblot bands) in ALPPS vs PVL. At 12h however, p21 was upregulated in ALPPS and associated with a drop in Ki67/pH3 counts, perhaps due to a small negative feedback to prevent exuberant proliferation in response to the massive regenerative activity elicited through ALPPS [13]. Together, these findings indicate that ALPPS accelerates liver weight regain and hepatocellular cell cycle at early times after surgery. Therefore, key pathways must operate early after ALPPS to accelerate regeneration.

Indian hedgehog as a candidate plasma factor associated with ALPPS

To obtain unbiased insight into potential ALPPS-associated molecular alterations in the liver, we deep-sequenced hepatic RNA during the first 12h after ALPPS, PVL, transection, LLLx, and sham operation. A distinct gene expression profile was evident for ALPPS as early as 4h post operation (Fig. 2A, Supplementary Fig. 3). At this time point, MetaCore analysis (Fig. 2B) revealed two pathways unique to ALPPS, the "TGF-beta-dependent induction of EMT via MAPK" ($P=5.9^{-14}$, false discovery rate [FDR]$=3.18^{-12}$) and the "Sirtiun6 regulation and function" ($P=1.17^{-13}$, $FDR=5.48^{-12}$) pathway (Supplementary Table 4). MetaCore analysis further revealed 50 independent genes unique to ALPPS (Fig. 2C, Supplementary Table 5). The only gene common to both the ALPPS-specific pathways and independent genes was *Ihh* (log_2ratio=6.0, $FDR=2.96^{-30}$), a secreted hedgehog ligand. PCR revealed an ALPPS-specific *Ihh* mRNA peak at 4h, while hepatic protein levels were reduced (Fig. 2D). Plasma protein levels however peaked at 4h after ALPPS (Fig. 2D), together suggesting newly produced Ihh was not being retained within cells but immediately secreted into plasma. Thus, Ihh may fit the role of a postulated plasma factor released through ALPPS. No ALPPS-specific changes were detected for other hedgehog ligands (desert hedgehog (Dhh), Supplementary Fig. 4). Non-parenchymal cells, particularly stellate cells, were positive for Ihh across samples (Fig. 2E,

Supplementary Fig 5), suggesting the ligand is sourced from the stellate population.

Ihh pathway activity is elevated after ALPPS

To substantiate Ihh as a candidate behind ALPPS-accelerated liver regeneration, we assessed hedgehog pathway components in liver. Ihh binds to its receptor Ptch1, relieving inhibition of Smo, which then causes nuclear translocation of the Gli transcription factors, the downstream effectors of hedgehog signaling [14]. No differences between ALPPS and PVL were observed for *Ptch1* and *Smo* expression, while *Gli1* and *Gli2* alterations showed significant differences. However, *Hhip* (encoding the hedgehog ligand inhibitor) was downregulated at 4h and particularly 8h post ALPPS, relative to PVL/transection (Fig. 3A). Immunoblots on cytosolic and nuclear fractions revealed that nuclear Gli1, but not Gli2, was upregulated at 4h in ALPPS vs PVL/transection. Immunofluorescence localized upregulation of Gli1 to hepatocyte nuclei of ALPPS liver (Fig. 3B). At 8h, Gli1 was not elevated in ALPPS nuclear fractions. Unlike in PVL/transection however, the main Gli1 signal remained in hepatocyte nuclei of ALPPS liver (Fig. 3B). Accordingly, both the Gli1 target cyclin D1 (Supplementary Fig. 6; Fig. 1C for mRNA) and mitotic counts (Fig. 1B) peaked at 8h, associating hedgehog activity in hepatocytes with their proliferation. Together with *Hhip* downregulation at 4-8h, Ihh signaling in liver may hence be conducive to acceleration of liver regeneration following ALPPS.

Recombinant Ihh accelerates PVL-induced liver regeneration

If Ihh mediates acceleration of regeneration after ALPPS, combining Ihh with PVL should mimic the effects of ALPPS. Mouse recombinant Ihh was administered after PVL instead of transection. When assessing body weight after injection, no differences were observed between PVL-Ihh and PVL-PBS animals. In contrast, liver weight was significantly elevated after PVL-Ihh compared to PVL-PBS - akin to levels after ALPPS surgery, albeit with different kinetics (Fig. 4A). The assessment of proliferation markers revealed increasing pH3 counts, with elevations particularly evident at 12h after PVL-Ihh (Fig. 4B). qPCR suggested relative *Gli1* and *Ccnd1* upregulation as well as *Hhip1* downregulation in PVL-Ihh liver over time (Fig. 4C). *Gli2* (Fig. 4C), *Ptch* and *Smo* were largely unaffected by Ihh (Fig. 4C). Nuclear protein levels of Gli1, but not Gli2, were upregulated through Ihh relative to PBS treatment, however at times later than 4h (Fig. 4D). Accordingly, cyclin D1 protein levels (Fig. 4E) and hepatocellular expression (Supplementary Fig. 7) were elevated after PVL-Ihh particularly at 12h. Altogether, the combination of PVL with Ihh has effects on regeneration similar to ALPPS, albeit in a delayed manner. These findings identify Ihh as an accelerator of PVL-induced liver growth.

Ihh neutralization deaccelerates ALPPS-induced liver regeneration.

If Ihh mediates accelerated regeneration after ALPPS, blocking Ihh should inhibit the ALPPS effects. A neutralizing antibody against Ihh was injected 1h prior to ALPPS surgery. Compared to PBS injection, body weight remained unaffected. Instead, Ihh neutralization reduced liver weight gain after ALPPS, although not to levels seen after PVL only (Fig. 5A). Proliferation parameters confirmed the deaccelerating effect of Ihh inhibition, illustrated through the suppression of the 8h-pH3 peak seen after ALPPS (Fig. 5B). Relative to PBS, αIhh upregulated *Hhip* but lowered *Gli1/2* and *Ccnd1* expression in liver of ALPPS mice (Fig. 5C). Moreover, nuclear levels of Gli1, but not Gli2, were reduced over time through αIhh-treatment (Fig. 5D). Finally, both cyclin D1 levels (Fig. 5E) and hepatocyte expression (Supplementary Fig. 7) were lowered in the ALPPS-αIhh relative to the ALPPS-PBS group. We conclude Ihh is an important mediator of the ALPPS effects.

Combined with our other data, these findings indicate that the elevations in plasma Ihh observed after ALPPS are central to the acceleration of liver regeneration achieved through this surgical technique.

IHH is induced in human ALPPS

Hedgehog signaling is conserved among animals [15]. To estimate whether ALPPS-induced Ihh elevations in mice are of human relevance, we measured plasma IHH levels from six consecutive patients having undergone ALPPS surgery at our clinic. During the first 24h, IHH levels were elevated over baseline levels at the time of surgery (Fig. 6). Given the slower regenerative pace in man relative to mouse, these observations are consistent with an early upregulation of IHH plasma levels in patients subjected to ALPPS surgery. No correlation was detected between IHH levels and postoperative liver volume or complication scores (IHH plasma levels correlated to % increase FLR, $R^2 = 0.1047$; IHH plasma levels correlated to comprehensive complication index (CCI) scores, $R^2 = 0.4973$), however analysis was hampered through the small and heterogeneous patient group (Supplementary Table 3). There was no 'control surgery' in the human patients, due to the nature of the clinical trial from which the tissue samples were obtained. Therefore, no statistical calculation were carried out.

Discussion

The development of ALPPS surgery has pushed the limits of resectability in liver surgery. The need to keep a certain remnant volume for liver to recover after tissue resection is a serious constraint that hinders the management of liver malignancy. The ALPPS approach illustrates that a conceptually simple combination of existing surgical techniques with a novel maneuver can unleash biological processes which are surprising in their extent. In other words, ALPPS demonstrates that the intrinsic capacity of liver to regenerate is larger than we think, but usually is cabined, likely to gain in stability and reliability needed for long-term function.

Mechanistically, liver regeneration after simple resection is highly complex [16]. How PVL leads to contralateral liver growth is ill-understood [17], and how regeneration is then accelerated by a transection step is unknown. The observation, however, that plasma obtained from ALPPS mice can mediate acceleration [11], pointed to circulating molecules being responsible for the effect of ALPPS. Here, we identify Ihh as one key plasma factor that is triggered by ALPPS step 1 to mediate early acceleration of liver regeneration.

Following an explorative transcriptome profiling approach, we found *Ihh* as the most likely gene to be specifically induced by ALPPS in liver. Its hepatic mRNA levels peak at 4h after surgery, paralleled by increases in Ihh plasma levels, consistent with Ihh acting as an auto/paracrine ligand following its secretion from stellate cells [14]. The time after the Ihh peak (4-8h) is associated with a marked increase in proliferation markers in ALPPS relative to PVL, along with an ALPPS-specific peak in the expression of *Ccnd1,* crucial for the hepatocellular cell cycle progression [12]. Cyclin D1 is a target of hedgehog signaling and required for successful liver regeneration after tissue loss [18, 19, 12], consistent with a key role for Ihh in the ALPPS effects. Although the levels of plasma Ihh and of nuclear Gli1 (the hedgehog effector inducing *Ccnd1*) in hepatocytes were highest at 4h after ALPPS, cyclin D1 and mitoses (pH3) did not peak before 8h. At 8h however, the nuclear Gli1 signal remained localized to hepatocytes particularly in ALPPS liver, despite similar overall expression levels to PVL and transection. On the other hand, the hedgehog ligand inhibitor *Hhip* was most downregulated in ALPPS at 8h relative to PVL/transection, providing an explanation for the persistence of

hepatocellular Gli1 activity at this time [14]. These findings suggest an ALPPS-specific Ihh wave induces sustained hedgehog activity in hepatocytes, eventually causing cyclin D1 upregulation to promote cell cycle progression. Therefore, ALPPS-triggered hedgehog pathway activity in hepatocytes appears to rely not only on the level of Gli1, but also on the duration and location of Gli1 activity. The associated proliferative peak at 8h is then likely to lead to the rapid gain in liver weight early post-surgery. Cellular hypertrophy or lipid accumulation might contribute to weight gain, however, ALPPS causes neither hypertrophy (Supplementary Fig. 8) nor significant steatosis (Fig. 1B, H&E) at early times.

To establish a role for Ihh in ALPPS, we injected recombinant protein into PVL mice. Indeed, regeneration was accelerated and accompanied by increases in proliferation, Gli1 and cyclin D1 along with *Hhip* downregulation. Of note, the response to recombinant Ihh was somewhat delayed compared to ALPPS. A likely explanation for this delay is that injection of recombinant Ihh cannot fully mimic the ALPPS-triggered Ihh wave, as both local Ihh concentrations and protein modifications will differ between ALPPS and Ihh injection [20]. Nonetheless, our findings demonstrate that plasma Ihh alone is sufficient to push regeneration induced by PVL. Conversely, ALPPS markedly lost its accelerating effects - again paralleled by according changes in proliferation and hedgehog components - when circulating Ihh was blocked, confirming that the regenerative potential unleashed by ALPPS strongly depends on the elevations in Ihh. However, some acceleration was still evident after Ihh neutralization, suggesting ALPPS induces additional factors with a pro-regenerative effect. In our screen, we did not detect ALPPS-specific changes in molecules classically involved in liver regeneration, such as Hgf, Egf or Tnf (Supplementary Fig. 9). However, we have already reported very early increases in plasma Il-6 after ALPPS surgery, suggesting this molecule may contribute to the ALPPS effects [11]. Altogether, our findings reveal a key role for Ihh in the acceleration of PVL-induced liver growth. Future research will need to explore the nature and kind of additional factors that participate in the accelerating effects of ALPPS.

Hedgehog signaling is known to be required for liver regeneration after both chemical insults and resection. Interestingly, the pathway is thought to operate in activated stellate cells that then promote parenchymal proliferation [21, 22]. At the Ihh mRNA/plasma peak after ALPPS, we observed Ihh staining in non-parenchymal cells, often displaying typical stellate morphology (Supplementary Fig. 5). Hence, ALPPS appears to trigger Ihh production in stellate cells but not hepatocytes [14]. Additional contributions to the elevations in circulating Ihh perhaps might come from other non-parenchymal cells or from the extracellular matrix, which can release the ligand during regenerative remodeling [23]. Early after hepatectomy, hedgehog signaling first acts in an autocrine way to promote the conversion of stellate cells into epithelial progenitors able to repopulate a part of the lost parenchymal mass [21, 22]. At 48h post-hepatectomy, signaling likewise becomes paracrine, resulting in Gli nuclear accumulation in hepatocytes to promote parenchymal reconstitution directly from epithelium [24]. After ALPPS, Gli1 is observed in nuclei of hepatocytes and stellate cells already at 4h, suggesting that the Ihh wave either simultaneously induces autocrine and paracrine signaling, or greatly accelerates the events observed after hepatectomy [21, 22, 24]. Therefore, while hedgehog signaling may not be specific to ALPPS, the timing of pathway activation through early Ihh release is unique to this procedure. Whether hedgehog signaling after ALPPS otherwise operates in analogy to hepatectomy or induces distinct processes will require further study. Moreover, the regenerative mechanisms associated with PVL alone will need clarification to appreciate

how Ihh signaling accelerates ALPPS-associated liver growth. However, our findings are consistent with the view that stellate cells are the main conveners of hedgehog signaling associated with ALPPS-triggered regeneration, akin to early regenerative responses after other liver insults.

The general involvement of hedgehog activity in various processes related to tissue remodeling, such as in response to growth or injury [14], portray Ihh signaling a plausible mechanism to contribute to ALPPS-enforced regeneration. Currently it is unclear how ALPPS may induce the Ihh-dependent cascade. Combining PVL with LLLx has no accelerating effect, because for ALPPS, the left lateral lobe is being occluded anyway before its resection. On the other hand, transection is the key factor differentiating ALPPS from PVL and would be an obvious candidate. Liver injury induced by transection conceivably might induce a repair response including Ihh secretion. Plasma Ihh levels did rise over time after transection only, however to much lower levels than following ALPPS, and without upregulating *Ihh* mRNA (Fig. 2). Therefore, transection is not the cause of active Ihh production seen after ALPPS (but may contribute perhaps by causing release of matrix-bound Ihh). Rather, the combination of PVL with transection appears to elicit a synergistic effect, with ALPPS triggering much higher Ihh plasma levels than the sum of Ihh seen after each procedure alone (Fig. 2). How the combination of occlusion and injury is leading to Ihh secretion will require further study. Injury, however, seems to be an important component, and even injection alone had some accelerating effect on PVL-induced regeneration (see PVL+PBS/Ihh versus PVL/ALPPS, Fig. 4A). Ihh signaling indeed is the first molecular insight into ALPPS-related mechanisms, and much more work will be needed to clarify triggers, contributing sources, and the various cellular crosstalks that underlie Ihh-dependent acceleration of liver regeneration in response to ALPPS.

The powerful promotion of regenerative speed seen in PVL mice after Ihh injection suggests therapeutic potential for this protein. In support of such potential, we observed early IHH elevations in ALPPS patients. Future studies should address specific clinical situations where hedgehog activation might be of benefit. At present, IHH may be of value for liver patients in need of but unsuitable - e.g. due to a critical health state - for major surgery such as ALPPS step 1. Given that the usual indication for resections is malignancy, the well-known cancer-promoting activities of hedgehog signaling [25] will have to be carefully balanced against the benefits for individual patients. In this regard, a single therapeutic IHH injection might have a small enough impact on neoplasia to be applied to patients at high risk of death due to unresectable disease. However, the tumorigenic risks associated with an IHH bolus are currently unknown and will need meticulous assessment in the settings of PVL. Of note, recent (but still limited) numbers suggests that ALPPS - as we show inducing IHH in patients - is not associated with higher recurrence rates than PVL [7] despite existing concerns [26]. Clearly, the tumorigenic potential of an IHH bolus in the settings of PVL will need to be addressed experimentally.

In summary, we report the first insight into the molecular principles underlying the acceleration of liver regeneration through ALPPS. The elevations in circulating Ihh early after ALPPS are both sufficient to accelerate compensatory liver growth following occlusion and required for ALPPS to develop full effect. Our findings highlight the dependency of ALPPS on humoral factors and provide a basis for a pharmaceutical promotion of compensatory liver growth in the clinic. The identification of Ihh as an accelerating factor is a first step in deciphering the mechanistic processes underlying ALPPS and in exploring according therapeutics for the expanded application of liver surgery.

Grant support

This study was funded by the Clinical Research Priority Program (CRPP) from the University of Zurich “non-resectable liver tumors – from palliation to cure” and the Swiss National Science Foundation (S-87002-09-01).

Authors’ contributions

Experimental design: ML, BH. Data acquisition and analyses: ML, AS, ES, ML, PB, BH. Data interpretation: BH, ML, PB, RG. Study concept and design: BH. Manuscript writing & critical revision: BH, ML, PAC. Funding: PAC, BH, RG. All authors approved the final version.

Acknowledgements

We would like to thank Marcel A. Schneider for collecting patient information as well as Udo Ungethüm, Ursula Süss, Eleanora Maurizio, and Pia Fuchs for the excellent technical assistance.

References

1. Lehman K, Tschuor C, Rickenbacher A, Jang JH, Oberkofler CE, Tschopp O, et al. Liver failure after extended hepatectomy in mice is mediated by a p21-dependent barrier to liver regeneration. Gastroenterology 2012;143:1609-1619.
2. Tschuor C, Kachaylo E, Limani P, Raptis DA, Linecker M, Tian Y, et al. Constitutive androstane receptor (Car)-driven regeneration protects liver from failure following tissue loss. J Hepatol 2016; in press
3. Clavien PA, Oberkofler C, Raptis DA, Lehmann K, Rickenbacher A, El-Badry A. What is critical for liver surgery and partial liver transplantation: size or quality? Hepatology 2010;52:712-729.
4. Clavien PA, Petrowsky H, DeOliveira M, Graf R. Strategies for safer liver surgery and partial liver transplantation. N Engl J Med 2007;356:1545-1559.
5. Jaeck D, Oussoultzoglou E, Rosso E, Greget M, Weber JC, Bachellier P. A two-stage hepatectomy procedure combined with portal vein embolization to achieve curative resection for initially unresectable multiple and bilobar colorectal liver metastases. Ann Surg 2004;240:1037-1049.
6. Donati M, Stavrou GA, Oldhafer KJ. Current position of ALPPS in the surgical landscape of CRLM treatment proposals. World J Gastroenterol 2013;19:6548-6554.
7. Schadde E, Ardiles V, Slankamenac K, Tschuor C, Sergeant G, Amacker N, et al. ALPPS offers a better chance of complete resection in patients with primarily unresectable liver tumors compared with conventional-staged hepatectomies: results of a multicenter analysis. World J Gastroenterol 2014;38:1510-1519.
8. de Santibañes E, Clavien PA. Playing Play-Doh to prevent postoperative liver failure: the "ALPPS" approach. Ann Surg 2012;255:415-417.
9. Schnitzbauer AA, Lang SA, Goessmann H, Nadalin S, Baumgart J, Farkas SA, et al. Right portal vein ligation combined with in situ splitting induces rapid left lateral liver lobe hypertrophy enabling 2-staged extended right hepatic resection in small-for-size settings. Ann Surg 2012;255:405-414.
10. Schadde E, Raptis DA, Schnitzbauer AA, Ardiles V, Tschuor C, Lesurtel M, et al. Prediction of Mortality After ALPPS Stage-1: An Analysis of 320 Patients From the International ALPPS Registry. Ann Surg 2015;262:780-785.
11. Schlegel A, Lesurtel M, Melloul E, Limani P, Tschuor C, Graf R, et al. ALPPS: from human to mice highlighting accelerated and novel mechanisms of liver regeneration. Ann Surg 2014;260:839-846.
12. Hanse EA, Nelsen CJ, Goggin MM, Anttila CK, Mullany LK, Berthet C, et al.

Cdk2 plays a critical role in hepatocyte cell cycle progression and survival in the setting of cyclin D1 expression in vivo. Cell Cycle. 2009;8(17):2802-9.
13. Auer KL, Park JS, Seth P, Coffey RJ, Darlington G, Abo A, McMahon M, Depinho RA, Fisher PB, Dent P. Prolonged activation of the mitogen-activated protein kinase pathway promotes DNA synthesis in primary hepatocytes from p21Cip-1/WAF1-null mice, but not in hepatocytes from p16INK4a-null mice. Biochem J 1998;336:551-60.
14. Omenetti A, Choi S, Michelotti G, Diehl AM. Hedgehog signaling in the liver. J Hepatol 2011;54:366-373.
15. Ryan KE, Chiang C. Hedgehog secretion and signal transduction in vertebrates. J Biol Chem 2012;287:17905-17913.
16. Michalopoulos GK. Liver regeneration. J Cell Physiol 2007;213:286-300.
17. Tashiro S. Mechanism of liver regeneration after liver resection and portal vein embolization (ligation) is different? J Hepatobiliary Pancreat Surg 2009;16:292-299.
18. Katoh Y, Katoh M. Hedgehog target genes: mechanisms of carcinogenesis induced by aberrant hedgehog signaling activation. Curr Mol Med 2009;9:873-886.
19. Patil MA, Zhang J, Ho C, Cheung ST, Fan ST, Chen X. Hedgehog signaling in human hepatocellular carcinoma. Cancer Biol Ther 2006;5:111-117.
20. Briscoe J, Therond PP. The mechanisms of Hedgehog signaling and its roles in development and disease. Nat Rev Mol Cell Biol 2013;14:416-429.
21. Michelotti GA, Xie G, Swiderska M, Choi SS, Karaca G, Krüger L, et al. Smoothened is a master regulator of adult liver repair. J Clin Invest 2013;123:2380-2394.
22. Swiderska-Syn M, Syn WK, Xie G, Krüger L, Machado MV, Karaca G, et al. Myofibroblastic cells function as progenitors to regenerate murine livers after partial hepatectomy. Gut 2014;63:1333-1344.
23. Bhave VS, Mars W, Donthamsetty S, Zhang X, Tan L, Luo J, et al. Regulation of liver growth by glypican 3, CD81, hedgehog, and Hhex. Am J Pathol 2013;183:153-159.
24. Swiderska-Syn M, Xie G, Michelotti GA, Jewell ML, Premont RT, Syn WK, et al. Hedgehog regulates Yes-associated protein 1 in regenerating mouse liver. Hepatology 2016; in press.
25. Amakye D, Jagani Z, Dorsch M. Unraveling the therapeutic potential of the Hedgehog pathway in cancer. Nat Med 2013;19:1410-1422.
26. Oldhafer KJ, Donati M, Jenner RM, Stang A, Stavrou GA. ALPPS for patients with colorectal liver metastases: effective liver hypertrophy, but early tumor recurrence. World J Surg 2014;38:1504-1509

Figures

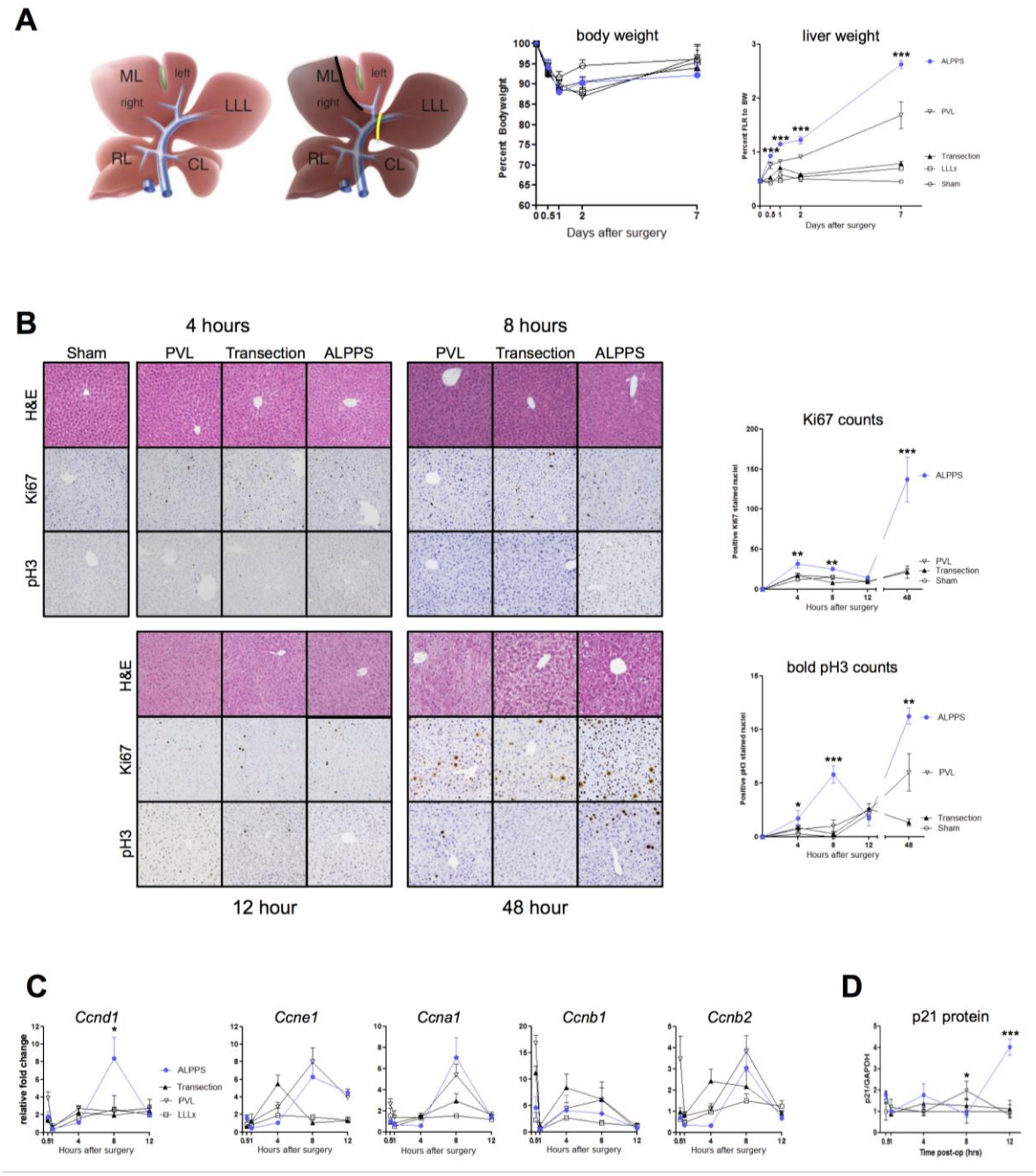

Figure 1. Acceleration of compensatory liver growth through ALPPS. *(A)* ALPPS surgery in mouse and its effects on liver re-growth. Gray shading indicates occluded liver parts following PVL. The black line indicates the transection step, and the yellow line the LLLx step. Percent body weight and liver weight regain (expressed as percent functional-liver-remnant-to-body-weight-ratio) after surgery are shown in the left and right graph, respectively. *(B)* H&E, Ki67, and pH3 staining of liver after surgery. Graphs show counts of hepatocytes positive for Ki67 or bold pH3. Histology (H&E) for sham was consistent over time. *(C)* Hepatic gene expression of *Ccnd1*, *Ccne1*, *Ccna2*, *Ccnb1*, and *Ccnb2* after surgery. *(D)* Hepatic protein expression (normalized to Gapdh) of p21 after surgery. N = 6/group. t-test, *p <0.05, ** p <0.01. ***p <0.001. Significances refer to ALPPS vs. PVL comparison unless otherwise stated.

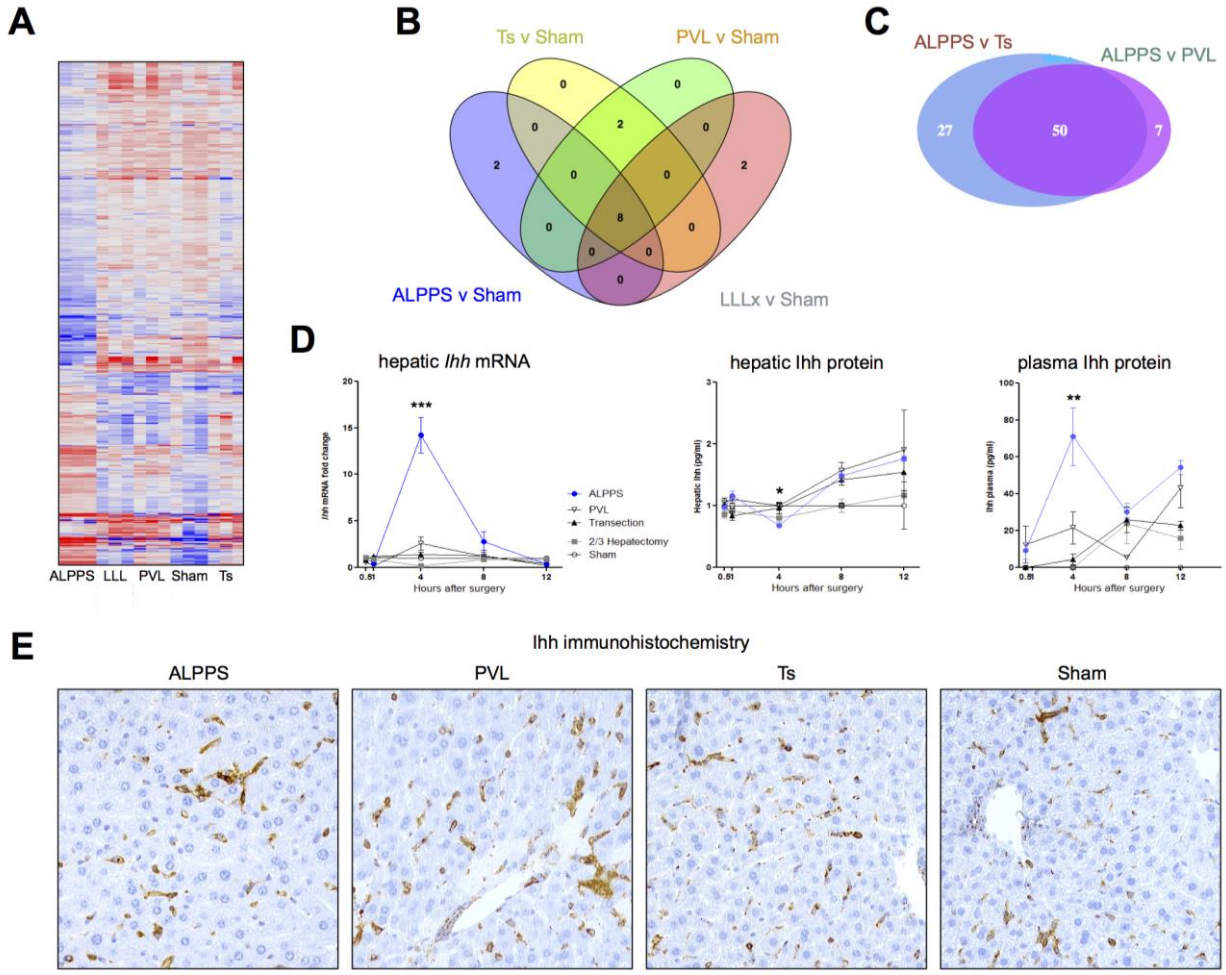

Figure 2. Ihh induction after ALPPS. *(A)* Hepatic gene expression profiles derived from RNA sequencing at 4h after surgery. Note the unique ALPPS profile. *(B)* Visual presentation (Venny 2.0) of overlaps between top dysregulated pathways (fold change ≥ 2, p >0.05) derived from MetaCore pathway analysis of 4h-expression profiles. *(C)* Venny visualization of dysregulated genes (fold change ≥ 4, p >0.05) in two-pair comparisons. N = 3/group for expression profiling. *(D)* Hepatic *Ihh* gene expression, hepatic Ihh protein expression (normalized to Gapdh), and plasma Ihh protein levels (ELISA) after surgery. (E) Ihh immunohistochemistry. Note the similar staining patterns across all groups. N = 6/group. t-test, *p <0.05, **p <0.01, ***p <0.001.

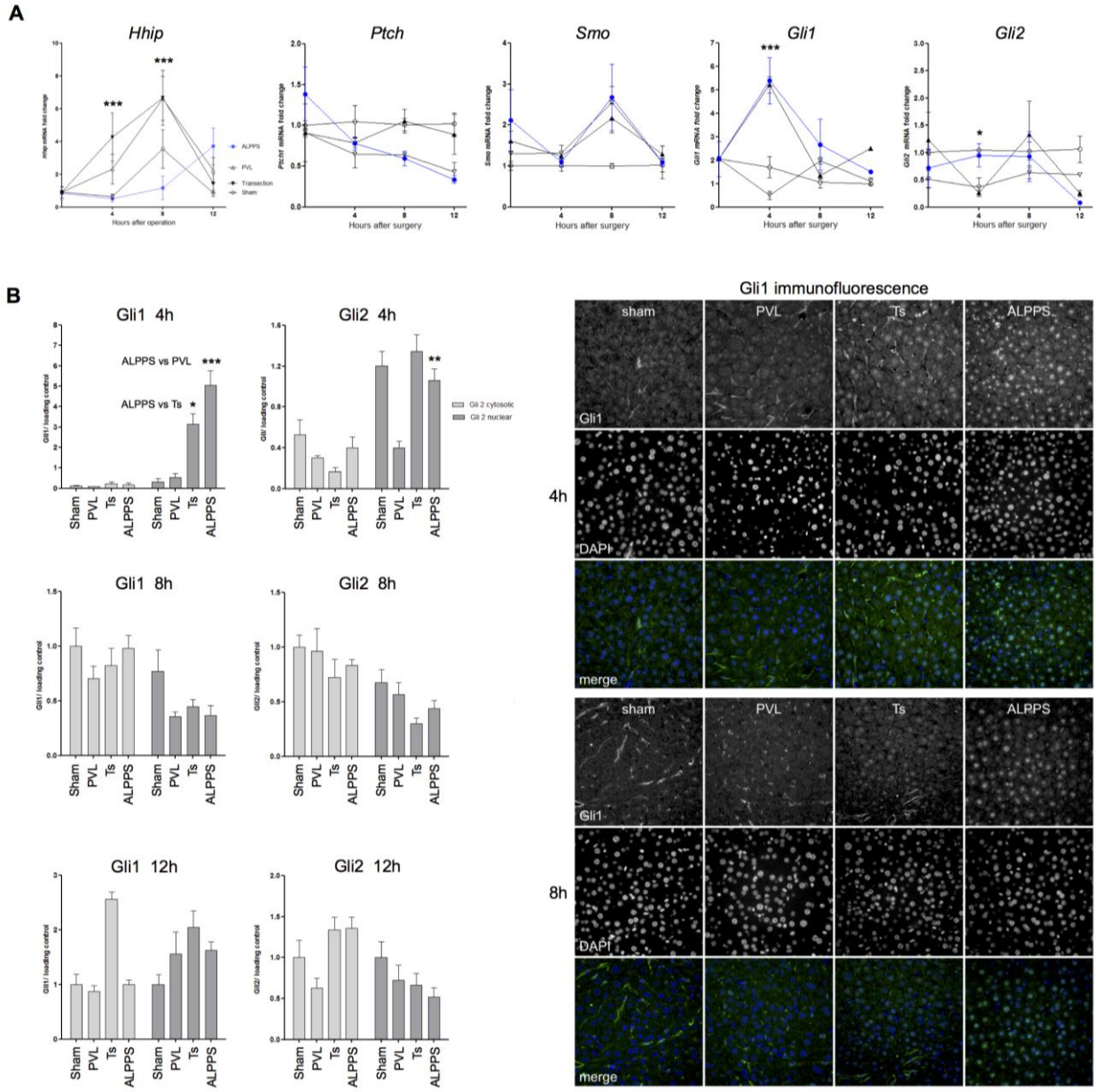

Figure 3. Hedgehog pathway components after surgery. *(A)* Gene expression for *Hhip1, Ptch1*, *Smo*, *Gli1*, and *Gli2*. N = 6/group. *(B)* Cytosolic and nuclear protein levels (normalized to β-tubulin and lamin B1, respectively; see immunoblots in Supplementary Fig. 2) of Gli1 and Gli2. N = 6/group. Right panels: immunofluorescence for hepatic Gli1. Note for ALPPS liver the nuclear staining predominantly in hepatocytes. At 8h, Gli1 expression was more prominent in parenchymal than non-parenchymal cells for ALPPS relative to transection, PVL and sham. In sham liver, cytoplasmic staining was increased in non-parenchymal cells at 8h relative to 4h. t-test, *p <0.05, **p <0.01, ***p <0.001 for PVL vs ALPPS unless indicated otherwise. ALPPS, associated liver partition and portal vein ligation for staged hepatectomy; PVL, portal vein ligation; Ts, transection.

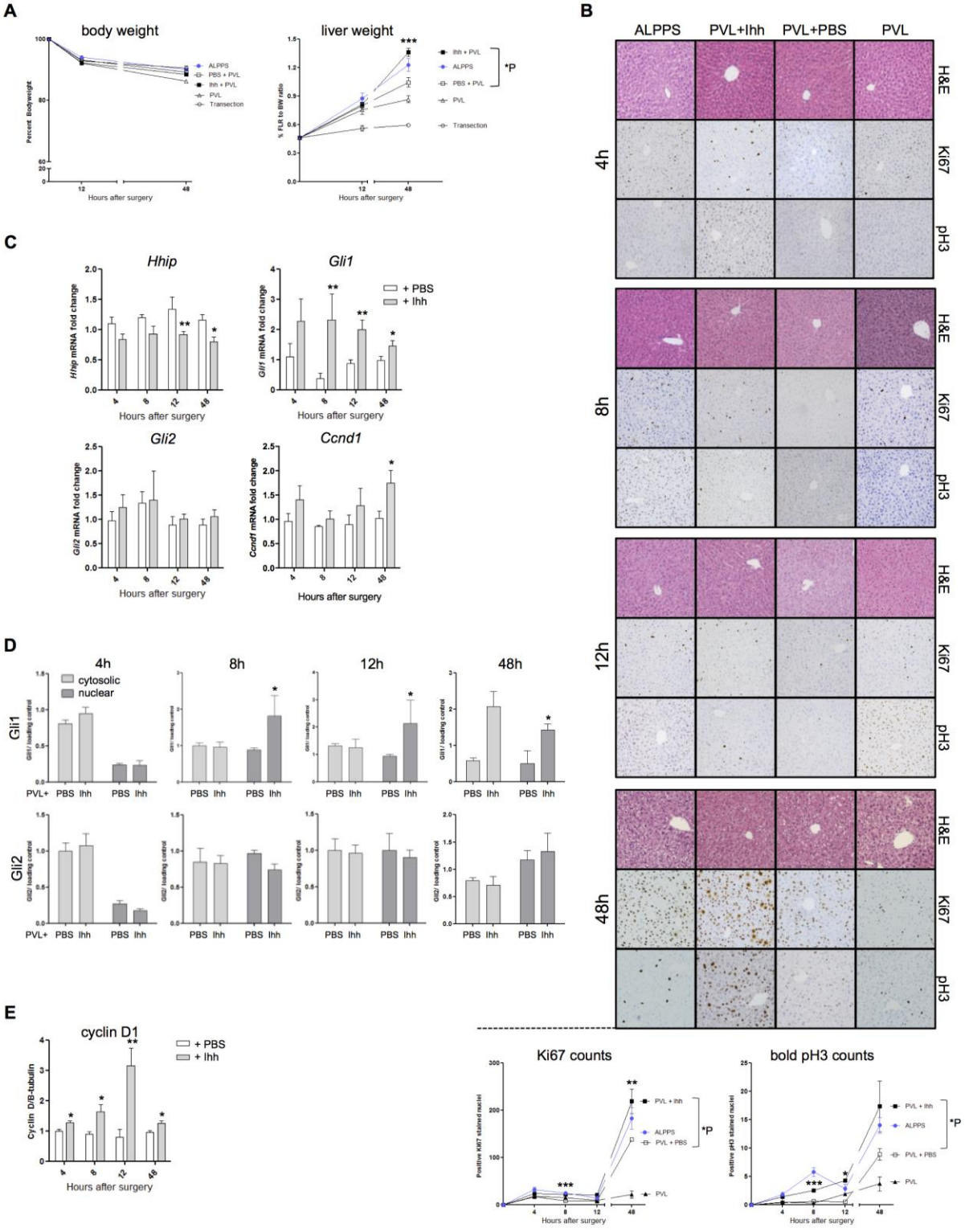

Figure 4. Effects of recombinant Ihh on PVL-induced liver regeneration. *(A)* Percent body weight and functional-liver-remnant-to-body-weight-ratio after PVL-Ihh, PVL-PBS, ALPPS, PVL and transection are shown in the left and right graph, respectively. *(B)* Corresponding H&E, Ki67, and pH3 staining of liver. Graphs show counts of hepatocytes positive for Ki67 or pH3. Note the increases in bold pH3-positive nuclei 12h after PVL-Ihh. *(C)* Hepatic gene expression of *Hhip*, *Gli1 Gli2*, and *Ccnd1* after PVL plus PBS or Ihh. *(D)* Cytosolic and nuclear protein levels (normalized to β-tubulin and lamin B1, respectively) of Gli1 and Gli2. (*E*) Quantified cyclin D1 immunoblots. N = 6/group. t-test, *p <0.05, **p <0.01, ***p <0.001 for PVL-PBS vs PVL-Ihh.

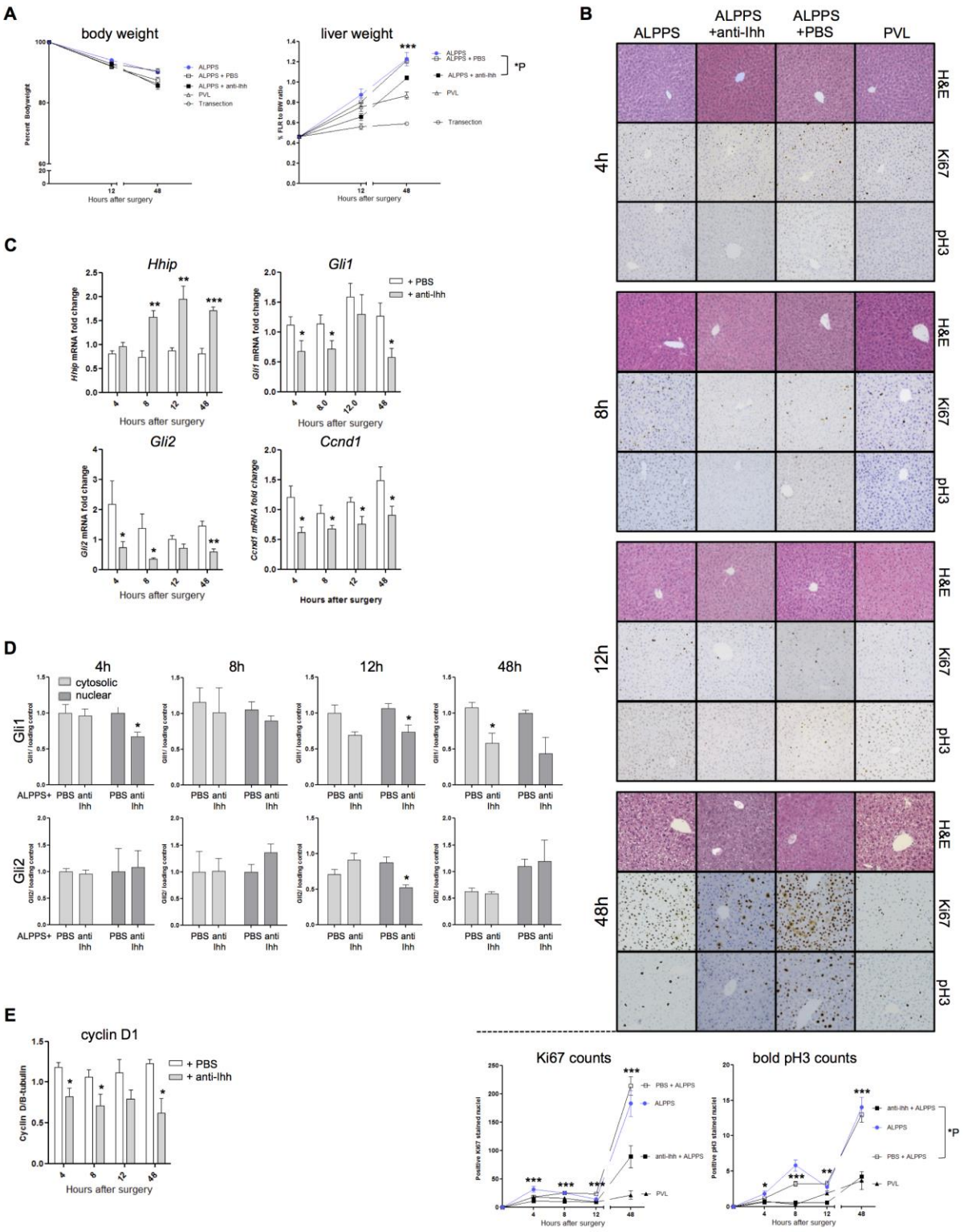

Figure 5. Effects of neutralizing Ihh antibody on ALPPS-induced liver regeneration. *(A)* Percent body weight and functional-liver-remnant-to-body-weight-ratio after ALPPS-αIhh antibody, ALPPS-PBS, ALPPS, PVL, and transection. *(B)* Corresponding H&E, Ki67, and pH3 staining of liver, with graphs showing Ki67 or pH3 counts. *(C)* Hepatic gene expression of *Hhip*, *Gli1, Gli2*, and *Ccnd1* after ALPPS plus PBS or αIhh antibody. *(D)* Cytosolic and nuclear protein levels of Gli1 and Gli2. (*E*) Quantified cyclin D1 immunoblots. t-test, *p <0.05, **p <0.01, ***p <0.001 for ALPPS-PBS vs ALPPS-αIhh

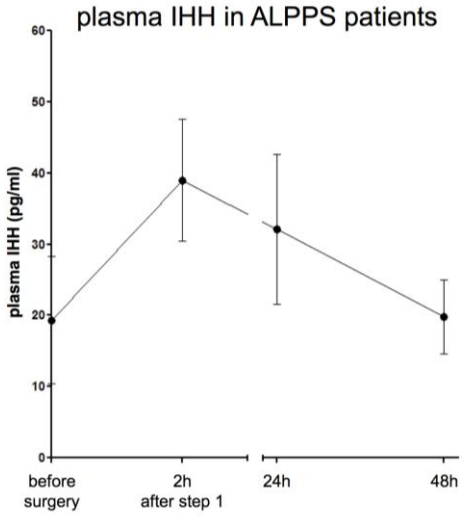

Figure 6. Human IHH levels in clinical material. Plasma from ALPPS patients was available at 0h (baseline), 2 h, 24 h, and 48 h after PVL and transection. IHH levels were assessed by ELISA.

Supplementary Materials

Supplementary Tables

Table S1. Taqman gene expression assays

gene name	Applied Biosystems order no.
Ccna1	Mm00438064_m1
Ccnb1	Mm00838401_m1
Ccnb2	Mm01171453_m1
Ccnd1	Mm00432359_m1
Ccne1	Mm00432367_m1
Gli1	Mm00494654_m1
Gli2	Mm01293117_m1
Hhip	Mm00469580_m1
Ihh	Mm00439613_m1
Ptch1	Mm00436026_m1
Smo	Mm01162710_m1
18S rRNA	Control reagents

Table S2. Antibodies

Antigene	Company (order no.)	Dilution
Ki67	Abcam, Cambridge, UK (ab16667)	1:200 (IHC)
pH3	Millipore, Schaffhausen, CH (06-570)	1:500 (IHC)
Ihh	Abcam, Cambridge, UK (ab39634)	1:500 (IHC)
secondary	Thermo Fischer, Rockford, IL, USA (62-9511)	1:50 (IF)
Gli1	R&D, Zug, CH (Mab3324)	1:50 (IF) 1:5000 (WB)
Gli2	Abcam, Cambridge, UK (ab26056)	1:500 (WB)
cyclin D	Abcam, Cambridge, UK (ab16663)	1:100 (IHC) 1:100 (WB)
lamin B1	Santa Cruz, CA USA (sc-377001)	1:500 (WB)
β-tubulin	Cell Signaling, MA USA (2128S)	1:1000 (WB)

Table S3. Patient information

Patient	Age	Gender	Weight	Indication	Co-morbidity	Histology	Increase in FLR volume*	Postoperative Complications	Postoperative Complication Score (CCI)
1	55	female	54 kg	synchronous liver metastases of adeno-carcinoma of the rectum	none	slight pericellular fibrosis, no higher fibrosis, no steatosis	20.5%	wound dehiscence, pneumothory, ohylothorax, electrolyte disorder, renal insufficiency	55.7
2	57	male	91 kg	synchronous liver metastases of adeno-carcinoma of the rectum	none	Macro-steatosis ca. 20%, no fibrosis	3.5%	VAC, antibiotics	29.6
3	35	female	61 kg	synchronous liver metastases of adeno-carcinoma of the rectum	cancer of right breast	none (slight pericellular fibrosis in 1 biopsy)	29.3%	none	0
4	37	female	65 kg	synchronous liver metastases of adeno-carcinoma of the sigmoid colon	none	minimal pericellular fibrosis without bridging	18.2%	blood transfusion	22.6
5	47	male	82 kg	metachronous liver metastases of adeno-carcinoma of the rectum	none	macro-steatosis ca. 30%	22.5%	bed side wound opening, antipyretics	8.7
6	55	male	105 kg	hepatocellular carcinoma	liver cirrhosis, child-pugh score A due to chronic hepatitis C, genotype 1B	moderate inflammatory activity (A2), fibrosis: metavir-stage F4	13.9%	none	0

**represents future liver remnant (FLR) volume before step 2 minus liver volume before step 1 of ALPPS*

Table S4. Differentially expressed pathways

	LLLx vs sham	P-value	FDR
1	Cytoskeleton remodeling_TGF, WNT, & cytoskeletal remodeling	4.758e-31	4.292e-28
2	Cytoskeleton remodeling_Cytoskeleton remodeling	1.666e-25	7.514e-23
3	Cell adhesion_Chemokines and adhesion	1.558e-19	3.512e-17
4	Development_Regulation of epithelial-to-mesenchymal transition	3.576e-18	6.451e-16
5	Development_EGFR signaling pathway	8.560e-17	1.103e-14
6	Development_TGF-beta receptor signaling	2.209e-16	2.490e-14
7	Transcription_Sin3 and NuRD in transcription regulation	4.431e-16	4.441e-14
8	Transport_Clathrin-coated vesicle cycle	1.003e-15	9.051e-14
9	Signal transduction_JNK pathway	2.222e-15	1.822e-13
10	Cell cycle_Influence of Ras and Rho proteins on G1/S Transition	1.462e-14	8.792e-13
	PVL vs sham	**P-value**	**FDR**
1	Cytoskeleton remodeling_TGF, WNT and cytoskeletal remodeling	9.008e-30	8.12e-27
2	Cytoskeleton remodeling_Cytoskeleton remodeling	1.435e-25	6.471e-23
3	Cell adhesion_Chemokines and adhesion	1.366e-19	3.081e-17
4	Development_Regulation of epithelial-to-mesenchymal transition	3.244e-18	5.851e-16
5	Development_EGFR signaling pathway	7.742e-17	9.977e-15
6	Transcription_Sin3 and NuRD in transcription regulation	2.780e-16	3.135e-14
7	Transport_Clathrin-coated vesicle cycle	9.103e-16	8.211e-14
8	Cell cycle_Influence of Ras and Rho proteins on G1/S Transition	1.351e-14	8.703e-13
9	Immune response_IL-18 signaling	1.742e-14	1.039e-12
10	Immune response_IL-1 signaling pathway	2.295e-14	1.150e-12
	transection vs sham	**P-value**	**FDR**
1	Cytoskeleton remodeling_TGF, WNT, and cytoskeletal remodeling	6.753e-27	6.092e-17
2	Cytoskeleton remodeling_Cytoskeleton remodeling	1.110e-25	5.005e-23
3	Cell adhesion_Chemokines and adhesion	1.091e-19	2.459e-17
4	Development_Regulation of epithelial-to-mesenchymal transition	2.743e-18	4.948e-16
5	Development_EGFR signaling pathway	6.516e-16	8.396e-15
6	Transcription_Sin3 and NuRD in transcription regulation	3.634e-16	4.097e-14
7	Transport_Clathrin-coated vesicle cycle	7.701e-16	7.718e-14
8	Transport_Clathrin-coated vesicle cycle	1.179e-14	7.596e-13
9	Immune response_IL-18 signaling	1.506e-14	8.856e-13
10	Immune response_IL-1 signaling pathway	2.034e-14	1.079e-12
	ALPPS vs sham	**P-value**	**FDR**
1	Cytoskeleton remodeling_TGF, WNT, and cytoskeletal remodeling	7.990e-30	7.207e-27
2	Cytoskeleton remodeling_Cytoskeleton remodeling	1.289e-25	5.815e-23
3	Cell adhesion_Chemokines and adhesion	1.244e-19	2.805e-17
4	Development_Regulation of epithelial-to-mesenchymal transition	5.850e-17	8.795e-15
5	Development_EGFR signaling pathway	7.206e-17	9.286e-15
6	Transcription_Sin3 and NuRD in transcription regulation	3.910e-16	4.408e-14
7	Transport_Clathrin-coated vesicle cycle	8.491e-16	8.510e-14
8	Cell cycle_influence of Ras and Rho proteins on G1/S Transition	1.276e-14	8.223e-13
9	Development_TGF-beta-dependent induction of EMT via MAPK	5.998e-14	3.182e-12
10	**Transcription_Sirtuin6 regulation and functions**	**1.169e-13**	**5.479e-12**

List of Metacore pathways used for Venny diagrams displaying ALPPS specific pathways. The Ihh gene was included in the the sirtuin 6 pathway (ALPPS vs. sham, no. 10. FDR, false discovery rate.

Table S5. Differentially expressed genes

gene	log2ratio	FDR
Dmbt1	13.7	4.39e-06
Atp2a1	8.2	1.01e-06
Akr1b7	7.8	1.80e-73
Cyp11b1	6.5	2.23e-05
Slc4a9	6.3	2.95e-06
Ihh	**6.0**	**2.96e-30**
Ly6k	5.8	9.12e-05
Sprr1a	5.4	8.79e-19
Fscn2	5.2	2.20e-13
Pax9	5.2	0.0004318
Tac1	5.2	2.20e-13
Otoa	5.1	0.00187
Slfn10-ps	4.9	0.001714
Bmp8b	4.8	1.77e-12
Ly6b	4.8	6.88e-18
Nes	4.8	8.01e-40
Fhl3	4.7	2.94e-19
Cd14	4.6	1.07e-09
Tubb3	4.5	1.78e-06
Sprr2a2	4.4	0.0001004
Mrap	4.3	1.07e-30
Ralgds	4.3	5.34e-25
Sphk1	4.3	2.13e-20
Ier3	4.2	2.13e-20
Krt8	4.2	2.84e-27
Duox2	4.1	0.03272
Nefm	4.1	3.68e-05
Tnfrsf12a	4.1	1.86e-24
Barx2	4.0	7.75e-07
Col12a1	4.0	9.99e-30
Krt18	4.0	3.49e-25
Mmp24	4.0	1.99e-09
Gm15348	-4.0	2.25e-07
Ciart	-4.1	4.26e-16
N4bp2l1	-4.1	1.57e-26
Gbp2b	-4.3	3.50e-06
Hist2h3c1	-4.3	5.58e-12
Gas 1	-4.5	1.74e-11
Gm17597	-4.6	0.01507
Hist2h3c2	-4.6	2.24e-08
Zfp936	-4.6	0.01401
Fbxo40	-4.7	0.01297
B4galnt3	-4.9	1.64e-06
Kif14	-4.9	0.004497
Ackr4	-5.0	0.006229
B230217C12Rik	-5.4	0.000462
3222401L13Rik	-5.4	0.0006822
Pif1	-5.5	0.0002963
Gm17435	-5.6	0.0001665

50 unique genes to ALPPS identified through Metacore (filter criteria: fold change ≥4, P≤0.05)

Supplementary Figures

Figure S1. Percentage liver weight gain after ALPPS versus hepatectomy.

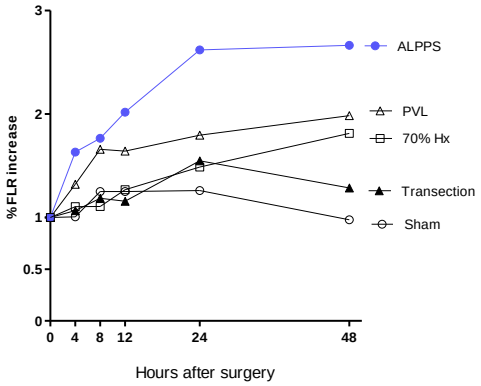

Supplementary Figure 1. Percentage liver weight gain after ALPPS compared to hepatectomy and the surgical controls. The weight of the remnant at surgery was set to one, enabling the comparison of ALPPS and PVL (10% remnant) with partial hepatectomy (30% remnant).

Figure S2. Immunoblots for protein quantifications

Figure 1

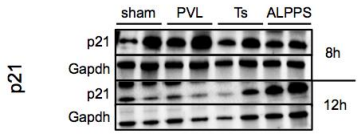

Figure 3

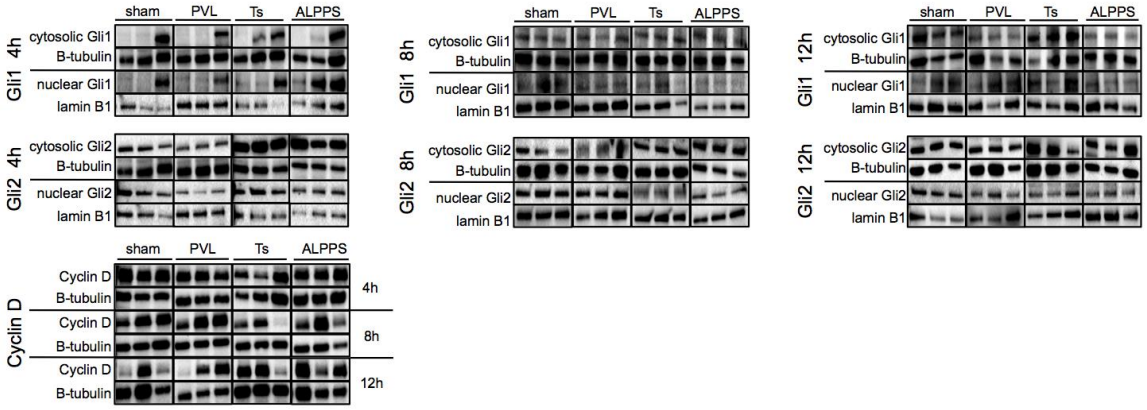

Figure 4

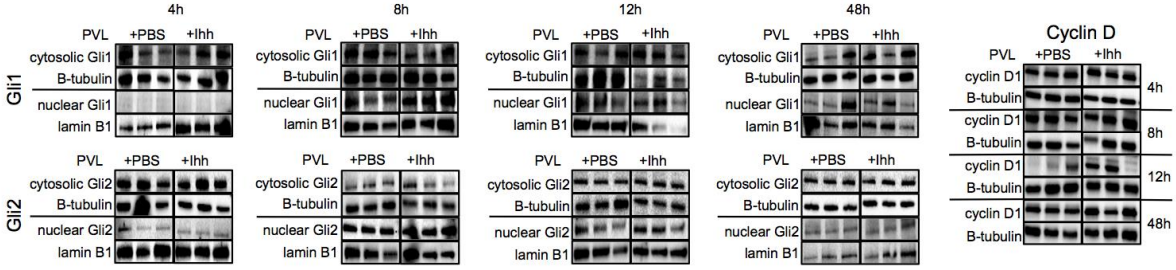

Figure 5

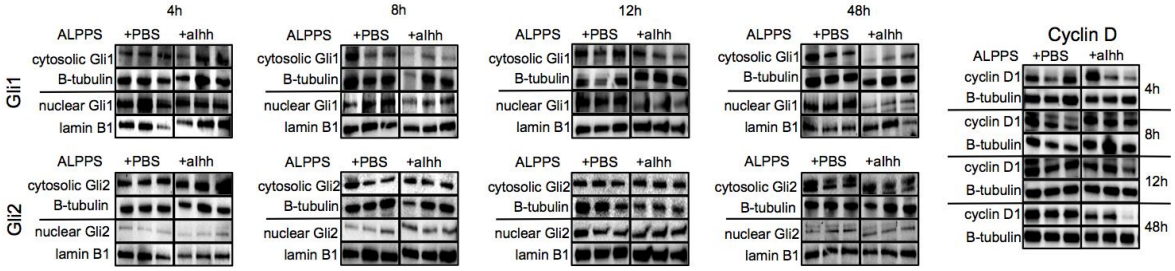

Supplementary Figure 2. Representative immunoblot bands corresponding to quantification graphs shown in the main figures 1, 3, 4 and 5. For quantifications, at least 6 samples/group were included.

Figure S3. Differentially expressed genes following surgery over time.

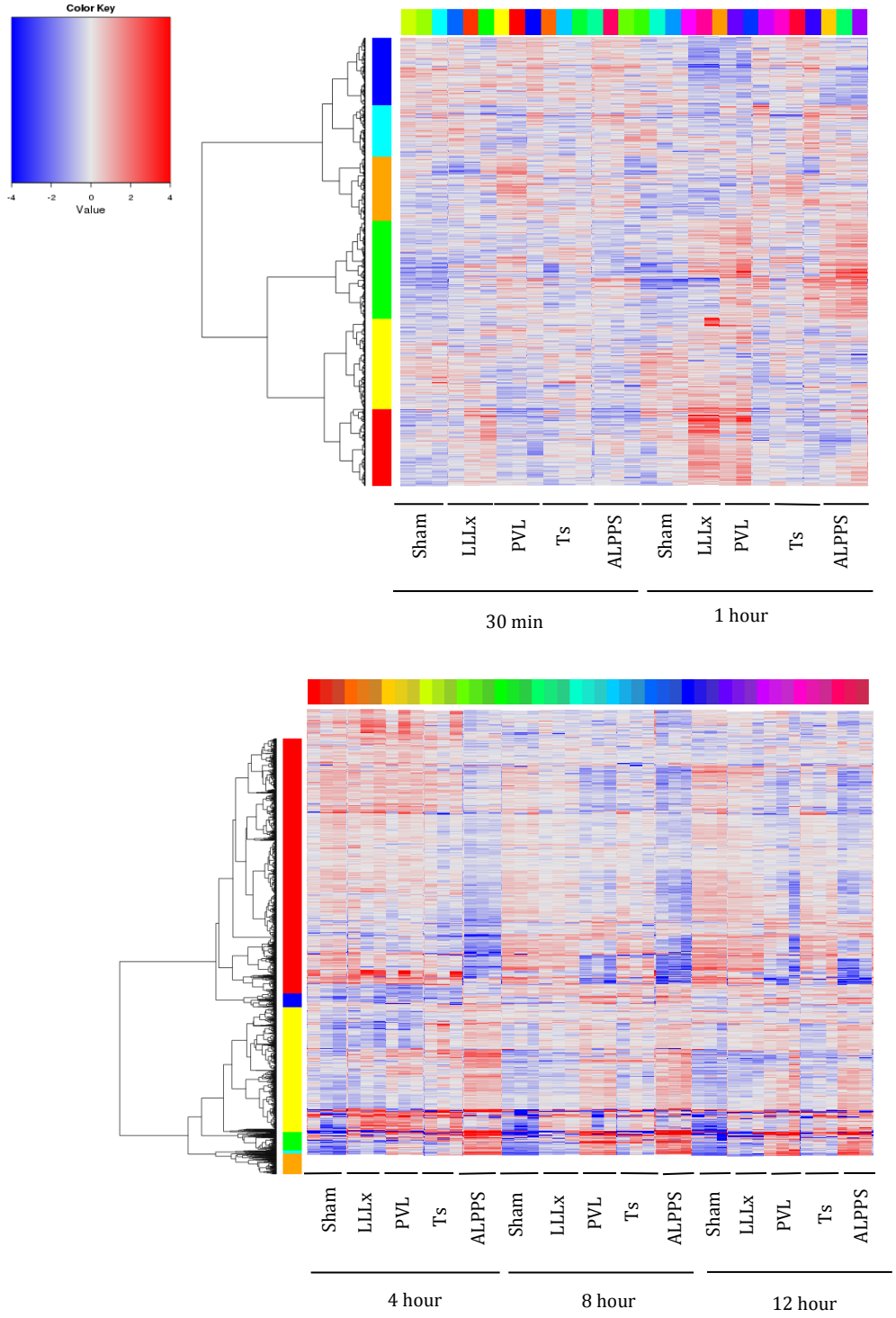

Supplementary Figure 3. Full heatmap of RNA deep sequencing data representing gene expression profiles at 0.5h, 1h, 4h, 8h, and 12h following ALPPS and control surgeries. Performed on the Illumina HiSeq 2500 by the Functional Genomic Center Zurich (FGCZ). Raw data was analyzed by EdgeR two-group analysis.

Figure S4. Shh/Dhh RNA sequencing data and Shh plasma levels.

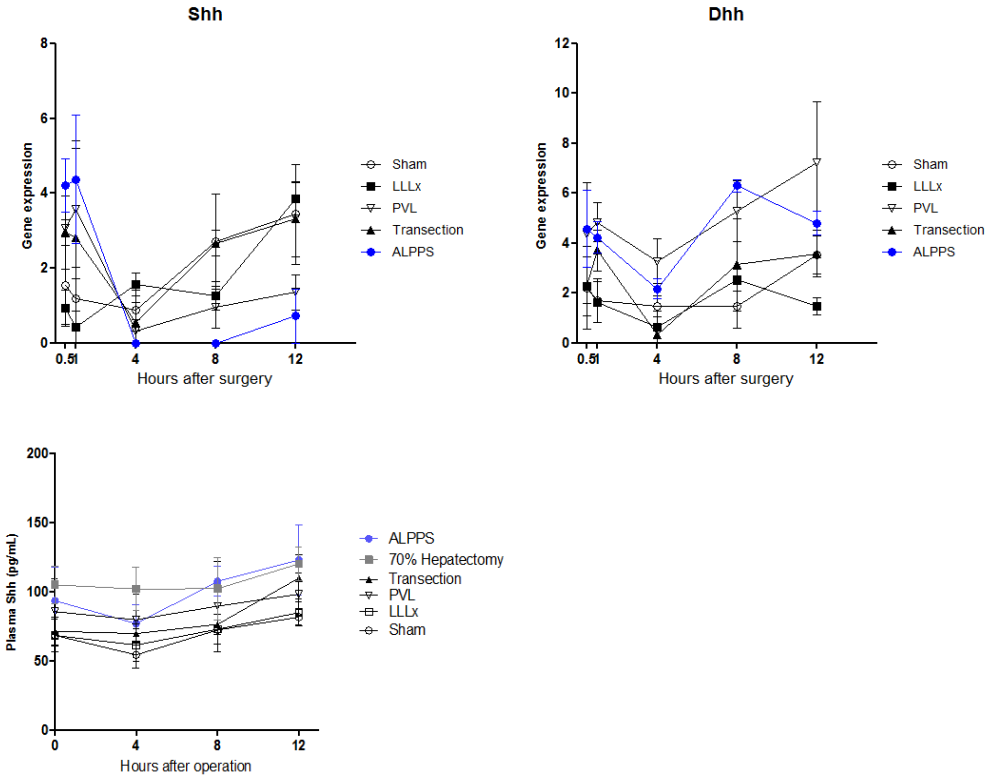

Supplementary Figure 4. Top: *Shh* and *Dhh* expression data derived from the RNA sequencing screen. No ALPPS-specific changes were detectable. Bottom: Shh plasma protein levels (ELISA) following surgical procedurs including standard hepatectomy. No ALPPS-specific changes were apparent.

Figure S5. Immunohistochemistry for Ihh.

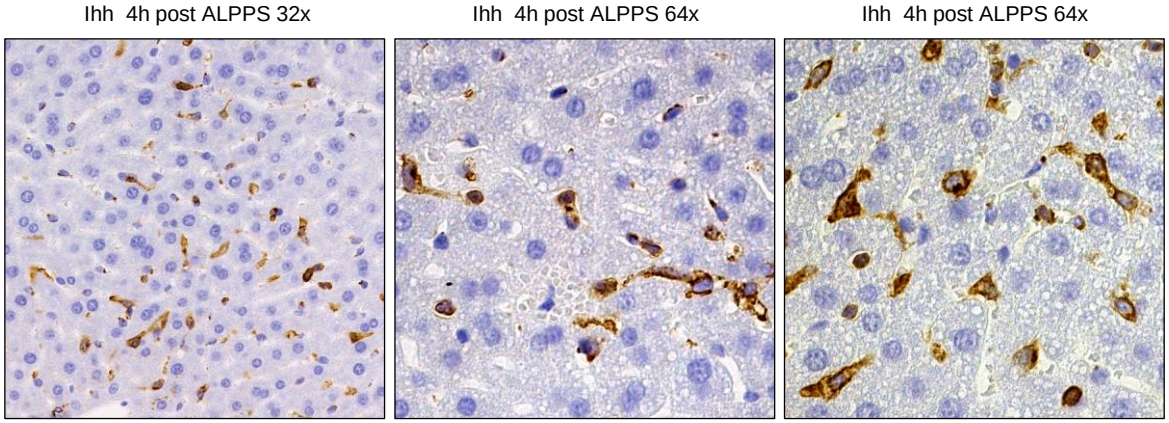

Supplementary Figure 5. Immunostainings for Ihh of liver 4h after ALPPS surgery. Ihh expression is observed in non-parenchymal cells, including cells with typical stellate morphology. At 4h after ALPPS, hepatic mRNA and plasma Ihh levels peak, suggesting Ihh is sourced from stellate cells and not hepatocytes.

Figure S6. Immunohistochemistry for cyclin D1 on liver post surgery

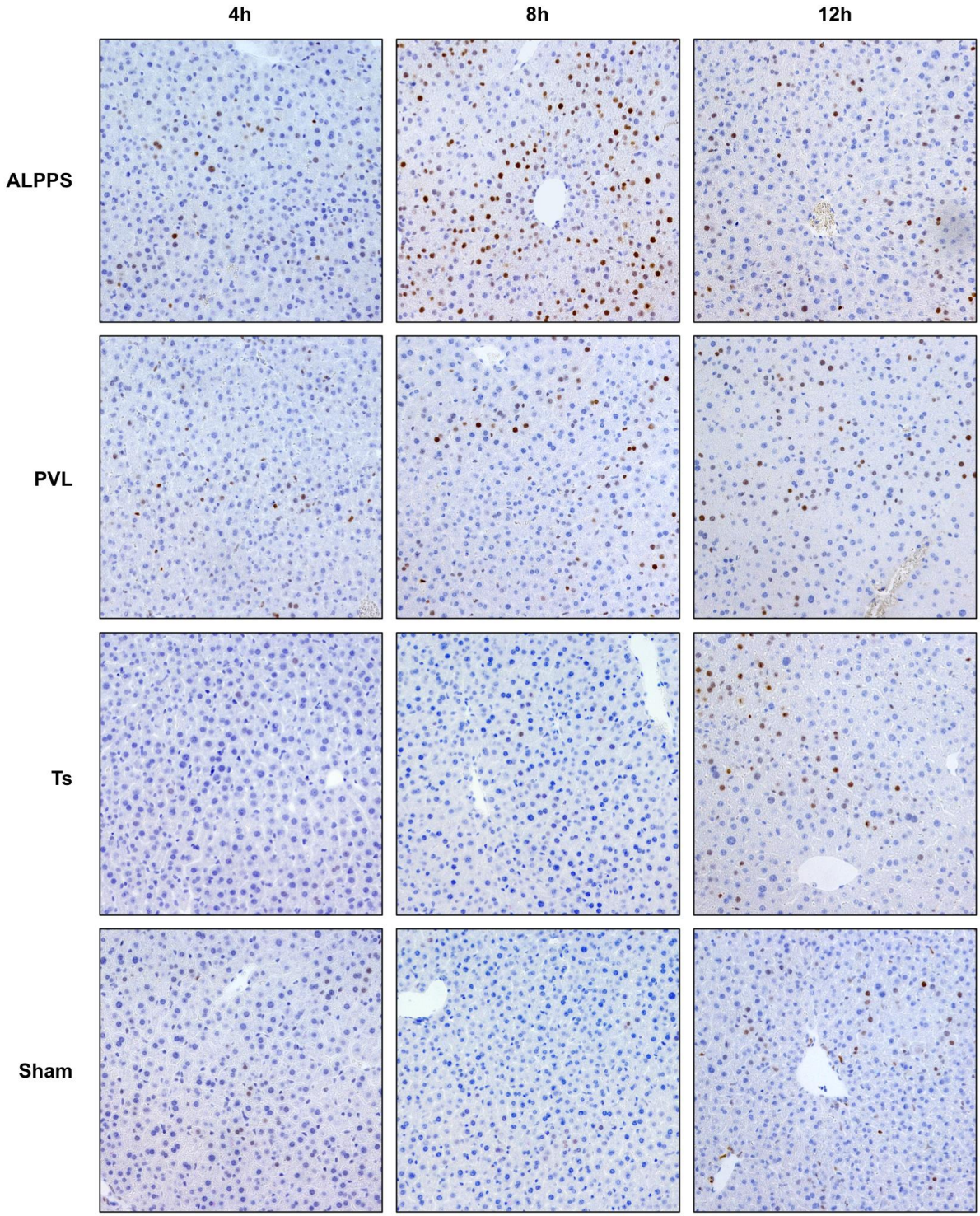

Supplementary Figure 6. Representative immunostainings for cyclin D1 on liver after ALPPS, PVL, transection and sham operation. Note the peak in nuclear positivity at 8h after ALPPS.

Figure S7. Immunohistochemistry for cyclin D1 on liver after Ihh gain or loss treatment.

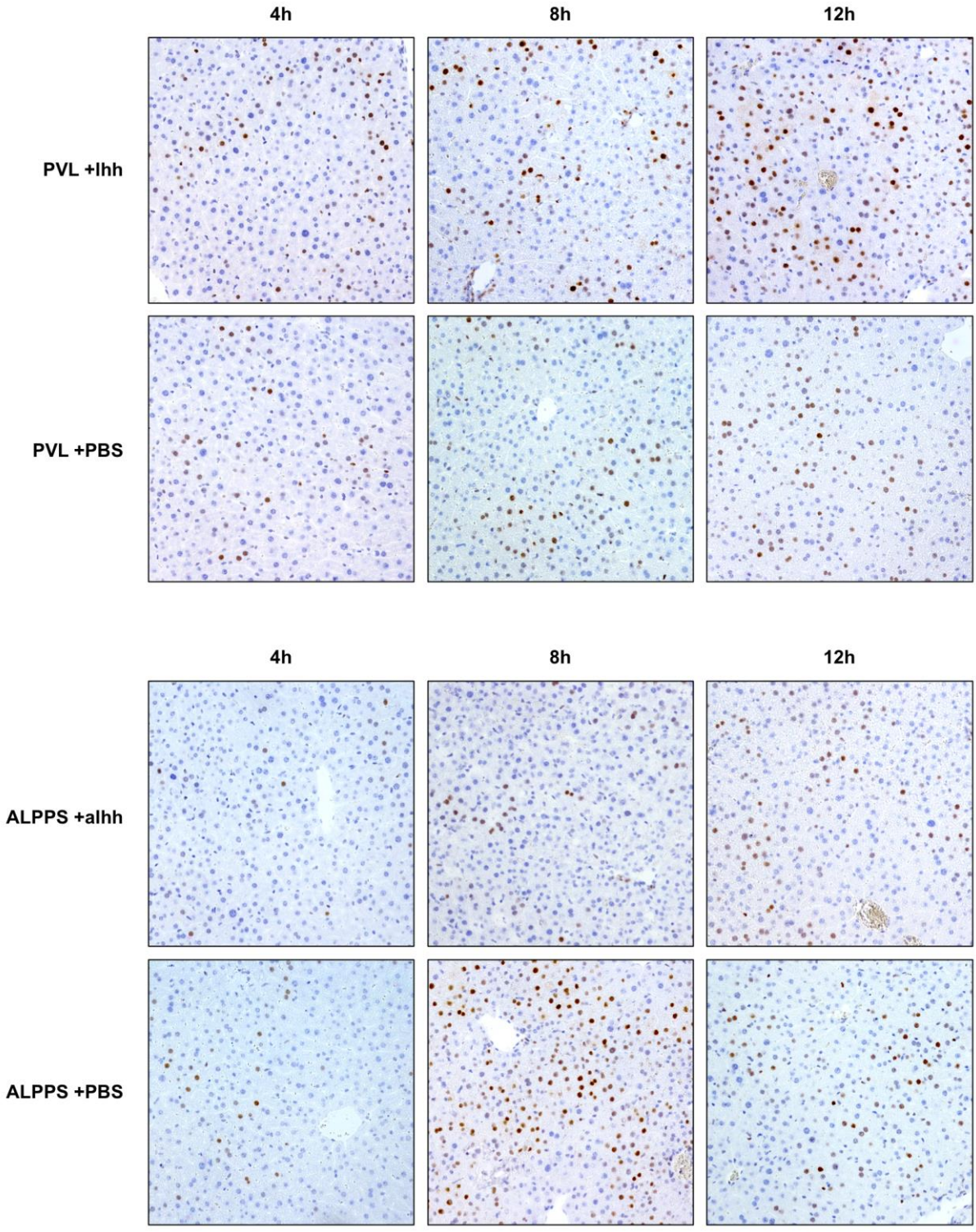

Supplementary Figure 7. Representative immunostainings for cyclin D1 on liver after treatment of PVL mice with Ihh/PBS (upper panels) or after treatment of ALPPS mice with αIhh/PBS (lower panels).

Figure S8. Estimation of cellular hypertrophy after ALPPS.

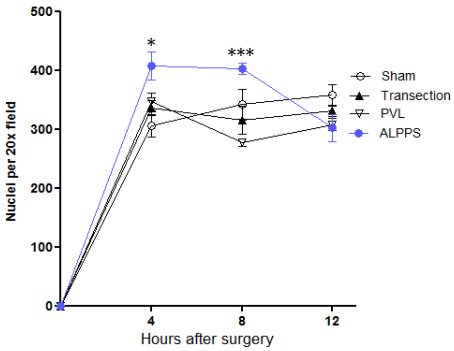

Supplementary Figure 8. Cellular hypertrophy following ALPPS, PVL, Ts and sham. Hypertrophy was estimated by counting hepatocyte nuclei per area, with higher counts correlating to smaller cell size. At 4h (*P<0.05, ALPPS vs PVL) and 8h (***P<0.001, ALPPS vs PVL), ALPPS liver displayed significantly elevated nuclear counts, pointing to a smaller cell size relative to PVL. At 12h however, counts were similar for all procedures. Therefore, cellular hypertrophy seems not to contribute to the increases in liver weight seen early after ALPPS. Five random visual fields (20x magnification) were counted per sample on H&E stains in a blinded way.

Figure S9: *Hgf*, *Egf*, and *Il6* expression after surgery.

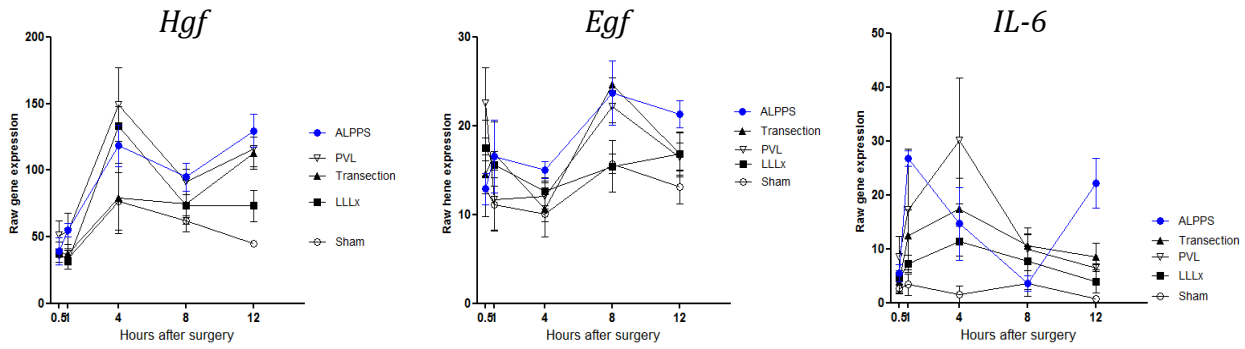

Supplementary Figure 9. Gene expression of classic promoters of liver regeneration after ALPPS and control surgeries. Gene expression was derived from RNA sequencing data. *Tnfa*, another classic regeneration molecule, was undetectable in the data set. n=3/group.

5. Manuscript B

JNK1 induces IHH signaling from stellate cells to accelerate liver regeneration after ligation and transection in mice

Magda Langiewicz[1], Rolf Graf[1], Bostjan Humar[1]±, Pierre A. Clavien[1]±

± shared senior authorship

[1]Laboratory of the Swiss Hepato-Pancreato-Biliary (HPB) and Transplantation Center, Department of Surgery, University Hospital Zurich, Switzerland.

Accepted *Journal of Hepatology*, 2018

Contribution: The second publication of my PhD project is a continuation of the first publication. I have done all experiments, data acquisitions, and analyses. I contributed to the experimental design under the supervision of Dr. Humar, the data interpretation, and in writing the manuscript.

JNK1 induces IHH signaling from stellate cells to accelerate liver regeneration after ligation and transection in mice

Authors: Magda Langiewicz[1], Rolf Graf[1], Bostjan Humar[1*], and Pierre A. Clavien[1*].

*shared senior authorship

[1]Laboratory of the Swiss Hepato-Pancreato-Biliary (HPB) and Transplantation Center, Department of Surgery, University Hospital Zurich, Raemistrasse 100, Zurich, CH-8091, Switzerland.

Corresponding author: Pierre-Alain Clavien, Department of Surgery & Transplantation, University Hospital Zurich, Raemistrasse 100, CH-8091 Zurich, Phone: +41 44 255 3300, email: clavien@access.uzh.ch

Abbreviations: ALPPS: Associating Liver Partition and Portal Vein Ligation Surgery, FLR: functional liver remnant, HSC: hepatic stellate cells, Ihh: Indian hedgehog, JNK1: c-Jun-N-terminal kinase, pH3: phosphohistone 3; PVL: Portal Vein Ligation, SFSS: small-for-size-syndrome, PH: partial hepatectomy

Transcript Profiling: ENA PRJEB15593

Abstract

Background & Aims: To improve outcomes of two-staged hepatectomies for large/multiple liver tumors, portal vein ligation (PVL) has been combined with parenchymal transection (coined ALPPS; *A*ssociated *L*iver *P*artition and *P*ortal vein ligation for *S*taged hepatectomy) to greatly accelerate liver regeneration. In a novel ALPPS mouse model, we have reported paracrine Indian hedgehog (IHH) signaling from stellate cells as an early contributor to augmented regeneration. Here, we sought to identify upstream regulators of IHH.

Methods: ALPPS in mice was compared against PVL and additional control surgeries. Potential IHH regulators were identified through *in silico* mining of transcriptomic data. JNK1 activity was reduced through SP600125 to evaluate its effects on IHH signaling. Recombinant IHH was injected after JNK diminution to substantiate their relationship during accelerated liver regeneration.

Results: Mining linked *Ihh* to *Mapk8*. JNK1 upregulation after ALPPS was validated and preceded the IHH peak. On immunofluorescence, JNK1 and IHH co-localized in ASMA-positive non-parenchymal cells. Inhibition of JNK1 prior to ALPPS surgery reduced liver weight gain to PVL levels and was accompanied by downregulation of hepatocellular proliferation and the IHH-GLI1-CCND1 axis. In JNK1-inhibited mice, recombinant IHH restored ALPPS-like acceleration of regeneration and re-elevated JNK1 activity, suggesting the presence of a positive IHH-JNK1 feedback loop.

Conclusions: JNK1-mediated induction of IHH paracrine signaling from HSCs is essential for accelerated regeneration of parenchymal mass. The JNK1-IHH axis is a mechanism unique to ALPPS surgery and may point to therapeutic alternatives for patients with insufficient regenerative capacity.

Keywords: compensatory hypertrophy; small-for-size syndrome; future liver remnant.

Introduction

The unique ability of mammalian liver to regain mass after tissue loss has revolutionized the treatment and cure of many patients with liver tumors. However, there are limitations to effective regeneration, as hepatic failure may develop after extensive liver resection. This entity, known as the small-for-size syndrome (SFSS), results from an insufficient functional volume of the liver remnant and remains the most frequent cause of death due to liver surgery [1,2]. Two-staged hepatectomies were introduced to reduce the SFSS risk. Typically, the portal vein draining the part of the liver containing the tumor is occluded (step 1), causing growth of the contralateral liver part (defined as the future remnant liver (FRL)); when the FRL has gained sufficient functional volume, step 2 (resection of the diseased part) is performed [2,3]. Nevertheless, in some cases regeneration is still insufficient, or the considerable time period between step 1 and 2 allows for further progression of the disease [4,5]. To additionally reduce the risk of SFSS in patients with large or multiple liver tumors, ALPPS (*A*ssociated *L*iver *P*artition and *P*ortal vein ligation for *S*taged hepatectomy: the combination of portal vein ligation with parenchymal transection) has been showcased as a procedure that induces accelerated liver regeneration and greatly reduces the interval between steps, allowing treatment of patients otherwise deemed as unresectable [6,7]. This procedure, introduced about five years ago, has gained sustained acceptance with more than 1000 cases included in an international registry (http://www.alpps.net/?q=registry).

Although there have been several clinical studies evaluating ALPPS in patients, reports on the molecular mechanisms underlying the regenerative acceleration following ALPPS-step 1 remain scarce. Several components known to be necessary for liver regeneration after partial hepatectomy have likewise been associated with accelerated regeneration. In rodent models, IL-6 and TNFα - established mediators of liver regeneration - have been found upregulated in ALPPS at the mRNA and protein level. Similarly, protein expression of STAT3, RELA, and YAP1 – known transcription factors in the regenerating liver - were elevated after ALPPS step 1 [8,9]. Furthermore, hypoxia has recently been shown to be an important driver of normal regeneration through HIF2α, with preliminary studies pointing to the importance of hypoxia also in ALPPS [10,11]. In human ALPPS tissues, IL-6 and TNFα have been validated on the mRNA level [12]. However, none of these molecules seems to be unique to the ALPPS-induced acceleration of regeneration.

We have developed a mouse model of ALPPS and documented the release of serum factors that can accelerate regeneration in mice following portal vein ligation (PVL) only to levels seen after the complete ALPPS-step 1 procedure [12]. These findings suggest that humoral factors must play essential roles in the early instigation of accelerated regeneration. With this mouse model, we established that the secretion of Indian Hedgehog (IHH) from hepatic stellate cells (HSCs) was necessary for the early activation and progression of accelerated regeneration [13]. Although hedgehog signaling has previously been reported to be required for regeneration after hepatectomy, the early elevations in serum IHH were unique to ALPPS, and not observed following hepatectomy or other surgeries [13].

Hedgehog activity is barely detectable in healthy adult liver. Upon hepatectomy, however, hepatocytes begin to proliferate and HSCs undergo differentiation into myofibroblastic and fibrogenic states [14,15]. Furthermore, there is increasing evidence that morphogenic signals - such as the hedgehog pathway - are mediators of the myofibroblastic HSC switch. When blocking or knocking out *Smo*, the receptor for hedgehog ligands, HSCs do not acquire myofibroblastic traits, and subsequent hepatocyte regeneration is inhibited [16,17,18].

Given the specific secretion of IHH after ALPPS, this study sought to identify upstream regulators of the ligand as to establish the role of IHH in ALPPS. On the other hand, expanding on the networks that act to accelerate regeneration after ALPPS may provide insight into new therapeutics for the pharmacological promotion of regeneration in clinical settings.

Materials and Methods

Animals

All animal experiments were performed in accordance with Swiss Federal Animal Regulations and approved by the Veterinary Office of Zurich. Male C57Bl/6 mice (Envigo, Horst, NL) aged 10-12 weeks kept on a 12-hour day/night cycle with free access to food and water were used.

Animal surgery and treatment

To mimic human ALPPS surgery in mice, 90% PVL was performed leaving a 10% functional remnant consisting of the left and a part of the right middle lobe. Then, a partial 80% transection was done through the middle lobe along the demarcation line of the occluded/non-occluded parenchyme. The left lateral lobe (LLL, 25% of liver volume) was also resected to simulate the cleaning of the liver from smaller tumors as often done in human ALPPS. Details on isoflurane anesthesia, buprenorphine analgesia, ALPPS procedures, and the control operations (90% PVL, 80% transection, and sham laparotomy) have been described [12,13]. After surgery, animals were allowed to recover on a warming pad in a separate cage until completely conscious. Animals were weighed before surgery and at sacrifice, where weight of resected and remnant liver was recorded. Tissue was formalin fixed or snap frozen, while plasma was stored at -80°C for analysis.

SP600125 (0.016mg/gram BW, InVivoGen, tlrl-sp60 Toulouse, FR), a specific JNK inhibitor, or DMSO in oil was injected I.P. one hour before operation. Recombinant Ihh (200 ng/kg, 160µl final volume; R&D, 1705-HH-025/CF Minneapolis, MN) or PBS was injected into the vena cava right after operation. Ihh antibody (4ug/kg, 160µl final volume; R&D MAB8048) or PBS was injected via tail vein one hour before operation.

Liver regeneration

Liver regeneration was assessed by the percentage of functional-liver-remnant-to-body weight ratio (FLR/BW) derived from six animals per group and time point.

Quantitative real-time PCR

Total RNA was extracted from 50 mg of tissue using Trizol reagent following provided instructions (Invitrogen, Basel, Switzerland). RNA quality/quantity was spectrometrically assessed. qPCR was performed with two replicates/sample on cDNA (Thermo Script reverse transcription PCR System, Invitrogen) using an ABI Prism 7500 Sequence Detector system (PE Applied Biosystems Rotkreuz, Switzerland). Taqman gene expression assays from Applied Biosystems are listed in Supplementary Table 1. Results represent mean fold induction ($2^{-\Delta Ct}$) ±SD relative to the normalization control *18S rRNA* [19].

Histological Examination

Archived liver sections (3 µm) were stained (antibodies in Supplementary Table 2) using the Dako Autostainer Link48 Instrument and the iView DAB kit (Dako Denmark A/S). Quantification of Ki67-, bold pH3- [19], cyclin D-, and pJNK-positive hepatocytes was achieved by blinded manual counting in 10 random visual fields (20x). For immunofluorescence, GLI1 antibody (R&D, Zug, Switzerland) was detected using an Alexa Fluor 488-conjugated anti-rat secondary antibody (Invitrogen, Zug, Switzerland). For co-immunofluorescence, primary antibodies are listed in Supplementary Table 2 and rabbit- and mouse-specific Alexa Fluor 488 and 594-conjugated secondary antibodies were used

respectively. Representative slides of five biological samples per group are shown.

In-silico analysis

RNA sequencing raw data of the accession number PRJEB15593 in the European Nucleotide Archive (ENA) was used for in-silico analysis via the online String Database (string-db.org).

Protein analysis

Western blotting was performed as described [19]. Antibodies are listed in Supplementary Table 2. NE-PER Nuclear and Cytoplasmic Extraction reagents (Thermo Fisher Scientific, Waltham, MA, PK207589) were used to isolate subcellular fractions, with their separation ascertained through β-tubulin (cytoplasmic) and lamin B1 (nuclear) blotting. IHH protein levels were measured by ELISA (mouse IHH: Cusabio, CSB-E16517m).

Statistical Analysis.

Data are expressed as mean ±SD. Differences between groups (n=6/group unless for expression profiling with n=3/group and for histological counting with n=5/group) were determined using unpaired, two-tailed t tests assuming unequal variance via GraphPad Prism v4.0 (GraphPad, San Diego CA), with significance set at $P<0.05$. Analyses were performed in a blinded way.

Results

Early upregulation of JNK1 in accelerated liver regeneration

To identify potential upstream regulators of the IHH pathway in accelerated liver regeneration we conducted an *in-silico* analysis of our RNA sequencing data sets derived from livers at early times after ALPPS, PVL, transection, or sham surgery [13]. Genes that discriminated ALPPS liver from other surgeries were included. Using string.db.org, *Mapk8* was text-mined to be linked to *Ihh* and *Ccnd1* of the hedgehog pathway (Fig 1A). Our RNA seq data suggested *Mapk8* upregulation at early times after ALPPS, which we confirmed by qPCR in a new set of animals subjected to the different surgeries (Figure 1B). The deregulation of JNK1 was further confirmed on the protein level. pJNK1, the active form of JNK phosphorylated on Thr183 and Tyr185, was upregulated as early as 1 hour after ALPPS (Fig 1C). Therefore, JNK1 activation through ALPPS surgery precedes the serum IHH peak that we have previously observed at 4h post operation [13]. From these findings, we hypothesized that JNK1 plays a part in accelerated liver regeneration as a potential instigator of IHH signaling.

Ihh and JNK1 are present in activated non-parenchymal cells

To establish an association between JNK1 and IHH signaling, we stained liver sections 4h after operation (ALPPS, PVL, transection, and sham) for IHH, ASMA (a marker of activated hepatic stellate cells [20,21]), and pJNK1. Non-parenchymal cells were positive for all the three proteins across samples (Supplementary Fig 1), suggesting pJNK1 and IHH may interact in stellate cells to accelerate regeneration. To assess localization of IHH and pJNK1 in activated hepatic stellate cells, we applied immunofluorescence (Fig 2A, Supplementary Fig 2) to paraffin-embedded liver sections after operation. pJNK1 co-localized with both αSMA and IHH, indicating their simultaneous presence in activated stellate cells.

JNK1 is thought to preferentially act in nuclei when phosphorylated [22,23]. To substantiate an JNK-IHH association, we prepared cytosolic and nuclear fractions from liver at 4h and 24h post surgery and assessed protein levels of pJNK1, the IHH downstream effector and transcription factor GLI1, and its proliferative target CCND1 [13]. Indeed, the nuclear increases in pJNK were paralleled by increases in GLI1, while nuclear levels of total JNK1 and GLI2 remained unchanged (Supplementary Fig 3). CCND1 was significantly elevated at 24h in nuclear fractions (Figure 2C), fitting its delayed induction seen on immunoblots 8h after ALPPS as previously reported [13]. On the other hand, a non-significant elevation in CCND1-positive hepatocyte nuclei was noted on immunohistochemistry at 4h post ALPPS, and was accompanied with increases in proliferative marker (Ki67, pH3) counts. Likewise, the elevated nuclear CCND1 positivity correlated with Ki67/pH3 increases at 24h post ALPPS (Figure 2C, Supplementary Fig 4).

These findings associate JNK1 activation with both the induction of IHH signaling and the promotion of proliferation following ALPPS. Therefore, JNK1 may foster regeneration in ALPPS by causing release of IHH from stellate cells to induce paracrine proliferation of hepatocytes via GLI1-CCND1. [13,22,24,25,26].

Reduction of JNK1 activity in ALPPS-treated mice abolishes regenerative acceleration

If the elevated activity of JNK1 after ALPPS is promoting acceleration of regeneration, inhibiting JNK should reduce the ALPPS effects. To decrease JNK1 activity, we chose SP600125, a specific JNK inhibitor that has been widely used in liver regeneration studies due to its specificity and ease of application [27,28]. SP600125 was injected 1h prior to

ALPPS surgery, and the assessment of pJNK1 levels in nuclear fractions confirmed a partial inhibition of the protein, with pJNK1 declining to levels seen in mice 4h after PVL (Fig 3A, Supplementary Fig 5).

DMSO vehicle injections had no significant impact on body and liver weight after ALPPS, although DMSO seemed to reduce the ALPPS effects slightly. In contrast, SP600125 significantly reduced the FLR/BW down to levels seen after PVL (Figure 3B). Congruent changes were observed for the proliferative markers Ki67 and pH3 in SP600125-treated animals (Figure 3C, Supplementary Figure 6). We conclude that partial JNK inhibition prior to ALPPS surgery reduces the regenerative speed to levels comparable to those after PVL. Therefore, JNK1 is an important instigator of the ALPPS-specific acceleration of liver regeneration.

The inhibition of JNK1 downregulates the IHH-GLI1-CCND1 axis in hedgehog signaling

To determine whether JNK1 may act through IHH signaling, we assessed the IHH pathway components in ALPPS mice treated with SP6100125 or control DMSO injection.

Following ALPPS, IHH protein levels peak in serum at 4h with little changes in the liver, consistent with the secretion of the ligand from stellate cells. The increases in serum IHH then promote GLI1 nuclear translocation, downregulation of the hedgehog inhibitor HHIP, and CCND1 upregulation from 4h onwards after ALPPS [13]. Treatment with SP600125 reduced both serum and hepatic levels of IHH 4h post ALPPS (Figure 4A), suggesting JNK1 inhibits production and/or release of the hedgehog ligand. Consistent with IHH downregulation, *Gli1* expression was decreased at 4h and 24h (Figure 4B), while *Hhip* expression was increased by SP600125 treatment at 4h after ALPPS (Figure 4C). Likewise, GLI1 protein and its target CCND1 were downregulated in nuclear fractions of ALPPS liver at 4h and 24h compared to vehicle controls (Figure 4C). Immunohistochemistry confirmed the reductions in nuclear GLI1 and CCND1 (Figure 4E-F, Supplementary Figure 9) with SP600125 treatment. No significant expression changes were observed for *Ptch1, Smo, Gli2* (Supplementary Figure 7) and nuclear GLI2 (Supplementary Figure 8), all molecules the expression of which does not change following IHH stimulation in ALPPS [13]. These findings identify IHH signaling as a potential mediator of JNK1's ability to accelerate regeneration in ALPPS.

Recombinant IHH rescues ALPPS-induced regeneration after JNK inhibition

If JNK1 is promoting its accelerating effects through IHH signaling, restoring IHH levels in SP600125-treated liver should re-accelerate the regenerative response after ALPPS surgery.

Mice were pretreated with SP600125, ALPPS-operated, injected with recombinant ligand (rIHH), and compared to vehicle (DMSO & PBS)-treated ALPPS controls. When assessing body weight after all treatments, no differences were observed between the groups. In contrast, the FLR/BW was significantly elevated after ALPPS+SP6+rIHH compared to ALPPS+SP6 (Figure 5A). Notably, DMSO/PBS injection on its own seemed to have some negative impact on ALPPS-regeneration. Nonetheless, liver weight was statistically similar for the ALPPS+DMSO+PBS and the ALPPS+SP6+rIHH groups (Figure 5A). Likewise, congruent changes were observed for the proliferative markers Ki67 and pH3 (Figure 5B, Supplementary Figure 10). Therefore, rIHH can compensate for the inhibition of JNK1 during ALPPS-associated regeneration.

Recombinant IHH re-instates hedgehog signaling and promotes JNK1 activity in SP600125-treated ALPPS liver

To further elucidate the relationship between JNK1 and IHH in ALPPS, we evaluated the levels of the individual pathway components. In SP600125-ALPPS-treated mice, rIHH increased *Gli1* and decreased *Hhip* expression (Figure 6A), as well as promoted nuclear GLI1 and CCND1 on immunoblots and immunochemistry (Figure 6B-D, Supplementary Figure 11). Again, *Ptch*, *Smo*, *Gli2* (Supplementary Figure 12), and GLI2 (Supplementary Figure 13) were not significantly affected. Intriguingly, when assessing JNK1, rIHH also increased the levels of nuclear JNK1 (Supplementary Figure 14) and of nuclear pJNK1 on both immunoblots (Figure 6E) and immunohistochemistry (Supplementary Figure 15). Therefore, IHH can increase the activity of JNK1 in ALPPS liver with partially inhibited JNK1, suggesting the presence of a positive feedback loop between JNK1 and IHH. Altogether, these findings establish IHH as a downstream effector of JNK1 in the acceleration of regeneration after ALPPS surgery.

Discussion

Liver regeneration is a complex molecular response unique in its ability to restore full function to the organ [29]. Many pathways have been identified to participate, such as signaling through the hedgehog pathway [18,28]. Nevertheless, liver regeneration does not occur in all patient scenarios, as liver failure ensues if the loss of functional tissue is too extensive [4]. With the introduction of ALPPS, the regenerative capacity has been extended and is expected to improve outcomes of two-staged hepatectomies in patients with marginal qualifications for resection. The unprecedented effect of ALPPS on liver recovery has provoked strong interest in the mechanisms underlying the acceleration of liver regeneration.

Here, we demonstrate a hitherto undescribed interaction between JNK1 and IHH in stellate cells that acts to instigate accelerated liver regeneration early after ALPPS step 1 surgery. More specifically, we demonstrate that (i) JNK1 activation is associated with liver weight gain and precedes the upregulation of IHH-GLI1-CCND1 signaling, (ii) partial inhibition of JNK1 reduces the rate of regeneration to that seen after PVL alone, along with congruent decreases in the IHH-GLI1-CCND1 axis, and that (iii) recombinant IHH is sufficient to restore ALPPS regeneration in JNK1-inhibited mice.

The alterations we observed following ALPPS, SP600125, and rIHH treatments were consistently reflected in GLI1-CCND1 nuclear levels and were strongly correlated with changes in proliferative markers as well as liver weight changes. On the other hand, molecules of the hedgehog pathway that were not affected through IHH (i.e. Ptch, Smo, GLI2) were also not altered through JNK1 manipulation. Moreover, the changes in these hedgehog components were examined via PCR, Western blots as well as immunohistochemical approaches. Therefore, we can reliably conclude that JNK1 initiates the IHH-GLI1-CCND1 axis in accelerated regeneration.

As a limitation to this study, pharmaceutical inhibition was employed to inhibit JNK1 activity during our ALPPS experiments. Genetic knockout models may provide more clear-cut evidence; however, we decided for a pharmacological approach to reduce rather than block JNK activity, given the presence of low levels of pJNK1 also after PVL, the main ALPPS control surgery. Knockdown strategies may be an alternative, however SP600125 has been widely used in liver research including regeneration studies [22,23,26,28,32], rendering our study comparable to existing work on hepatic JNK.

JNK1's role after partial hepatectomy has been revealed by the observation that its inhibition blocks hepatocyte proliferation and liver regeneration [18,28,30]. JNK1 is activated within one hour after partial hepatectomy, leading to AP-1 activation, the promotion of

cyclin D1 expression, and hepatocellular G0-G1 transition [22,30,31]. Interestingly, through studies in fibrosis, JNK1 was found to be involved in HSC activation, where it promotes ASMA expression and HSC proliferation [22,32]. The morphogenic hedgehog network likewise is recognized to be essential to liver regeneration and to promote expansion of activated HSCs [13,15,18,33]. However, whether JNK1 interacts with the Hedgehog pathway after partial hepatectomy is unknown.

In analogy to regeneration after partial hepatectomy, we observed JNK1 upregulation one hour after ALPPS. Furthermore, JNK1 localized to activated HSCs. The co-localization of IHH and JNK1 in activated HSCs suggested a novel link between these two molecules, which we could demonstrate through SP600125 and recombinant IHH. Indeed, studies in skin cancer have revealed a link between JNK1 and the hedgehog pathway; there, JUN (the canonical JNK1 target) required synergistic interaction with GLI1 for full activation of downstream molecules [34]. Therefore, complex interactions appear to exist between JNK1 and hedgehog signaling.

Unlike after partial hepatectomy, ALPPS did not increase the number of ASMA-positive cells, suggesting JNK1 activity does not promote HSC activation in these settings. While JNK1 clearly promotes regeneration after hepatectomy and ALPPS, the associated mechanisms seem to differ in some aspects. In ALPPS, the interaction between JNK1 and IHH is key in instigating accelerated regeneration. The extent to which IHH participates in regeneration after hepatectomy is unknown; however, the early, strong IHH secretion is unique after ALPPS, as plasma IHH increases occur at much later times and only at modest levels after resection [13,18]. On the other hand, we observed a statistically significant elevation of serum SHH at 4h after partial hepatectomy relative to ALPPS [13], suggesting SHH rather than IHH may be the hedgehog ligand relevant after resection. However, whether JNK1 is interacting with SHH after hepatectomy remains unknown. In mice, hepatectomy leads to little parenchymal injury, whereas in ALPPS, liver injury through parenchymal transection is preceded by ligation, which on its own induces regeneration through mechanisms that are ill-defined. Therefore, the divergent nature of the initial regenerative stimuli may underlie the timing and the set of interacting proteins/pathways that define the speed of regeneration after a given surgery.

In this regard, an intriguing observation is that recombinant IHH not only restored accelerated regeneration in SP600125-treated mice, but in parallel increased the activity of the partially inhibited JNK1. These findings imply IHH enhances JNK1 activities in retrograde to promote its own secretion. While further evidence is required to establish such mechanisms, a positive feedback loop between JNK1 and IHH would provide an attractive explanation for the enhanced IHH secretion and the regenerative acceleration unique to ALPPS.

Interestingly, both JNK and Hedgehog have prominent roles in the handling of liver injury. JNK is most notably activated by TNF-alpha, a cytokine involved in the pathophysiology of many types of liver injury, including viral hepatitis, alcoholic liver disease, and ischemia-reperfusion injury. Activated JNK phosphorylates its targets (c-Jun, ATF-2, and JunD), and these transcription factors then activate genes that are involved in the regulation of inflammation, proliferation, and cell death. In the past few years, the use of JNK inhibitors has led to the understanding that the duration of JNK activation is critical for its pro-apoptotic effects in injury [35]. For example, *Gunawan et al* showed that transient blockade of JNK activity through SP600125 was able to rescue mice from acetaminophen-induced liver injury [36]. Similarly, the Hedgehog pathway has been identified to play a role in liver repair such as in regeneration and acute liver injury. In fibrogenic repair, production of Hedgehog ligands increases to

permit ligand-receptor interaction and activation of the Hedgehog signaling pathway, which is thought to be vital for the reconstitution of normal liver architecture [37]. In other tissues such as skin, reduced SHH production has been associated with the delayed healing seen in mice with diabetes, a condition closely related to liver disease [38]. Therefore, transient activation of JNK and Hedgehog pathways are important physiological processes fostering the repair of injured liver tissue.

Chronic activation of JNK1, however, has been associated with the development and progression of hepatocellular carcinoma (HCC) [39]. Consistent JNK1 activity has been reported to predict a bad outcome in HCC, an aspect that perhaps relates to JNK1 activation secondary to chronic liver injury, an accepted cause of HCC. Although the pro-apoptotic function of JNK1 has been related to anti-cancerous actions [40], recent evidence indicates a more complex situation, as JNK1 may directly promote the repair of DNA breaks [39]. These observations suggest a disturbed balance between the removal or repair of damaged hepatocytes that underlies JNK1's association with a bad HCC outcome [39]. Indeed, a dual role of JNK1 in HCC has been postulated through animal models, where either its loss or its overactivation contribute to the development of malignancy [22]. Similarly, chronic hedgehog signaling has been linked to HCC. High levels of hedgehog components in HCC seem to maintain the proliferation of cancer stem cells, thereby contributing to HCC progression [41]. Likewise, liver diseases associated with chronic injury and an elevated HCC risk (i.e. nonalcoholic fatty liver disease) are accompanied by a chronic overactivation of the hedgehog pathway [42]. On the other hand, JNK1 and hedgehog activities remain associated with the successful healing of tissue injury, consistent with the view that transient activity of these molecules may be beneficial for the liver. [16,18,28,31,38,43]

The first cases of ALPPS occurred in patients in Germany where the technique to induce accelerated regeneration of the liver was discovered by chance [6,7]. By combination of portal vein ligation and transection, extensive tumor resection was performed and patient recovery occurred in record time [44,45,46]. The understanding of ALPPS-triggered processes is in its infancy; however, underlying mechanisms begin to emerge, with the JNK1-IHH axis a first example of ALPPS-specific molecular events that can be associated with the unprecedented regenerative acceleration. Short-term activation of JNK1 and IHH might be of use in the clinic. Not every patient requiring ALPPS may qualify for this major surgery; for example, highly morbid patients that may tolerate PVL, but not the more invasive ALPPS, may benefit from a JNK1-IHH-based promotion of regeneration. Although the oncological risks associated with long-term activation will not vanish, the prevention of imminent death due to liver failure may justify the use of compounds activating the JNK1-IHH pathway. Understanding the extent to which the JNK1 and IHH signals can be stimulated may open the opportunity for pharmacological administration to encourage regeneration in at-risk-patients, eventually expanding the boundaries of success in the treatment of liver disease one step further.

Grant support

This study was funded by the Clinical Research Priority Program (CRPP) from the University of Zurich “non-resectable liver tumors – from palliation to cure” and the Swiss National Science Foundation (S-87002-09-01).

Authors’ contributions

Experimental design: ML, BH. Data acquisition and analyses: ML, BH. Data interpretation: BH, ML, RG. Study concept and design: BH. Manuscript writing & critical revision: ML, BH, PAC. Funding: PAC, BH, RG. All authors approved the final version.

Acknowledgements

We would like to Udo Ungethüm, Ursula Süss, and Pia Fuchs for excellent technical assistance.

References

1. Clavien PA, Oberkofler C, Raptis DA, et al. What is critical for liver surgery and partial liver transplantation: size or quality? Hepatology 2010; 52:712-729.
2. Clavien PA, Petrowsky H, DeOliveira M, et al. Strategies for safer liver surgery and partial liver transplantation. N Engl J Med 2007; 356:1545-1559.
3. Jaeck D, Oussoultzoglou E, Rosso E, et al. A two-stage hepatectomy procedure combined with portal vein embolization to achieve curative resection for initially unresectable multiple and bilobar colorectal liver metastases. Ann Surg 2004; 240:1037-1049.
4. Donati M, Stavrou GA, Oldhafer KJ. Current position of ALPPS in the surgical landscape of CRLM treatment proposals. World J Gastroenterol 2013; 19:6548-6554.
5. Schadde E, Ardiles V, Slankamenac K, et al. ALPPS offers a better chance of complete resection in patients with primarily unresectable liver tumors compared with conventional-staged hepatectomies: results of a multicenter analysis. World J Gastroenterol 2014; 38:1510-1519.
6. de Santibañes E, Clavien PA. Playing Play-Doh to prevent postoperative liver failure: the "ALPPS" approach. Ann Surg 2012; 255:415-417.
7. Schnitzbauer AA, Lang SA, Goessmann H, et al. Right portal vein ligation combined with in situ splitting induces rapid left lateral liver lobe hypertrophy enabling 2-staged extended right hepatic resection in small-for-size settings. Ann Surg 2012; 255:405-414.
8. Garcia-Perez R, Revilla-Nuin B, Martines CM, et al. Associated Liver Partition and Portal Vein Ligation (ALPPS) vs Selective Portal Vein Ligation (PVL) for Staged Hepatectomy in a rat model. Similar regenerative response? PLoS One. 2015; 10:e0144096.
9. Shi H, Yang G, Zheng T, et al. A preliminary study of ALPPS procedure in a rat model. Sci Rep. 2015; 5:17567.
10. Kron P, Linecker M, Limani P, et al. Hypoxia-driven Hif2a coordinates mouse liver regeneration by coupling parenchymal growth to vascular expansion. Hepatology. 2016; 64: 2198-2209.
11. Schadde E, Tsatsaris C, Swiderska-Syn M, et al. Hypoxia of the growing liver accelerates regeneration. Surgery. 2017; 161: 666-679.
12. Schlegel A, Lesurtel M, Melloul E, et al. ALPPS: from human to mice highlighting accelerated and novel mechanisms of liver regeneration. Ann Surg 2014; 260:839-846.
13. Langiewicz M, Schlegel A, Saponara E, et al. Hedgehog pathway mediates early acceleration of liver regeneration induced by a novel two-staged hepatectomy in mice. J Hepatol. 2017; 66:560-570.
14. Friedman SL. Evolving challenges in hepatic fibrosis. Nat Rev Gastroenterol Hepatol. 2010; 7:425-436.
15. Swiderska-Syn M, Xie G, Michelotti GA, et al. Hedgehog regulates Yes-Associated Protein 1 in regeneration mouse liver. Hepatology. 2016; 64:232-244.
16. Michelotti GA, Xie G, Swiderska M, et al. Smoothened is a master regulator of adult liver repair. J Clin Invest. 2013; 126:2380-2394.
17. Swiderska-Syn M, Syn WK, Xie G, et al. Myofibroblastic cells function as progenitors to regenerate murine livers after partial hepatectomy. Gut. 2014; 63:1333-1344.
18. Ochoa B, Syn WK, Delgado I, et al. Hedgehog signaling is critical for normal liver regeneration after partial hepatectomy in mice. Hepatology. 2010; 51:1712-1723.
19. Lehman K, Tschuor C, Rickenbacher A, et al. Liver failure after extended hepatectomy in mice is mediated by a

p21-dependent barrier to liver regeneration. Gastroenterology 2012; 143:1609-1619.
20. DeLeve LD, Wang X, Guo Y. Sinusoidal endothelial cells prevent rat stellate cell activation and promote reversion to quiescence. Hepatology 2008; 48:920-930.
21. Mabuchi A, Mullaney I, Sheard P, et al. Role of hepatic stellate cells in the early phase of liver regeneration in rat: formation of tight adhesion to parenchymal cells. Comp Hepatol 2004; 3:S29.
22. Seki E, Brenner DA, Karin M. A liver full of JNK: signaling in regulation of cell function and disease pathogenesis, and clinical approaches. Gastroenterology 2012; 142:307-320.
23. Davies C, Tournier C. Exploring the function of the JNK (c-Jun N-terminal kinase) signaling pathway in physiological and pathological processes to design novel therapeutic strategies. Biochem Soc Trans 2012. 40:85-89.
24. Farzan SF, Singh S, Schilling NS, et al. The adventures of sonic hedgehog in development and repair. III Hedgehog processing and biological activity. Am J Physiol Gastrointest Liver Physiol 2008; 294:G844-G849.
25. Ingham PW, McMahon AP. Hedgehog signaling in animal development: paradigms and principles. Genes & Dev 2001; 15:3059-3087.
26. Kluwe J, Pradere JP, Gwak GY, et al. Modulation of hepatic fibrosis by c-Jun-N-terminal kinase inhibition. Gastroenterology 2010; 138:347-359.
27. Bennet BL, Sasaki DT, Murray BW, et al. SP600125, an anthrapyrazolone inhibitor of Jun N-terminal kinase. Proc Natl Acad Sci USA 2001; 98:13681-13686.
28. Schwabe RF, Bradham CA, Uehara T, et al. c-Jun-N-terminal kinase drives cyclin D1 expression and proliferation during liver regeneration. Hepatology 2003; 37:824–832.
29. Michalopoulos GK. Liver regeneration. J Cell Physiol 2007; 213:286-300.
30. Westwick JK, Weitzel C, Leffert HL, et al. Activation of Jun kinase is an early event in hepatic regeneration. J Clin Invest 1995; 95:803-810.
31. Alcorn JA, Feitelberg SP, Brenner DA. Transient induction of c-jun during hepatic regeneration. Hepatology 1990; 11:909–915.
32. Schnabl B, Bradham CA, Bennett BL, et al. TAK1/JNK and p38 have opposite effects on rat hepatic stellate cells. Hepatology 2001; 34:953–963.
33. Omenetti A, Choi S, Michelotti G, et al. Hedgehog signaling in the liver. J Hepatol 2011; 54:366-373.
34. Laner-Plamberger S, Kaser A, Paulischta M, et al. Cooperation between GLI and JUN enhances transcription of JUN and selected GLI target genes. Oncogene 2009; 2:1639-1651.
35. Schwabe RF, Brenner DA. Mechanisms of Liver Injury. I. TNF-alpha-induced liver injury: role of IKK, JNK, and ROS pathways. Am J Physiol Gastrointest Liver Physiol 2006; 290:G583-589.
36. Gunawan BK, Liu ZX, Han D, et al. c-Jun N-terminal kinase plays a major role in murine acetaminophen hepatotoxicity. Gastroenterology 2006; 131:165-178.
37. Choi SS, Omenetti A, Syn WK, et al. The role of hedgehog signaling in fibrogenic liver repair. Int J Biochem Cell Biol 2011; 43:238-44.
38. Luo JD, Hu TP, Wang L, et al. Sonic hedgehog improves would healing via enhancing cutaneous nitric oxide function in diabetes. Am J Physiol Endocrinol Metab 2009; 297:E525-531
39. Boege Y, Malehmir M, Healy ME, et al. A dual role of caspase-8 in triggering and sensing proliferation-associated DNA damage, a key

determinant of liver cancer development. Cancer Cell 2017; 32:342-359.
40. Iansante V, Choy PM, Fung SW et al. PARP14 promotes the Warburg effect in hepatocellular carcinoma by inhibiting JNK1-dependent PKM2 phosphorylation and activation. Nat Commun 2015; 10:7882.
41. Della Corte CM, Viscardi G, Papaccio F, et al. Implicaiton of the hedgehog pathway in hepatocellular carcinoma. World J Gastroenterol 2017; 23:4330-4340.
42. Guy CD, Suzuki A, Zdanowicz M, et al. Hedgehog pathway activation parallels histologic severity of injury and fibrosis in human nonalcoholic fatty liver disease. Hepatology 2012; 55:1711-1721.
43. Behrens A, Sibilia M, David JP, et al. Impaired postnatal hepatocyte proliferation and liver regeneration in mice lacking c-jun in the liver. EMBO J 2002; 21:1782-1790.
44. Baumgart J, Lang S, Lang H. A new method for induction of liver hypertrophy prior to right trisectionectomy: a report of three cases. *HPB (Oxford)* 2011; 13 (Suppl 2):71–72.
45. de Santibanes E, Alvarez FA, Ardiles V. How to avoid postoperative liver failure: a novel method. *World J Surg* 2012; 36:125–128.
46. Alvarez FA, Iniesta J, de Santibanes E, et al. New method of hepatic regeneration. *Cir Esp* 2011; 89:645–64

Figures

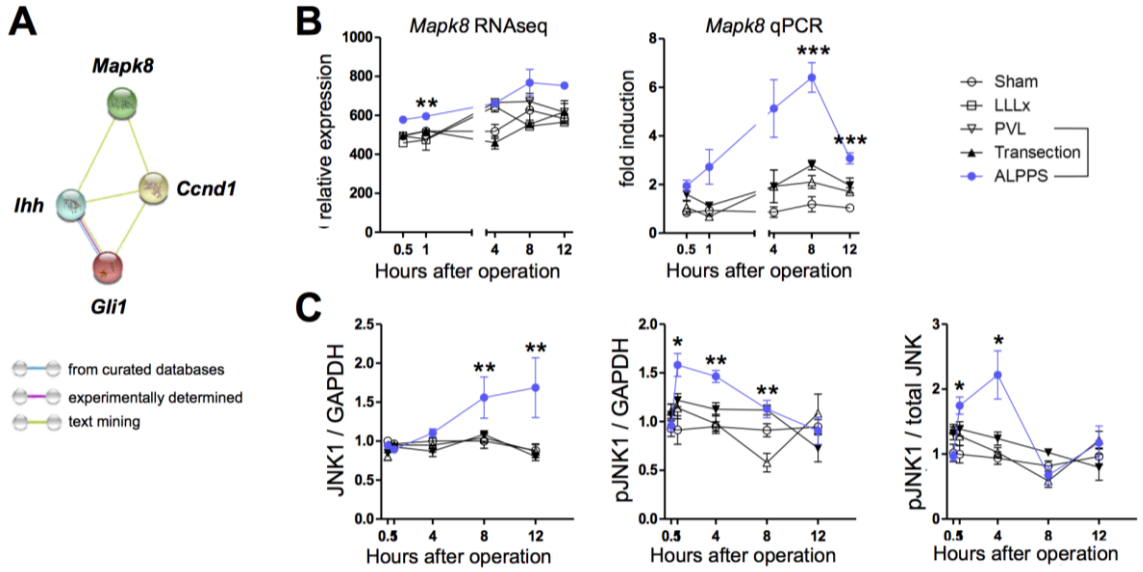

Figure 1. JNK1 is upregulated early after ALPPS. *(A)* In-silico analysis linking components of the hedgehog pathways to *Mapk8* (JNK1) by the String database. Green lines represent suspected links between genes from their database of publications. Blue and pink lines represent experimentally determined links between genes. *(B)* Raw hepatic gene expression values of *Mapk8* from RNA sequencing data and corresponding qPCR validation. *(C)* Hepatic protein expression (normalized to GAPDH) of JNK1 and pJNK1 after surgery. N=5/group, t-test, *P<0.05, ** P<0.01. ***P<0.001. Significances refer to ALPPS vs. PVL comparison.

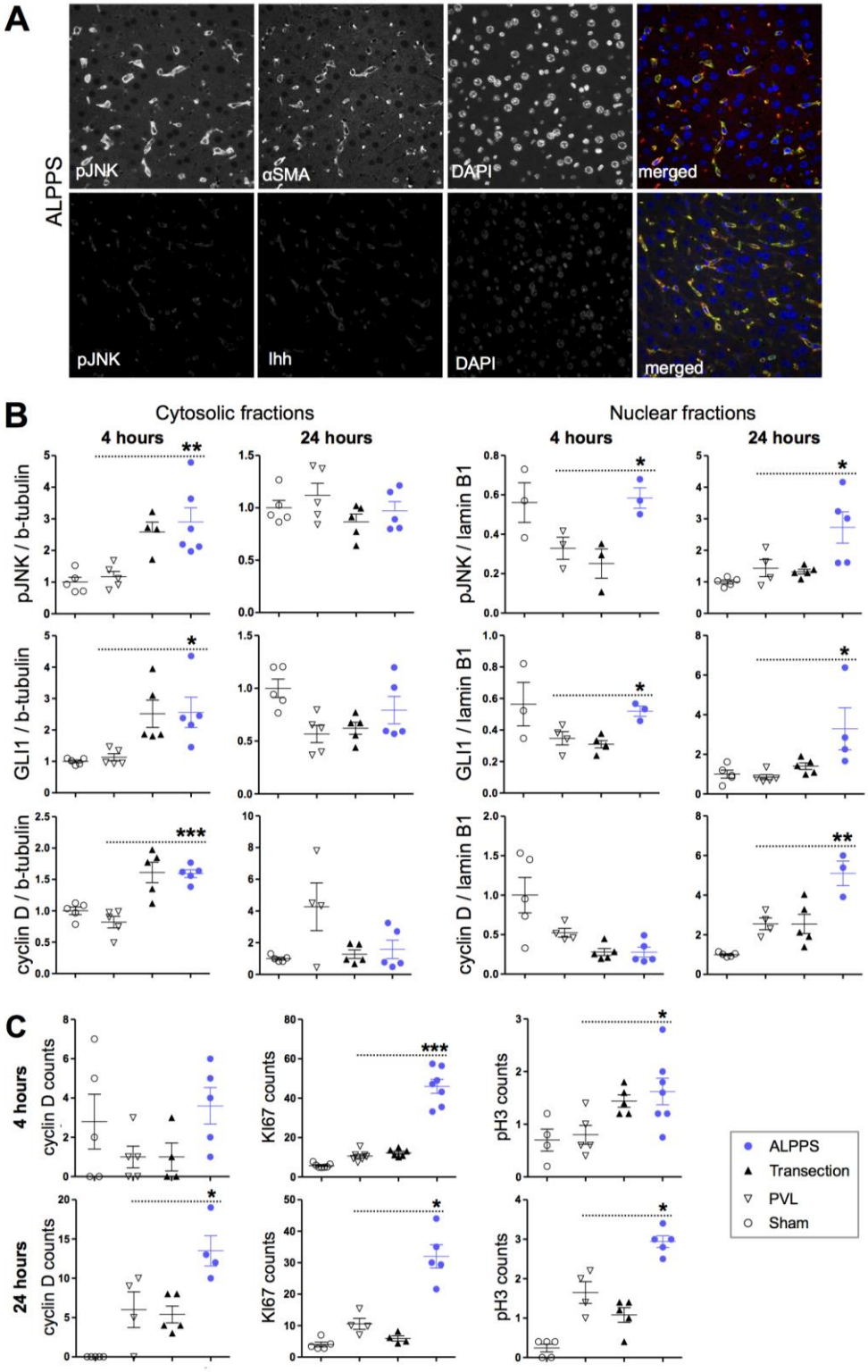

Figure 2. JNK1/IHH cellular location and associated downstream signaling in liver *(A)* pJNK1/alpha-SMA and pJNK1/Ihh immunofluorescence co-stain showing co-localization of both proteins in nonparenchymal cells (see Supplementary Figure 1 and 2 for stainings in control surgeries) . *(B)* Cytosolic and nuclear protein levels (normalized to β-tubulin and lamin B1, respectively; see immunoblots in Supplementary Figure 16) of pJNK1, GLI1, and Cyclin D. *(C)* Counts of cyclin D, Ki67, and bold pH3-positive hepatocyte nuclei hepatocyte counts(see Supplementary Figure 4 for corresponding stains). N=5/group. t-test, *P<0.05,** P<0.01, ***P<0.001. Significances refer to ALPPS vs. PVL comparison.

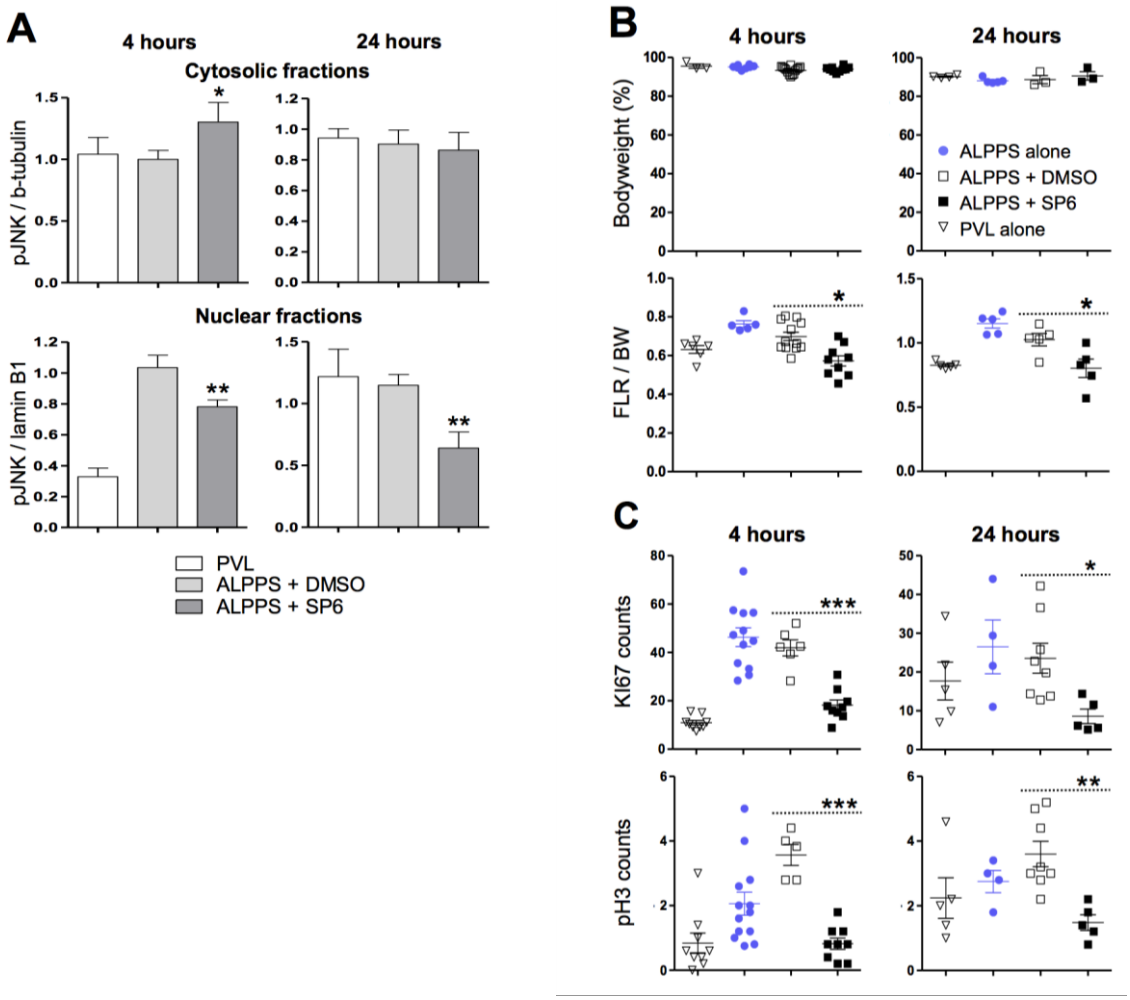

Figure 3. JNK1 inhibition reduces the regenerative speed after ALPPS. *(A)* Cytosolic and nuclear pJNK1 levels (normalized to β-tubulin and lamin B1, respectively; see Supplementary Fig. 16 for immunoblots in). N=5/group. *(B)* Body weight and liver weight regain (expressed as percent FLR/BW) after surgery and treatment with SP600125 are shown in the left and right graph, respectively. *(C)* Corresponding Ki67 and pH3 counts (see Supplementary Fig. 6 for stains). N=5/group, t-test, *P<0.05, **P<0.01, ***P<0.001 for ALPPS + DMSO *versus* ALPPS + SP6 unless otherwise indicated.

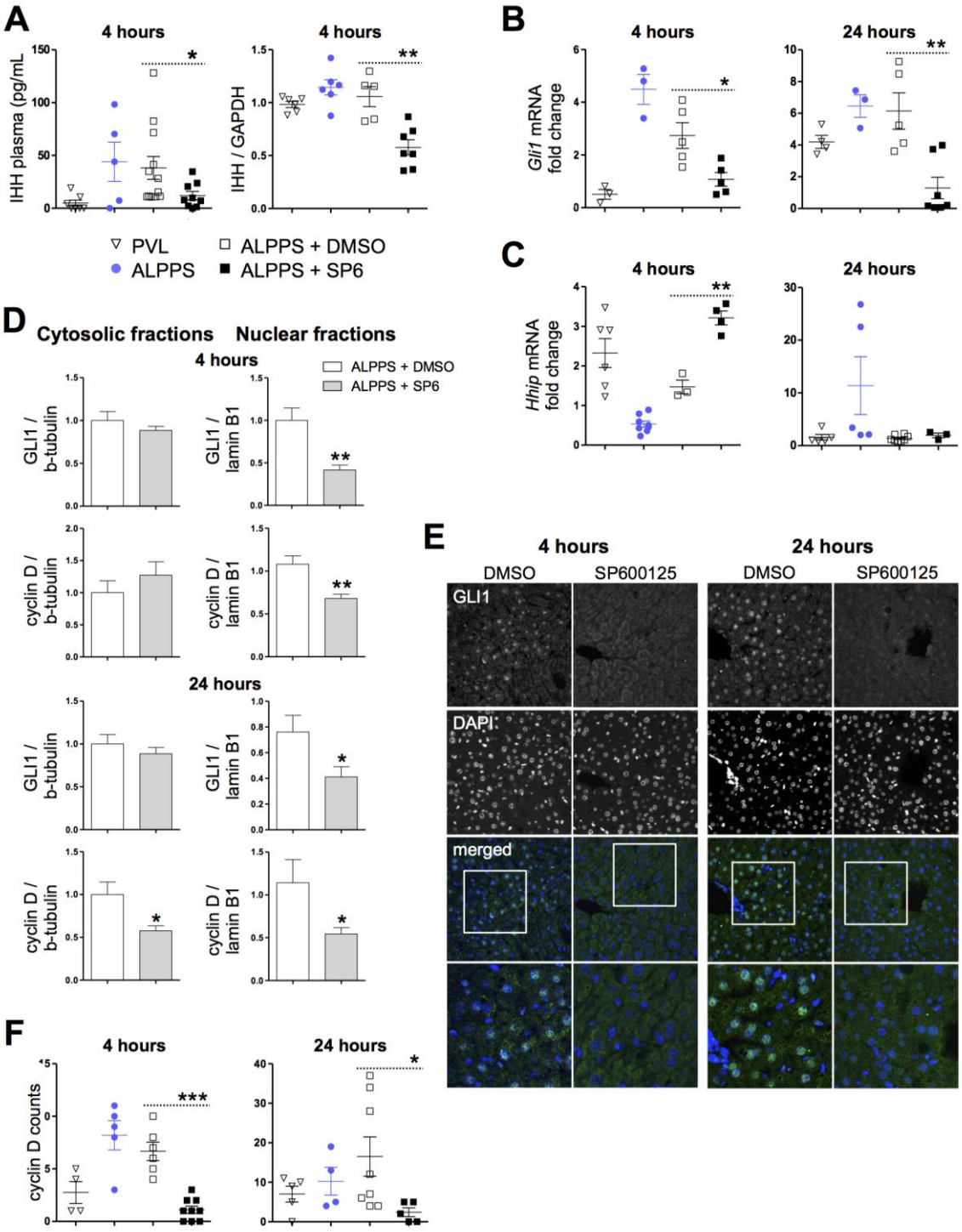

Figure 4. JNK1 inhibition dpwnregulates the IHH pathway after ALPPS. *(A)* Plasma IHH levels (ELISA) and hepatic protein expression (normalized to GAPDH) after surgery and treatment. Hepatic gene expression of *(B) Gli1* and *(C) Hhip* after surgery and treatment. *(D)* Cytosolic and nuclear protein levels (normalized to β-tubulin and lamin B1, respectively) of GLI1 and Cyclin D. *(E)* Immunofluorescence for hepatic GLI1. Note that SP600125 treatment reduces nuclear staining in hepatocytes. (*F*) Cyclin D counts (see Supplementary Fig. 9 for stains). N=5/group, t-test, *P<0.05, **P<0.01, ***P<0.001 for ALPPS + DMSO vs ALPPS + SP6.

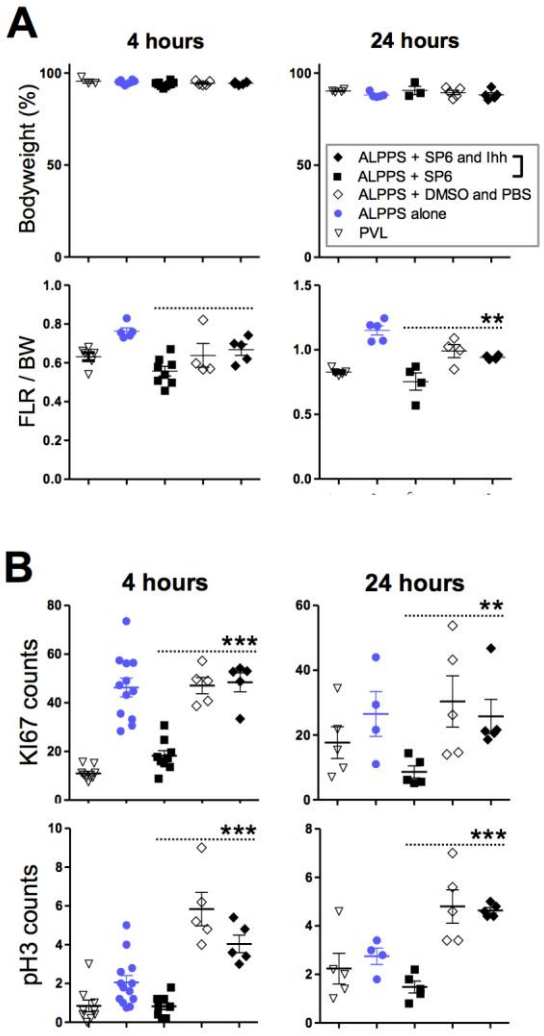

Figure 5. Effects of JNK1 inhibition combined with recombinant IHH treatment on regeneration after ALPPS. *(A)* Body weight and liver weight (FLR/BW) after ALPPS+ SP6 with/without rIHH *versus* corresponding vehicle controls and ALPPS or PVL alone. *(B)* Corresponding Ki67 and pH3 counts (see Supplementary Fig. 10 for stain). N=5/group, t-test, *P<0.05, **P<0.01, ***P<0.001 for ALPPS + SP6 *versus* ALPPS + SP6 and recombinant Ihh.

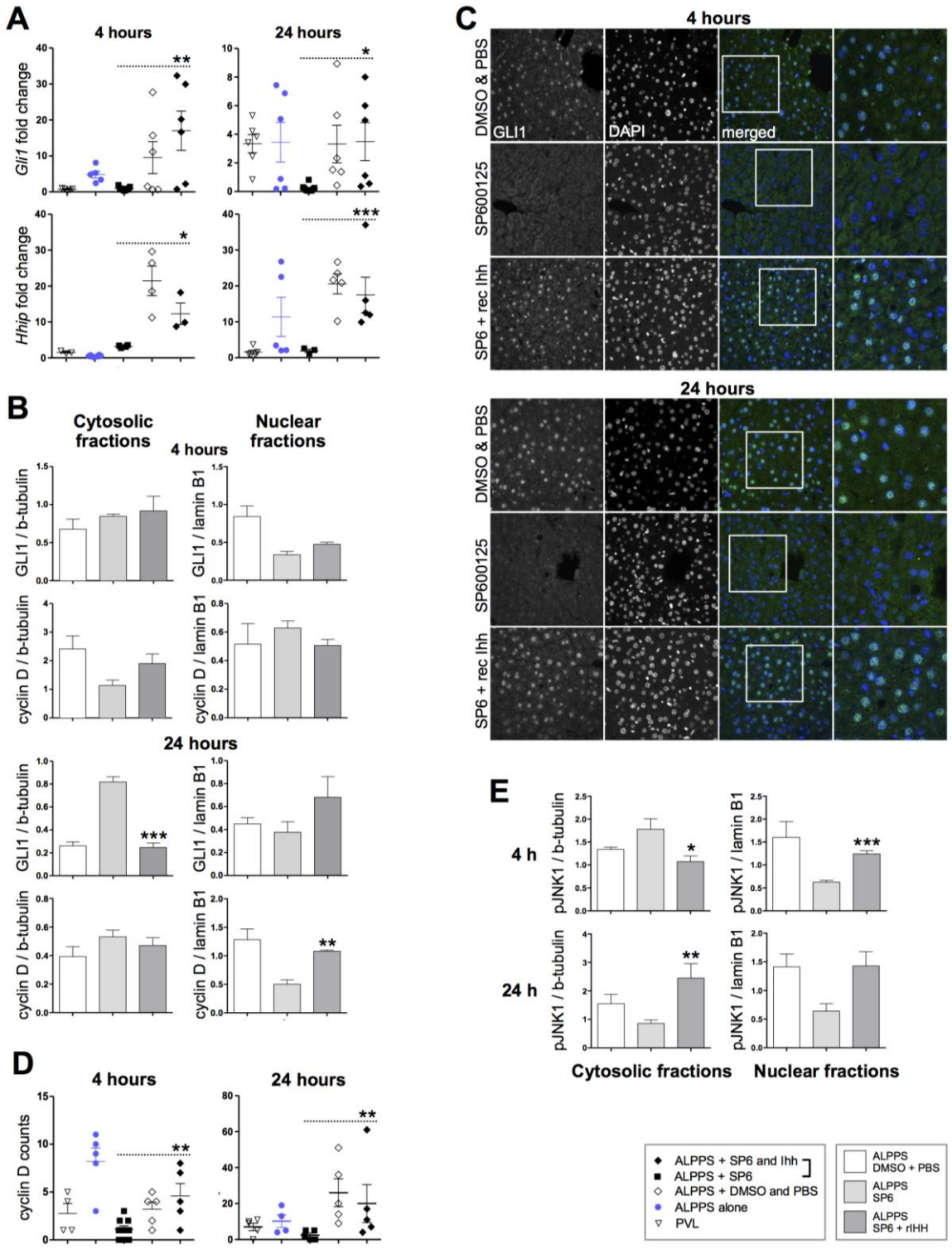

Figure 6. Effects of JNK1 inhibition combined with recombinant IHH treatment on hedgehog signaling after ALPPS. *(A)* Hepatic gene expression of *Gli1* and *Hhip* after surgery and treatment. *(B)* Cytosolic and nuclear protein levels (normalized to β-tubulin and lamin B1, respectively) of GLI1 and Cyclin D. *(C)* Immunofluorescence for hepatic GLI1. Note the restoration of nuclear GLI1 expression in SP600125-treated liver through rIHH. *(D)* Cyclin D nuclear counts see Supplementary Figure 11 for stains) *(E)* Cytosolic and nuclear protein levels of pJNK1. N=5/group, t-test, *P<0.05, **P<0.01, ***P<0.001 for ALPPS + SP6 *versus* ALPPS + SP6 and rIHH.

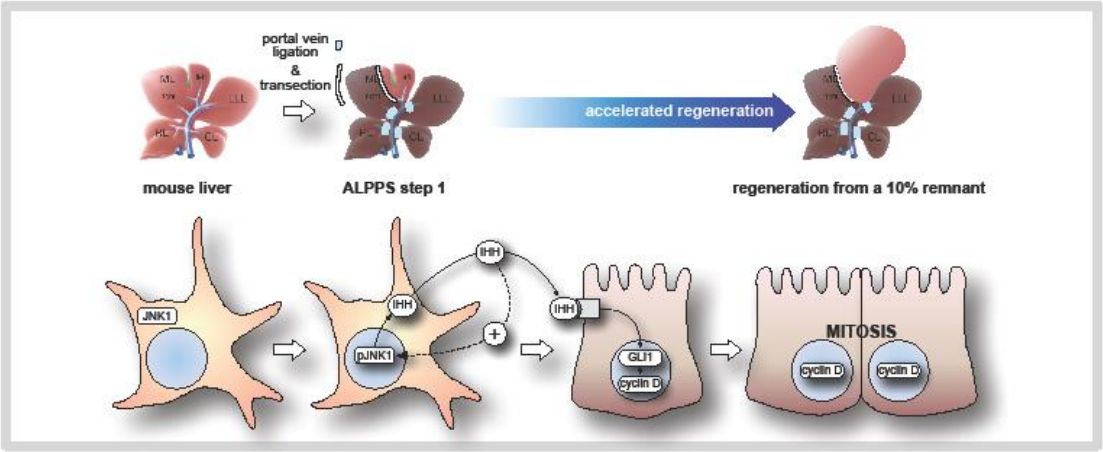

Figure 7. JNK1-IHH signaling from stellate cells as an accelerator of liver regeneration following ALPPS surgery. Upon ligation and transection, JNK1 is activated in stellate cells to induce IHH secretion. Paracrine activation of the IHH downstream effector GLI1 promotes cyclin D expression in hepatocytes, accelerating the cell cycle to enable the regeneration of functional liver remnants as small as 10% of the original hepatic volume. IHH further seems to elevate JNK1 activity, suggesting a feed forward mechanism that may contribute to the acceleration of regeneration.

Supplementary Materials

Supplementary Tables

Table S1. Taqman gene expression assays

gene name	Applied Biosystems order no.
Gli1	Mm00494654_m1
Gli2	Mm01293117_m1
Hhip	Mm00469580_m1
Ptch1	Mm00436026_m1
Smo	Mm01162710_m1
18S rRNA	Control reagents

Table S2. Antibodies

Antigene	Company (order no.)	Dilution
Ki67	Abcam, Cambridge, UK (ab16667)	1:200 (IHC)
pH3	Millipore, Schaffhausen, CH (06-570)	1:500 (IHC)
Ihh	Abcam, Cambridge, UK (ab39634)	1:500 (IHC)
Gli1	R&D, Zug, CH (Mab3324)	1:50 (IF) 1:5000 (WB)
Gli2	Abcam, Cambridge, UK (ab26056)	1:500 (WB)
cyclin D	Abcam, Cambridge, UK (ab16663)	1:100 (IHC) 1:100 (WB)
Alpha-SMA	Abcam, Cambridge, UK (ab32575)	(IF)
pJNK	Santa Cruz, CA USA (sc6254)	(IF)
pJNK	R&D, Zug, CH (AF1205)	(IHC)
Ihh	Abcam, Cambridge, UK (ab39634)	(IF) (IHC)
lamin B1	Santa Cruz, CA USA (sc-377001)	1:500 (WB)
β-tubulin	Cell Signaling, MA USA (2128S)	1:1000 (WB)

Supplementary Figures

Figure S1. Immunohistochemistry for IHH, ASMA, and pJNK1 on liver post surgery.

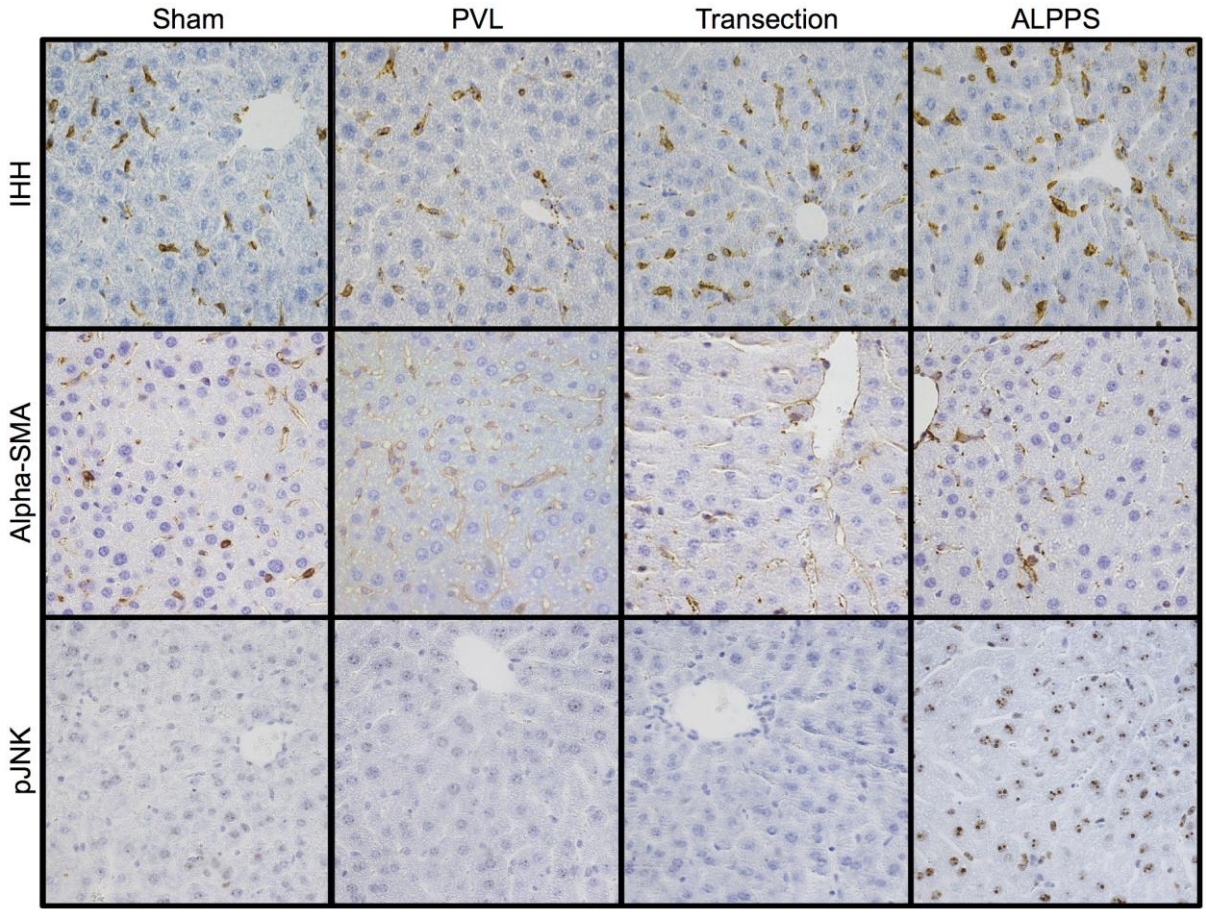

Supplementary Figure 1. Representative immunostainings for IHH, ASMA, and pJNK1 on liver at four hours after ALPPS, PVL, transection, and sham operations. 40x magnification.

Figure S2. Immunofluorescent co-stains for pJNK1/ASMA and pJNK1/IHH on liver post control surgeries.

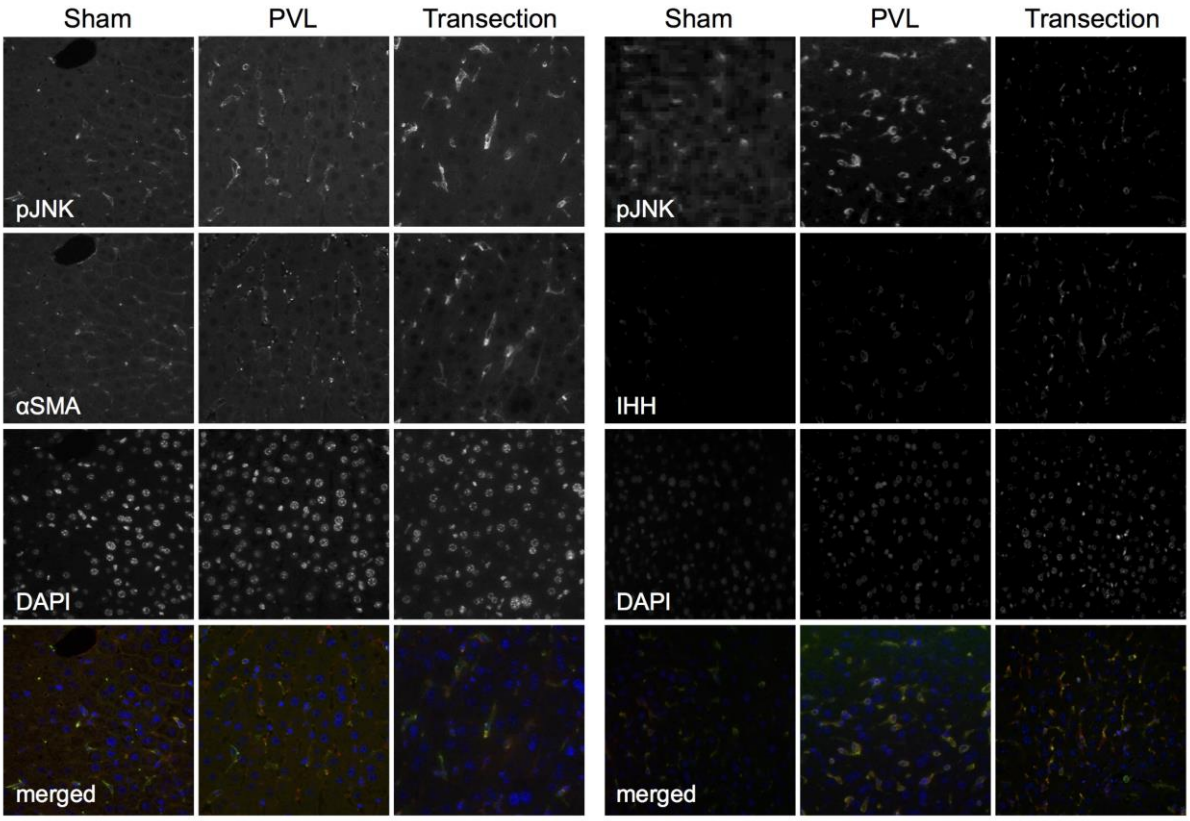

Supplementary Figure 2. Representative immunofluorescent co-stains for pJNK1/ASMA and pJNK/IHH on liver four hours after PVL, transection, and sham operations. 40x magnification.

Figure S3. JNK1 and GLI2 protein expression in ALPPS versus control surgeries

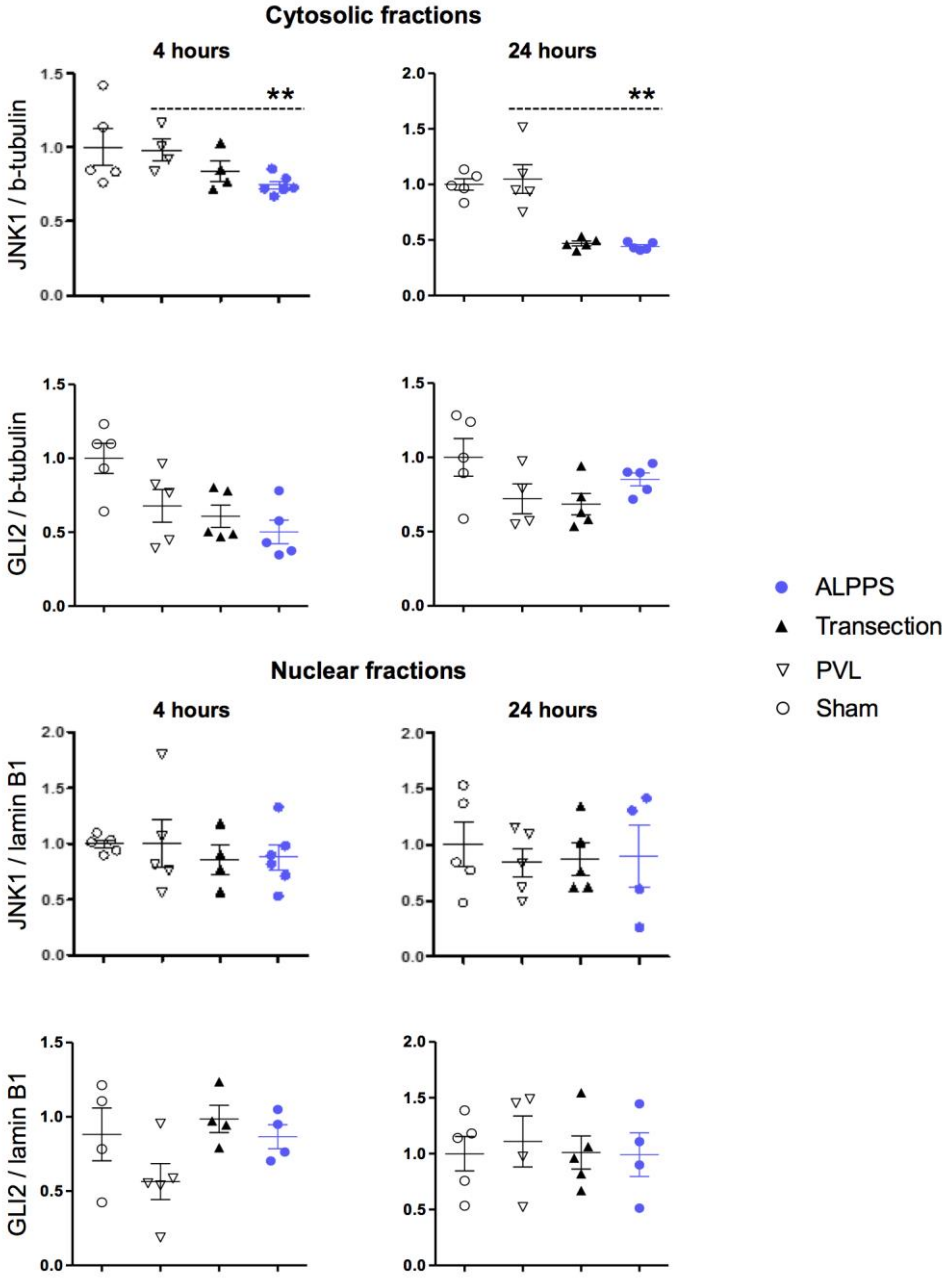

Supplementary Figure 3. JNK1 and GLI2 cytosolic and nuclear protein levels after ALPPS or its surgical controls. N=5 per group. t-test, *P<0.05, **P<0.01. ***P<0.001. Significances refer to ALPPS vs. PVL comparison unless otherwise stated.

Figure S4. H&E staining and immunohistochemistry for Ki67, pH3, and cyclin D on liver post surgery.

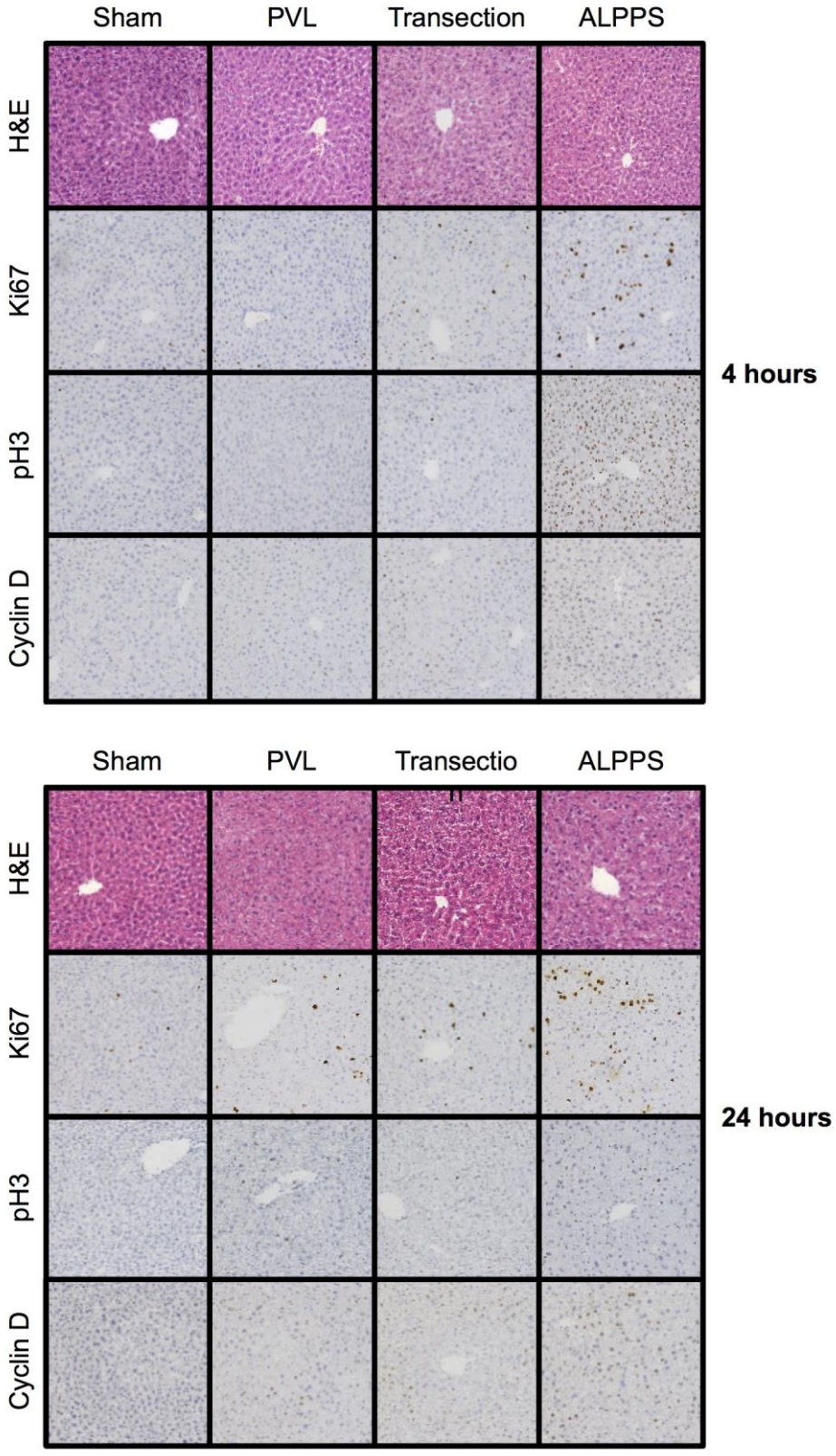

Supplementary Figure 4. Representative immunostainings for H&E, Ki67, pH3, and cyclin 1 on liver after ALPPS, PVL, transection, and sham operations. Quantitations are shown in Figure 1E. 20x magnification.

Figure S5. JNK1 nuclear and cytosolic protein levels after JNK inhibition with SP600125.

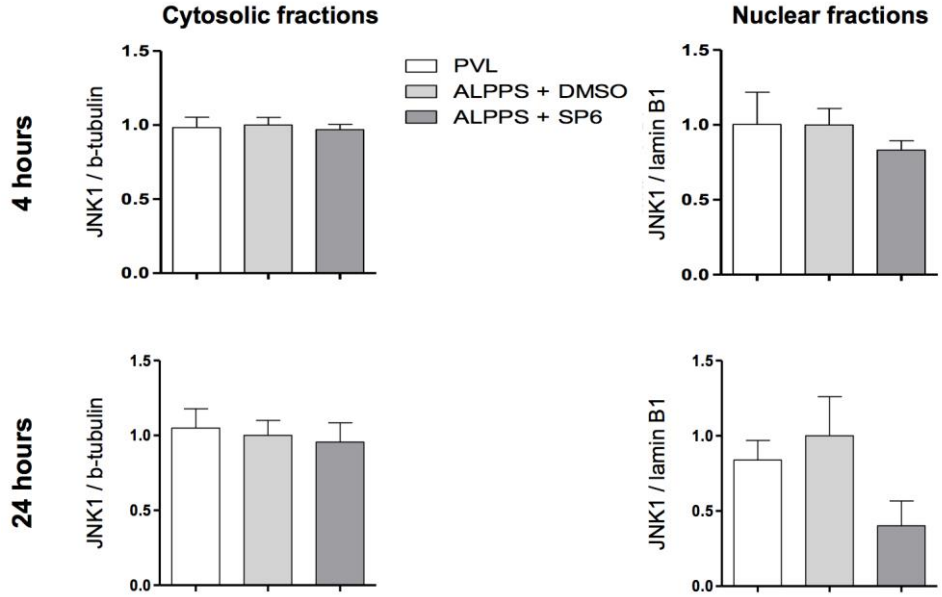

Supplementary Figure 5. JNK1 nuclear and cytosolic protein levels determined by western blot in ALPPS livers with control injection (DMSO) or SP600125. N=5 per group. No significant differences between ALPPS+DMSO and ALPPS+SP6 group comparisons.

Figure S6. Immunohistochemistry for H&E, Ki67, and pH3 on liver after JNK1 inhibition by SP6.

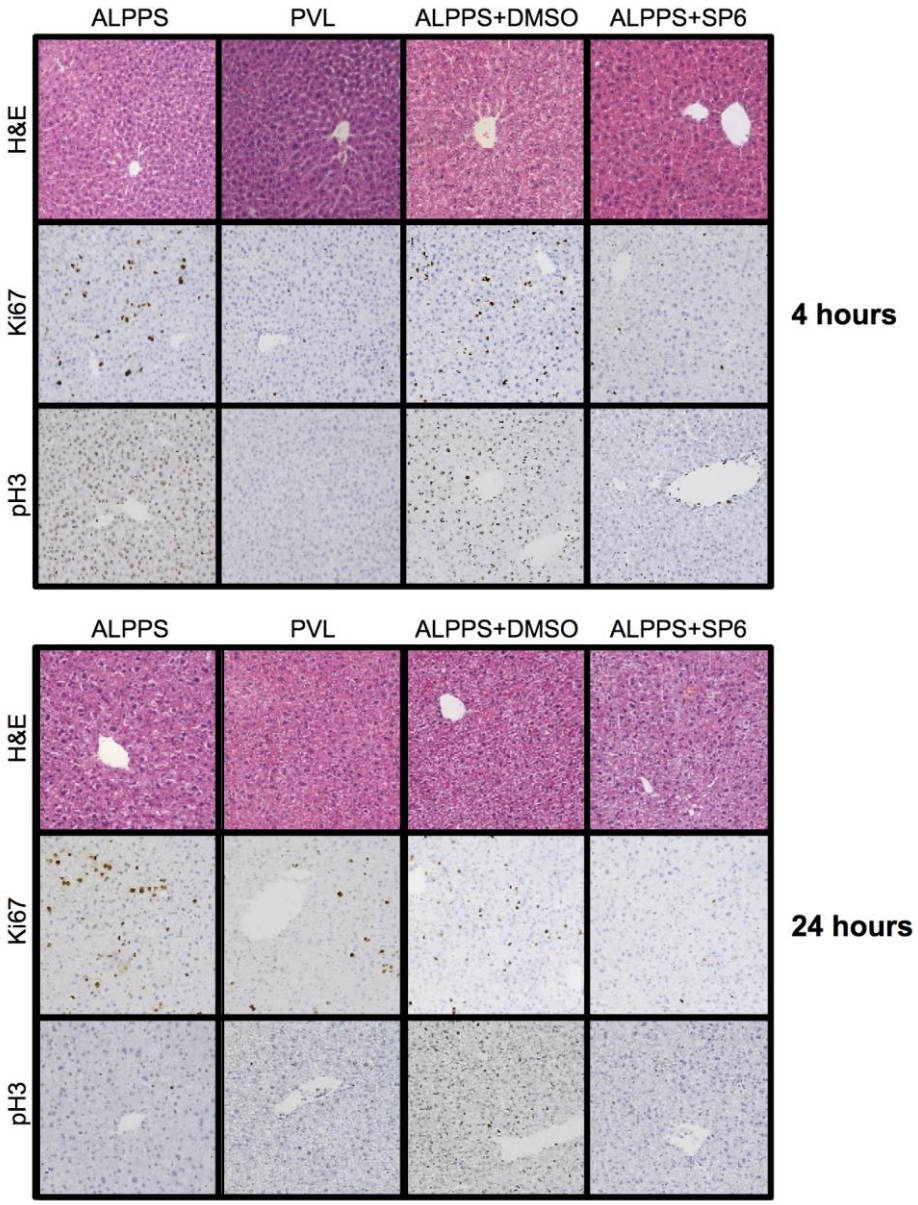

Supplementary Figure 6. Representative immunostainings for H&E, KI67, and pH3 on liver after treatment of ALPPS mice with DMSO, vehicle, or SP600125. 20x magnification.

Figure S7. mRNA analysis of *Smo*, *Ptch1*, *Gli2*, and *Hhip* in livers with JNK1 inhibition by SP6.

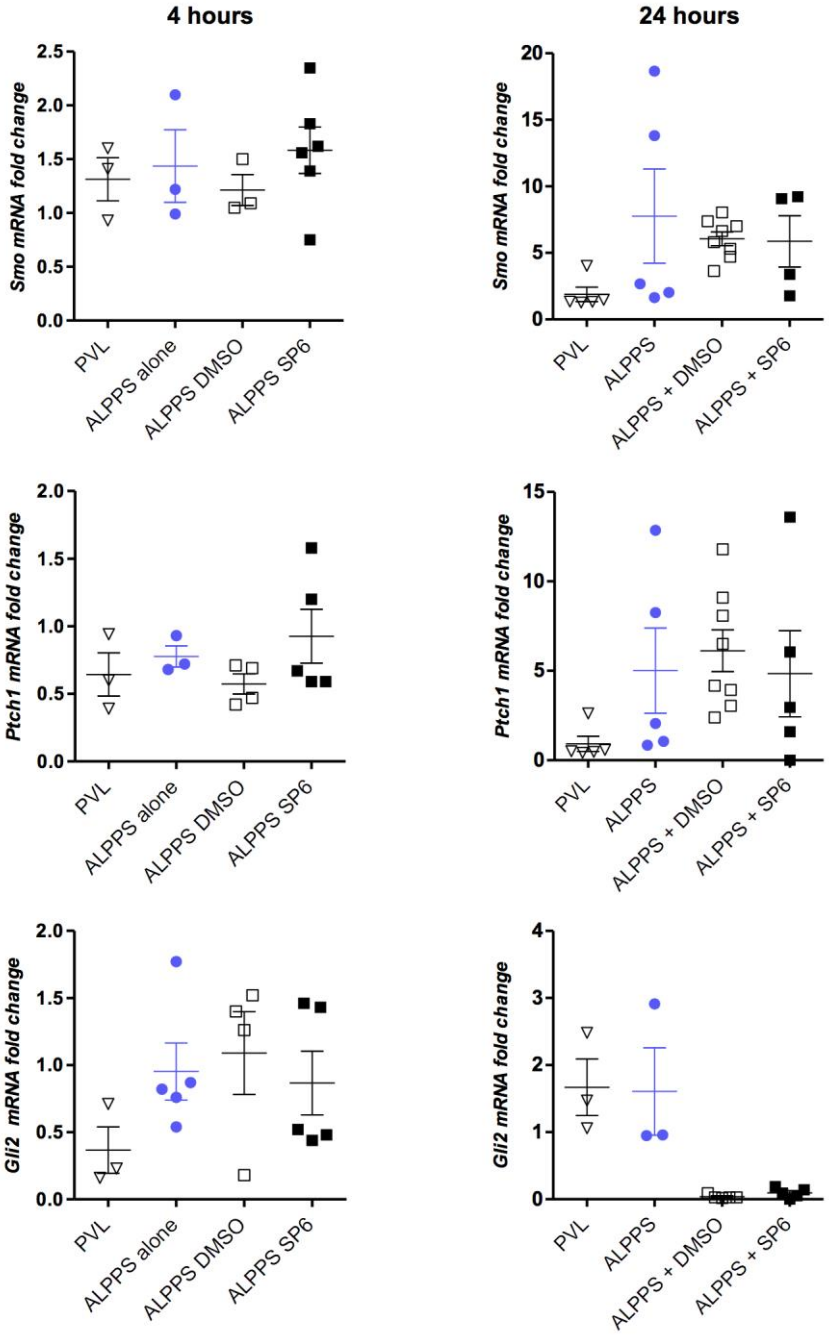

Supplementary Figure 7. mRNA expression analysis of downstream components of IHH signaling in livers with JNK1 inhibition. N=5 per group. No significant differences between ALPPS+DMSO and ALPPS+SP6 group comparison.

Figure S8. GLI2 protein levels in livers with JNK1 inhibition by SP6.

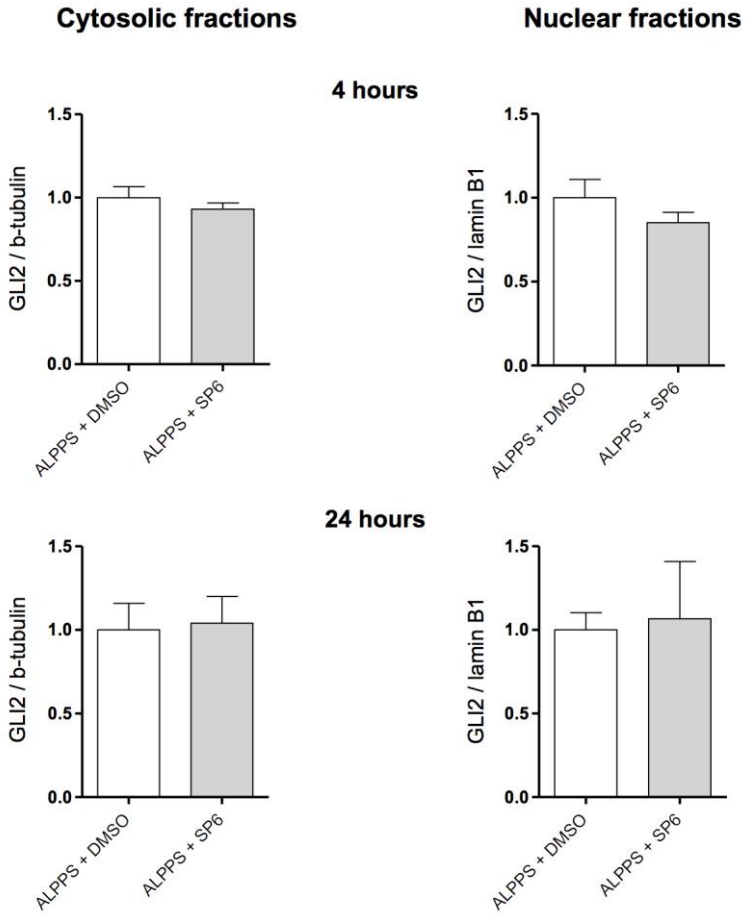

Supplementary Figure 8. Hepatic GLI2 protein levels in nuclear and cytosolic fractions after vehicle (DMSO) or SP600125 treatment followed by ALPPS. N=5 per group. No significant differences between ALPPS+DMSO and ALPPS+SP6 group comparison.

Figure S9. Immunohistochemistry for cyclin D1 on liver after JNK1 inhibition by SP6.

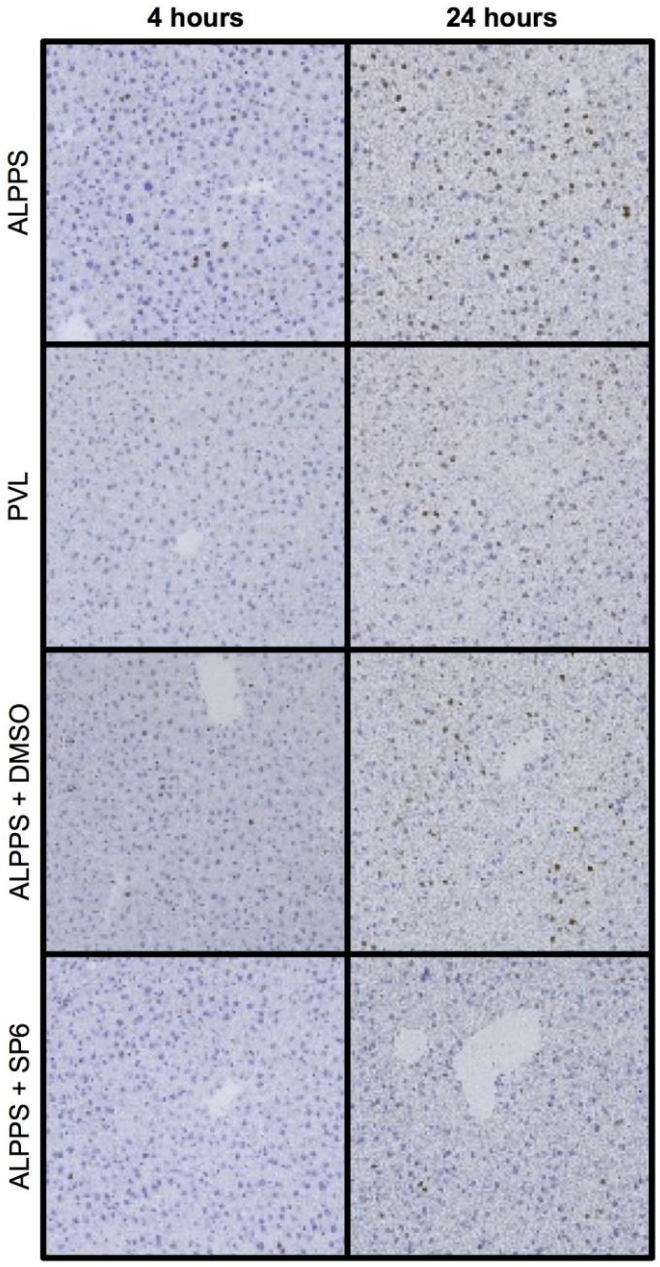

Supplementary Figure 9. Representative immunostainings for pJNK and cyclin D on liver after treatment of ALPPS mice with DMSO vehicle or SP600125. 20x magnification.

Figure S10. Immunohistochemistry for H&E, Ki67, and pH3 on livers with JNK1 inhibition by SP6 and recombinant IHH treatment.

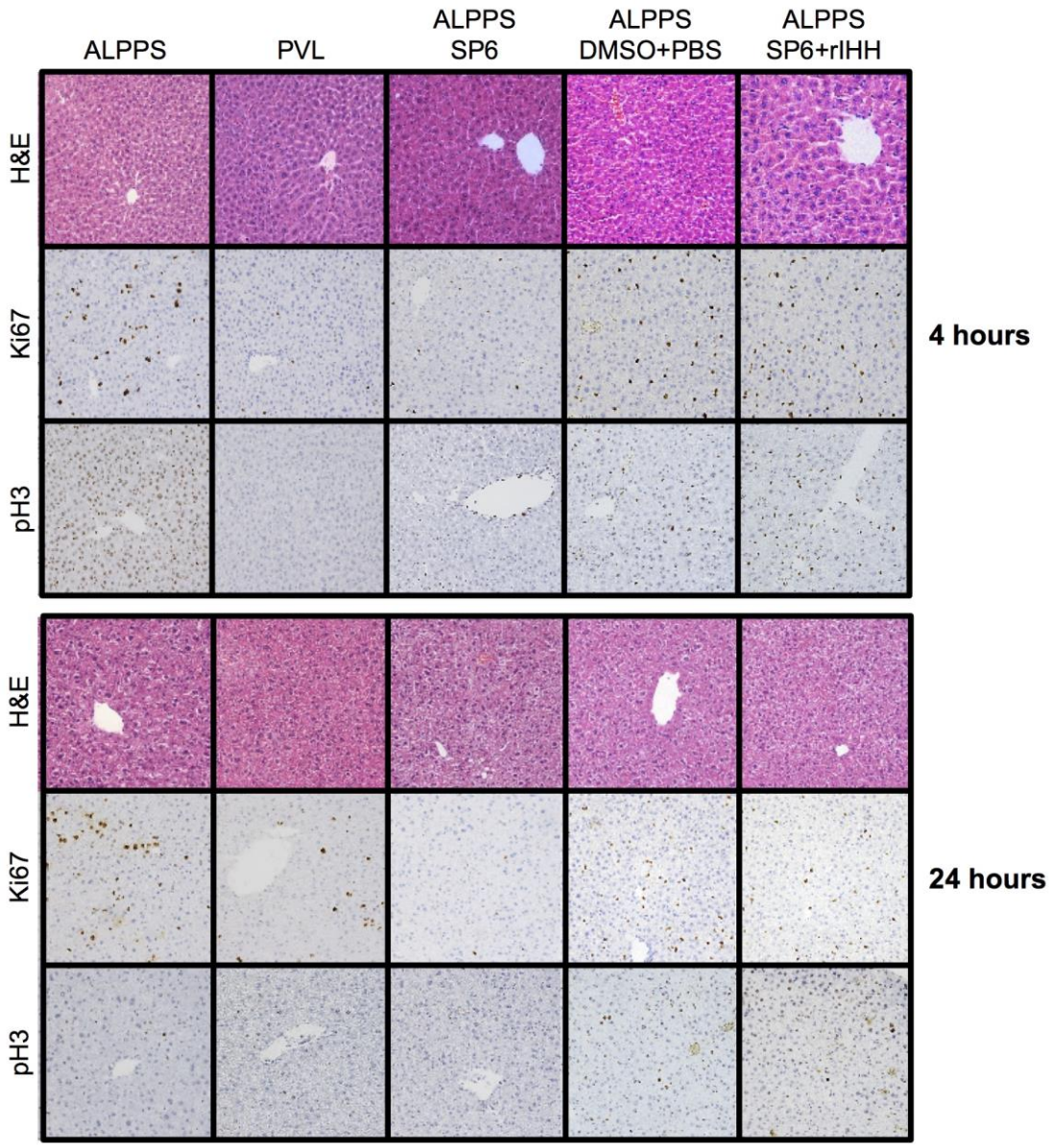

Supplementary Figure 10. Representative immunostainings for H&E, KI67, and pH3 on liver after treatment of ALPPS mice with vehicle injections (DMSO and PBS), or SP600125, or SP600124 and recombinant IHH injections. 20x magnification.

Figure S11. Immunohistochemistry for cyclin D on liver after JNK1 inhibition and recombinant IHH treatment.

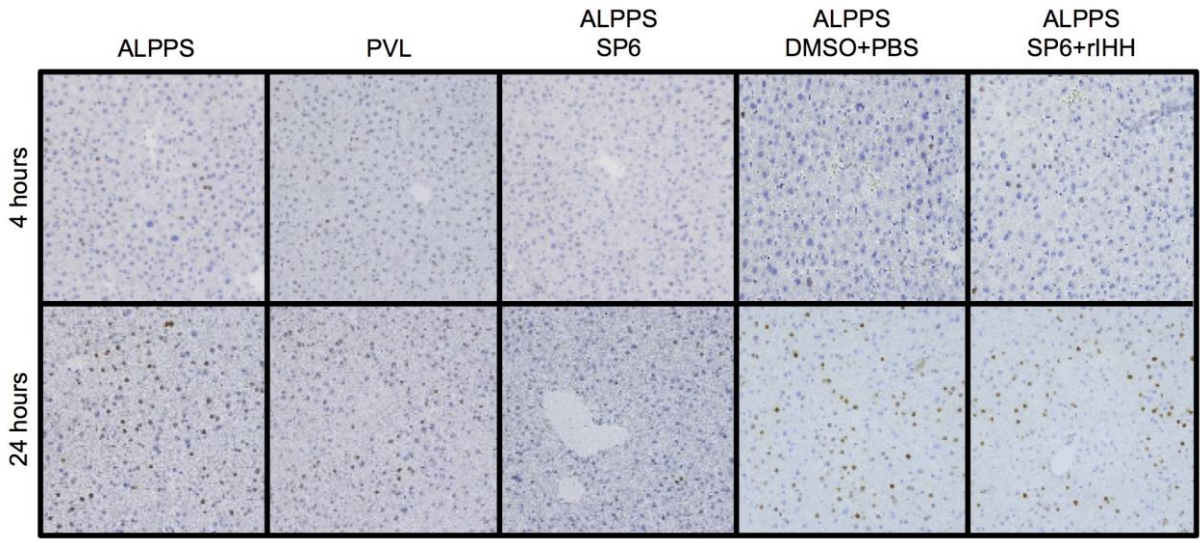

Supplementary Figure 11. Representative immunostainings for pJNK and cyclin D1 on liver after treatment of ALPPS mice with vehicle (DMSO and PBS), or SP600125, or SP600125 and recombinant IHH treatment. 20x magnification.

Figure S12. mRNA analysis of *Ptch1*, *Smo*, *Gli2*, and *Hhip* in livers with JNK1 inhibition and recombinant IHH treatment.

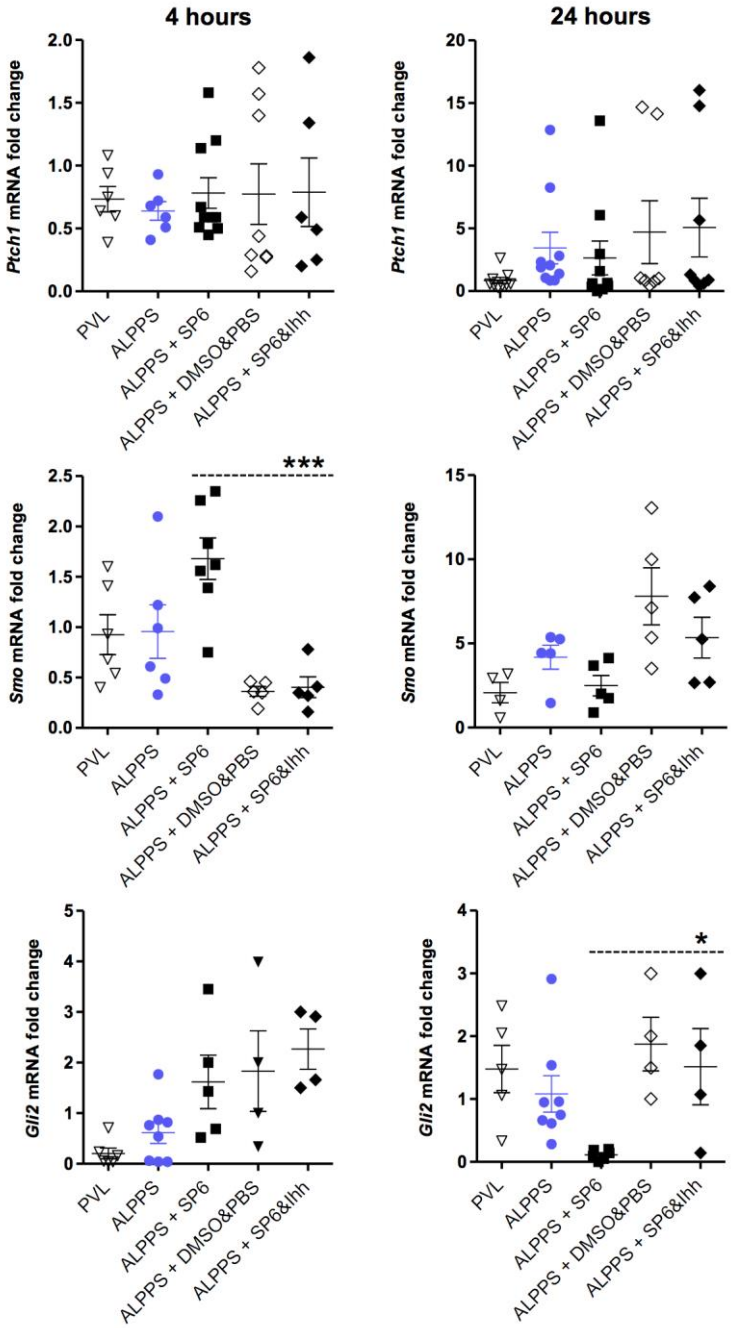

Supplementary Figure 12. mRNA expression analysis of downstream components of IHH signaling in livers with JNK inhibition and recombinant IHH treatment. N=5 per group. t-test, *P < 0.05, **P < 0.01. ***P < 0.001. Significances refer to ALPPS+SP6 vs. ALPPS+SP6+rIHH comparison.

Figure S13. GLI2 protein levels in livers with JNK1 inhibition and recombinant IHH treatment.

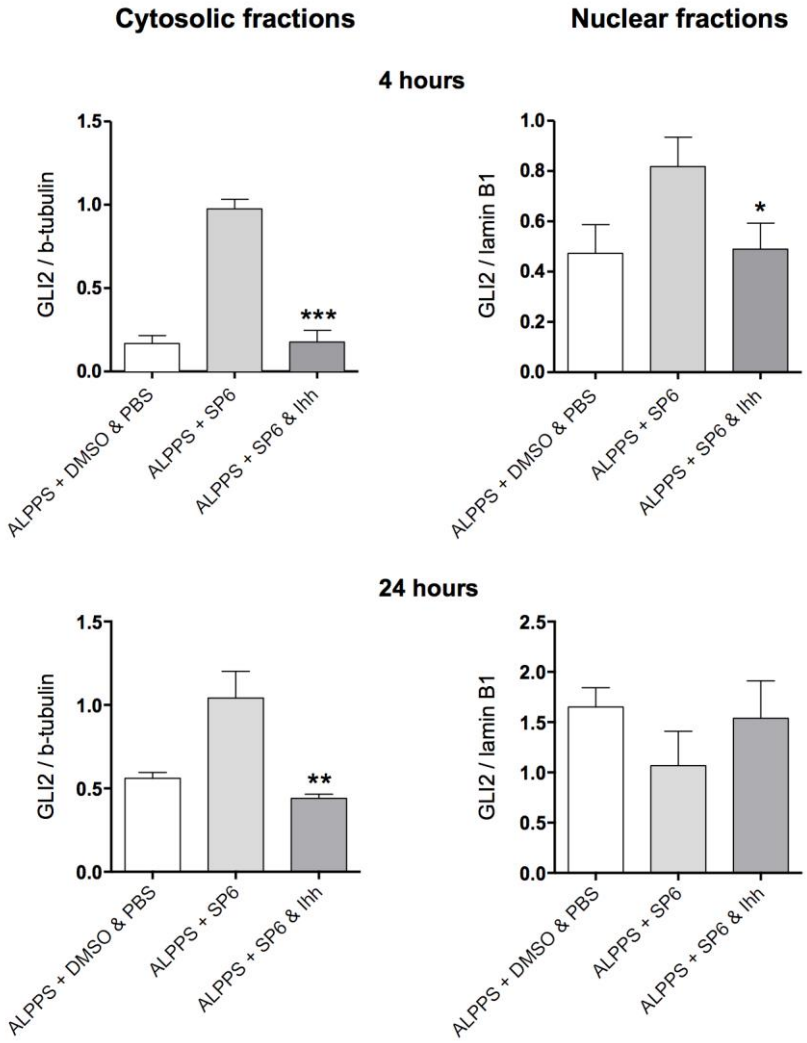

Supplementary Figure 13. GLI2 protein levels in nuclear and cytosolic fractions in livers with vehicle (DMSO&PBS), or SP600125, or SP600125 and recombinant IHH treatment. N=5 per group. t-test, *P < 0.05, **P < 0.01. ***P < 0.001. Significances refer to ALPPS+SP6 vs. ALPPS+SP6+rIHH comparison.

Figure S14. JNK1 protein levels in livers after JNK loss treatment and recombinant Ihh treatment.

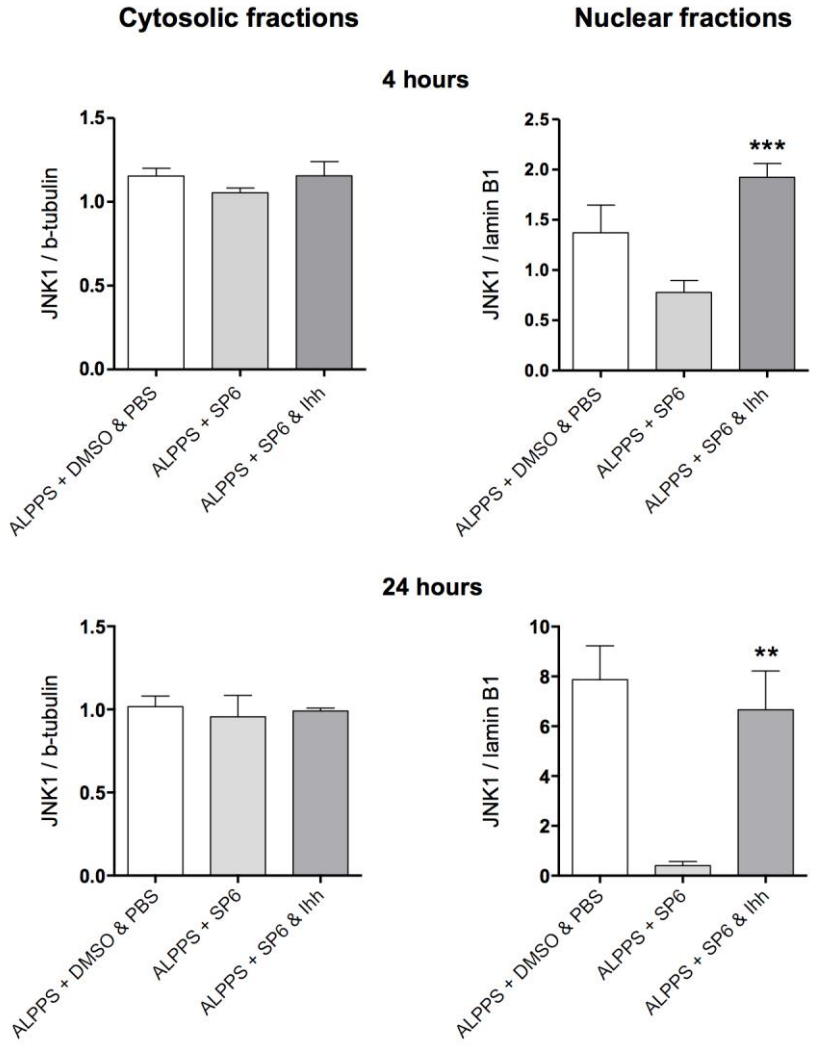

Supplementary Figure 14. JNK1 protein levels in nuclear and cytosolic fractions in livers of ALPPS mice treated with vehicle injection (DMSO & PBS), or SP600125, or SP600125 and recombinant IHH (referring to Figure 6E). N=5 per group. t-test, *P < 0.05, **P < 0.01. ***P < 0.001. Significances refer to ALPPS+SP6 vs. ALPPS+SP6+rIHH comparison.

Figure S15. Immunohistochemistry for pJNK1 on liver after JNK1 inhibition and recombinant IHH treatment.

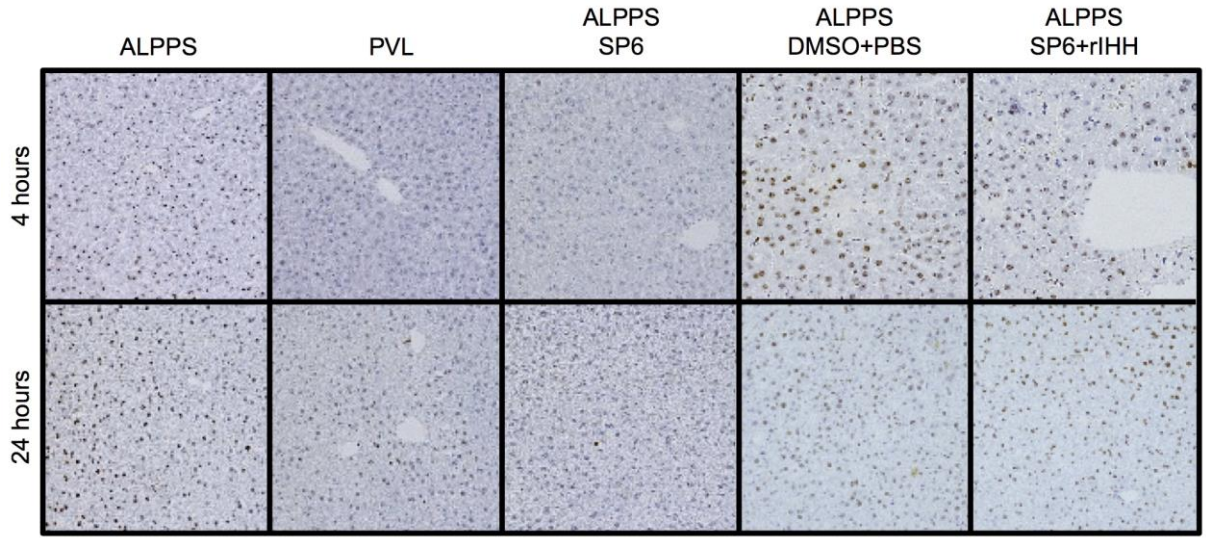

Supplementary Figure 15. Representative immunostainings for pJNK1 on liver after treatment of ALPPS mice with vehicle (DMSO and PBS), or SP600125, or SP600125 and recombinant IHH treatment. 20x magnification. Note the moderate re-elevation in pJNK1 nuclear expression in SP600125-rIHH-treated liver, consistent with a positive feedback between IHH and JNK1.

Discussion

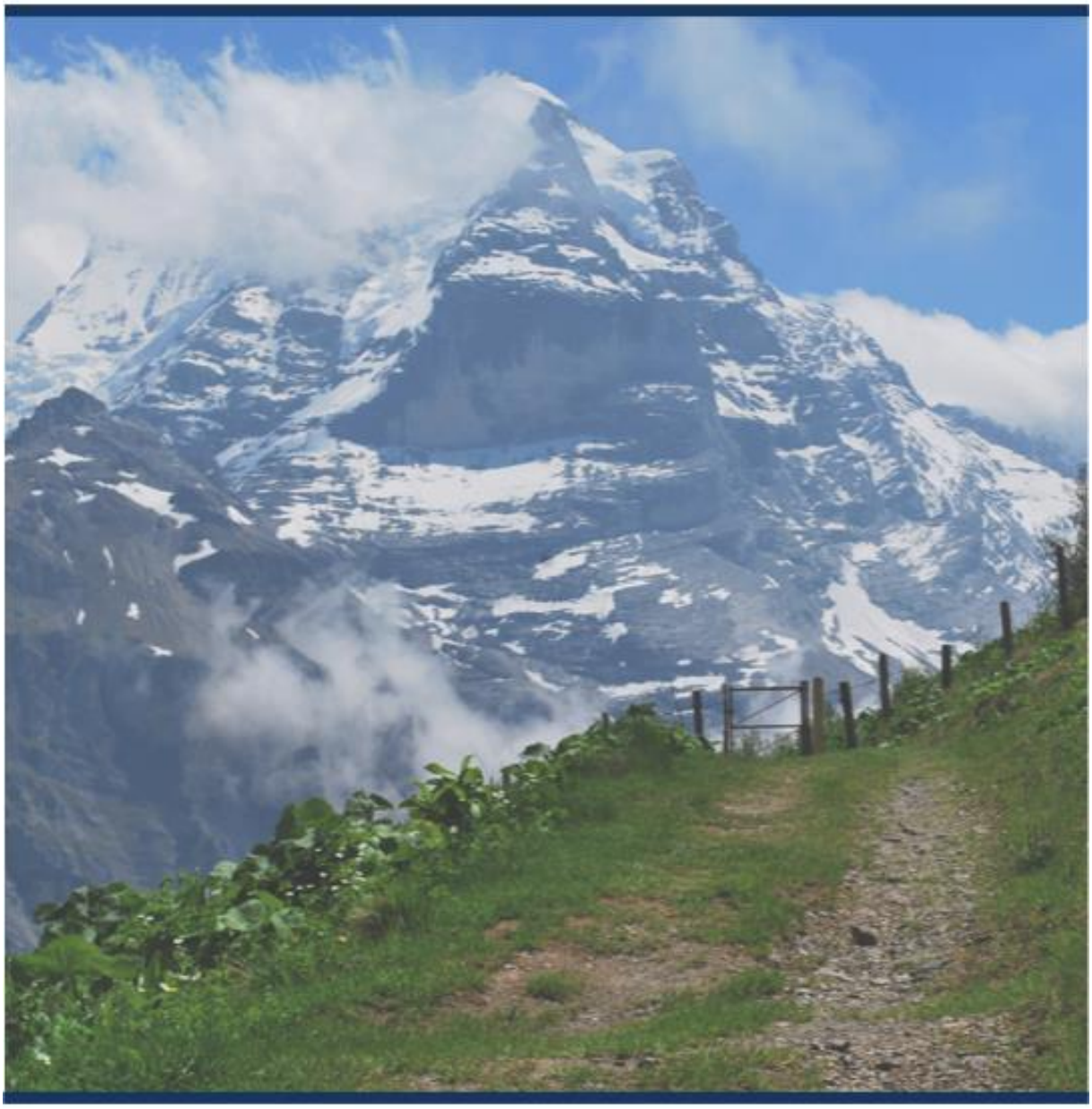

6. Discussion

The development of ALPPS surgery has pushed the limits of resectability in liver surgery and has introduced a novel management of severe liver malignancy. The innovation of ALPPS illustrates that a conceptually simple combination of existing surgical techniques can unleash regenerative responses that are beyond our expectations. ALPPS demonstrates that the intrinsic capacity of the liver to regenerate is larger than previously thought, yet is usually confined. The unprecedented effect of ALPPS on liver recovery has provoked strong interest in the mechanisms that account for this acceleration of liver regeneration.

Mechanistically, liver regeneration after simple sHx is highly complex [8]. Furthermore, how contralateral liver growth after simple portal vein ligation (PVL) occurs is ill-understood [103]. More so, how regeneration is then accelerated by parenchymal transection is completely unknown. The observation that plasma obtained from ALPPS mice can mediate this acceleration [76] in PVL mice pointed to circulating molecules as mediators of the ALPPS effects, perhaps reflecting the outcomes of an injury response.

During these past few years of my PhD, my aim was to elucidate unique pathways underlying ALPPS using different Omics approaches. I used (i) genomics to explore the pathways dysregulated after ALPPS relative to surgical controls, and (ii) proteomics approaches on ALPPS plasma to identify the circulating factors that mediate the regenerative effects. In brief, my research revealed the following undescribed interaction between JNK1 and IHH in stellate cells as an early instigation of accelerated liver regeneration after ALPPS stage 1 surgery:

a) IHH and JNK1 reside in stellate cells and activation of each is associated with liver weight gain, while the peak in JNK1 precedes the upregulation of IHH, which precedes the activation of its downstream targets GLI1 and cyclin D1 in hepatocytes.
b) Individual partial inhibition of IHH and JNK1 reduced the rate of regeneration to that seen after PVL alone, along with congruent decreases in the IHH-GLI1-cyclin D1 axis and in hepatocellular proliferation.
c) Recombinant IHH is sufficient to restore ALPPS regeneration in PVL mice and in JNK1-inhibited mice, providing evidence that JNK1 accelerates regeneration through IHH.

In brief, we report the first insights into the molecular principles underlying the acceleration of liver regeneration through ALPPS surgery.

6.1 The role of the JNK1-IHH-Cyclin D-axis

The role of JNK1 in regeneration and other liver diseases is being discussed in Manuscript B, while the regenerative role of IHH has already been addressed in Manuscript A. However, the link between JNK1 and the described IHH-GLI1-cyclin D axis has not been reported in any other regenerative model. In regeneration after sHx, JNK1 is upregulated at 1 hour [92,96,104], similarly to ALPPS. Unlike the 4 hours after ALPPS, however, *Ihh* mRNA peaks at 48 after sHx [78,85] and is not upregulated at early timepoints (Fig 11), suggesting no comprehensible link between these two molecules exists in a normal regenerating liver. Further experiments including the inhibition of JNK and the concomitant analysis of the hedgehog pathway before and at 48 hours would need evaluation to determine whether regulation of IHH through JNK1 indeed is unique to ALPPS. *Schwabe et al* used SP600125 to inhibit JNK after sHx, but only illustrated the decrease of proliferation along with cyclin D1 downregulation at 24h after sHx [96]. On the other hand, we observed a modest elevation of SHH at 4 hours after sHx relative to ALPPS and sham (Supplementary Fig. 4, manuscript A), implying JNK1 may regulate SHH rather than IHH after sHx provided JNK-hedgehog interactions exist after normal resection.

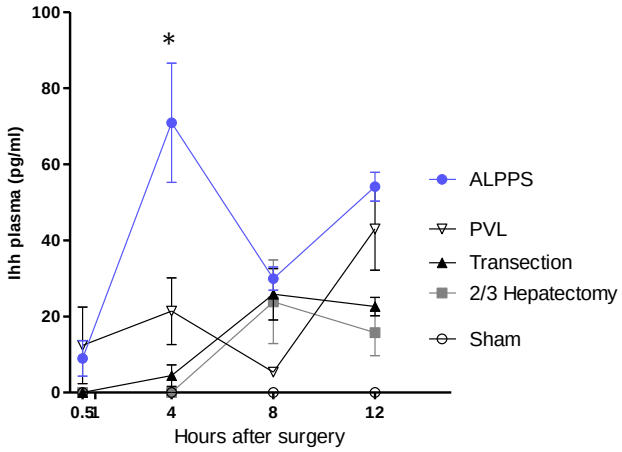

Figure 11. IHH is not upregulated after sHx in plasma at early time points after surgery, compared to ALPPS.

Furthermore, investigating potential upstream regulators of JNK, such as MKK4 and MKK7, may further elucidate the mechanistic differences of JNK1 in sHx *versus* ALPPS. *Wuestefeld et al* show that MKK4 silencing increased the regenerative capacity of hepatocytes in models of liver regeneration [105]. Puzzlingly, our preliminary experiments showed a potential increase in pMKK4 expression at one hour after ALPPS (but not on the mRNA level, Fig 12), suggesting early activation rather than silencing. A detailed analysis of the

MAPK cascade early after ALPPS and sHx will be needed to reveal any contributions of MKKs to accelerated regeneration.

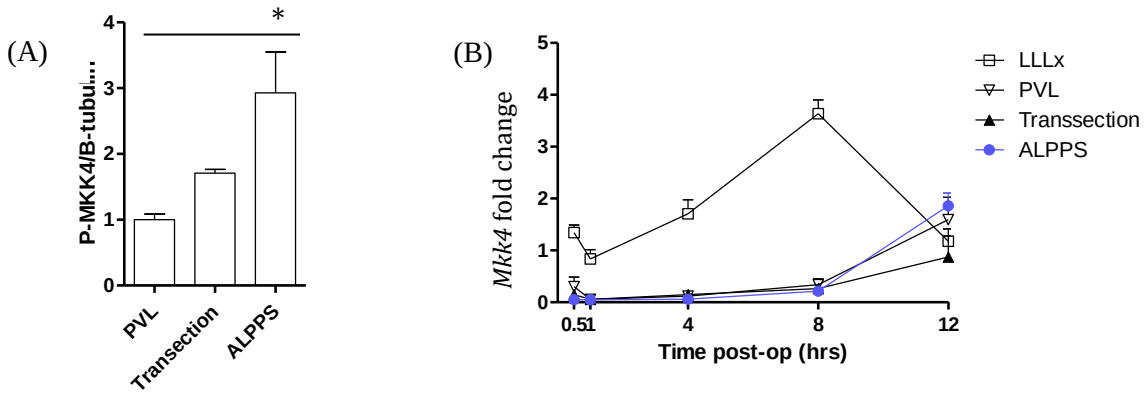

Figure 12. Evaluation of MKK4 in ALPPS. (A) pMKK4 may be upregulated on the protein level in ALPPS TIME, however (B) no differences are observed at the MRNA expression levels.

An important aspect concerns the potential role of the JNK1-IHH-cyclin D axis in tumor biology. Ideally, stimulating this mechanism in a small, timely limited dose would instigate a signal large enough to induce regeneration in an otherwise incapable organ, but small enough to avoid the promotion of cancer or other disease (in the case of fibrosis and NASH). As far as we understand from pilot experiments and human ALPPS registry data, ALPPS does not induce further tumor progression [Patryk Kambakamba, unpublished] allowing us to hypothesize that in the right conditions, the JNK1-IHH-cyclin D-axis could be manipulated in a controlled way as to promote regeneration without further effects.

6.2 Limits to proteomics

The main techniques in the explorative approach to screen for potential mechanisms behind ALPPS regeneration relied on large data sets obtained from genomics and proteomics. The two publications listed in this thesis resulted from extensive analysis of the gene expression data incurred by RNA deep sequencing. However, *Schlegel et al* demonstrated that ALPPS plasma harvested 30 minutes after operation was sufficient to propagate accelerated regeneration when injected into PVL mice. In an effort to identify the kind of plasma molecules contributing to these effects, I depleted and concentrated the plasma proteins into two fractions (one with 95% protein depletion, the other with 95% protein concentration). Only the protein-concentrated fraction elicited the ALPPS regenerative response (and the protein-depleted fraction prompted a PVL-like regenerative response, Fig 13), identifying

proteins as the likely accelerators. Therefore, proteomics approaches were coveted to identify the circulating proteins involved in ALPPS regeneration - particularly because identifying such proteins would have c

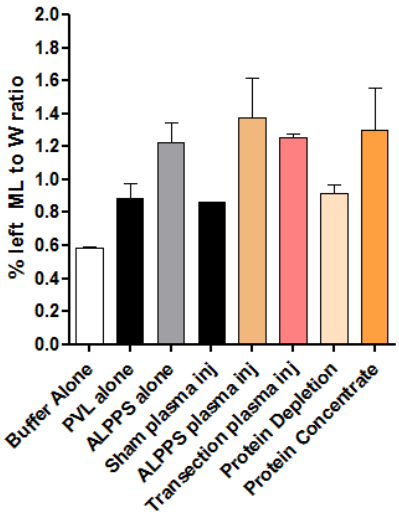

Figure 13. ALPPS plasma protein depletion and concentration using the BindPro Metabolomics Kit (Biotech Support Group, New Jersey USA).

However, the proteomics approach sustained many challenges that inhibited the completion of some of our aims within this project. For one, proteomics profiling on regenerative tissue after sHx is variable and not very well defined [106]. Secondly, we conducted proteomics research on plasma samples from ALPPS mice and their appropriate controls 30 minutes after operation. This alone presents many obstacles, as proteomics is not a very well established technique on the complex sample content that is plasma [107,108]. One huge trial is the fact that approximately 52% of the proteins in plasma are albumin, making it very difficult to identify other small proteins because they are 'blocked' by the abundance of albumin, or are bound to albumin and cannot be distinguished separately [109,110]. Regardless of this obstacle, I attempted several protocols to generate the most easily identifiable proteins in our plasma samples. Using a discovering approach (shotgun proteomics), I began with trypsin digestion and mass spectrometry (MS) on whole plasma. With this method, the MS instrument runs in data-dependent acquisition (DDA) mode generating fragment ion spectra for selected precursor ions detectable in a survey scan. The fragment ion spectra are then assigned to their corresponding peptide sequences by sequence database searching. This method led to the identification of only <1000 plasma proteins. To increase the protein detection number, I depleted the top 7 abundant proteins (Seppro Mouse Spin Columns, Sigma-Aldrich, Germany) from whole plasma before trypsin digestion and MS. However, after many trials, our Mascot search and Spectronaut analysis (peptide sequence databases to identify proteins) did not yield an increase in the detection number. As

a final push in obtaining optimal proteomics data, we utilized a new technique described as Swath MS/MS [111]. This method uses a new strategy labeled data-independent acquisition (DIA). Using a cyclic recording (the MS steps within 2-4 seconds cycle time) through a set of consecutive survey scans (with acquisition windows designed to cover 400-1200 m/z), the whole peptide mass range is readily covered by the mass analyzer in a time frame where most of the tryptic peptide precursors of the organism are present [112,113]. This technique evades the low sensitivity and propagation of errors normally attained with DDA and allows for a more in-depth identification of peptides present in a protein sample. Using whole plasma, target spectrum library assays were generated using DDA experiment on a Q-Exactive HF instrument. Data were searched with Mascot v2.4 and search results were further processed using the Bioc R package specL. DDA and DIA were acquired back-to-back in a randomized order on the MS for full peptide identification coverage. This sample preparation method and analysis allowed for the identification of over 4700 proteins, giving us the largest chance in identifying plasma proteins unique to ALPPS. As the sham operated group were distinct in their clustering from the other operated groups (PVL, transection, and ALPPS), the sham group was excluded from analysis for the identification of dysregulated proteins in ALPPS plasma.

One further observation that adds to the limitations of these results is that all ALPPS samples had a good correlation (pearson correlation above 0.9); however the PVL and transection groups had correlation scores below 0.8, suggesting a 'batch effect' in the sample preparation process (although I tried to prevent this as much as possible with mice from the same cage, operated at the same time, etc). This higher-than-expected variability could affect the analysis of proteins that are differentially expressed. As a result of these limitations, the top dysregulated proteins were still very difficult to validate on the protein level in plasma, marking this section of my PhD thesis as incomplete. Further details of the proteomics results are described below in Future Directions.

6.3 Regeneration and wound healing

It is very well known that the mechanisms of regeneration and wound healing are intermixed. After all, regeneration is a repair mechanism in response to liver tissue loss. Wound healing is categorized into three consecutive, yet overlying phases (akin to regeneration, see section 3.2) that occur in parallel with the initial response of hemostasis:

inflammation, proliferation, and remodeling [114,115]. Mechanisms similar between organ regeneration and wound healing include the increase of inflammation, in particular macrophage/Kupffer cell activation, blood clots, fibroblast migration, MMP upregulation, ECM reorganization, wound epithelium formation, and angiogenesis. However, processes unique to regeneration include those associated with new growth to completely restore portions of damaged tissue to its normal state. Meanwhile, severely damaged or non-regenerative tissue may be replaced with collagen deposits and fibrosis, often leading to an end point of scarring, and are processes unique to wound healing [116,117]. As there are many types of injury leading to wound healing processes, we will focus on repair mechanisms in cutaneous wounds.

Hedgehog in wound healing

Wounding triggers a cascade of signaling events to ensure a normal re-epithelialization. Although the hedgehog pathway's involvement during development has been extensively studied, much less is known about its role in wound repair. Recently, an increasing number of studies evaluated the effect of sonic hedgehog (SHH) on dermal repair and wound vascularization [118]. Interestingly, diabetic mice treated with topical application of human SHH-expressing plasmids exhibited improvements in re-epithelialization and dermal healing [119]. On the other hand, mice treated with the SHH inhibitor cyclopamine after wounding showed delayed wound closure and reduced dermal granulation tissue formation [120]. Therefore, the hedgehog pathway has the potential to influence several aspects of wound healing, including dermal repair and vascularization. This further suggests parallels between wound healing and liver regeneration, albeit the specific roles of SHH and IHH in cutaneous wound healing need to be further defined.

JNK in wound healing

JNK signaling has also been shown to be critical to the cascade of events in wound healing. For example, inhibition of JNK impairs keratinocyte migration and the healing of an *in vitro* wound, while maintaining keratinocyte differentitation [121]. Furthermore, mice deficient in MEKK1, an upstream kinase of JNK, exhibit a significant healing delay due to impaired activation of JNK and reduced expression of genes involved in ECM homeostasis [122]. Although the specific role of each JNK isoform has not been addressed in many of these studies, a combinatory redundant role between JNK1 and JNK2 appears plausible. JNK1 has been the most implicated in liver regeneration; nevertheless, the role of JNK2 is not

discounted as conflicting publications show divergent roles for JNK2. *Sabapathy et al* indicated that the loss of JNK2 accelerated liver regeneration [95], while *Das et al* illustrated that JNK2 has no role in liver regeneration [102]. Defining the time course of activities for each JNK gene could help pinpoint the true differences or parallels between organ regeneration and cutaneous wound healing.

Inflammation in wound healing

The inflammatory phase is well-characterized in cutaneous wound healing and therefore is of relevance for accelerated regeneration after ALPPS. The inflammatory response is characterized by an influx of immune cells in response to damage-associated molecular patterns (DAMPs), where leukocytes enter the wound area while chemoattractants recruit neutrophils. Later on (48 hours after the lesion), monocytes infiltrate the area and are differentiated into macrophages, which release growth factors (i.e. PDGF and VEGF) necessary for triggering and propagating new tissue in the lesion area [123]. Importantly, the activation of these cells is eventually settled by the reorganization of the ECM the newly formed blood vessels [115]. Tissue regeneration is in part promoted by the early acting leukocytes that interact with tissue scaffolds, while in wound healing lymphocytes foster chronic inflammation and favor scarring over regeneration. Furthermore, the identification of CD4+ T cells role in terminating inflammatory responses could be important in propagating regeneration over chronic inflammation and scarring [124,125]. Therefore, in both regeneration and wound healing, the inflammatory response is essential in initiating, mitigating, and terminating the injury. However, regeneration will occur not only if the injured cells are capable of proliferation but also only if the underlying stromal framework is intact. If injury is so severe that there is damage to the stromal framework of the tissue, regeneration will not occur [117].

Lastly, an important component to take into account for all repair mechanisms are the circulating factors such as cytokines, immune cells, and other mitogens. Many of these factors have been identified in both wound healing and regeneration (IL-6, TGF-beta, FGF, etc); nevertheless, parallel profiling should be conducted to ascertain new molecules specific to each process. This comparison could either lead to identification of unknown pathways in these injury responses, or identify unique pathways to each, distinguishing differences between regeneration and wound healing. Furthermore, understanding the full extent of these circulating factors could also help extend knowledge to wound healing occurring in diseased tissues, perhaps in cases where repair would not occur successfully because the repair

mechanisms have already been activated to an extent where healing is faulty and is rather incurring further damage.

Altogether, it appears that many similarities exist between ALPPS, regeneration, and wound healing. JNK and hedgehog pathways are known to partake in all three cases; however, at different timepoints, in varied combinations, and possibly propagating different downstream targets. Therefore, exploring the timing, involvement of other ligands, and interactions with different molecules could characterize the quality and outcome of an injury response.

Future Directions

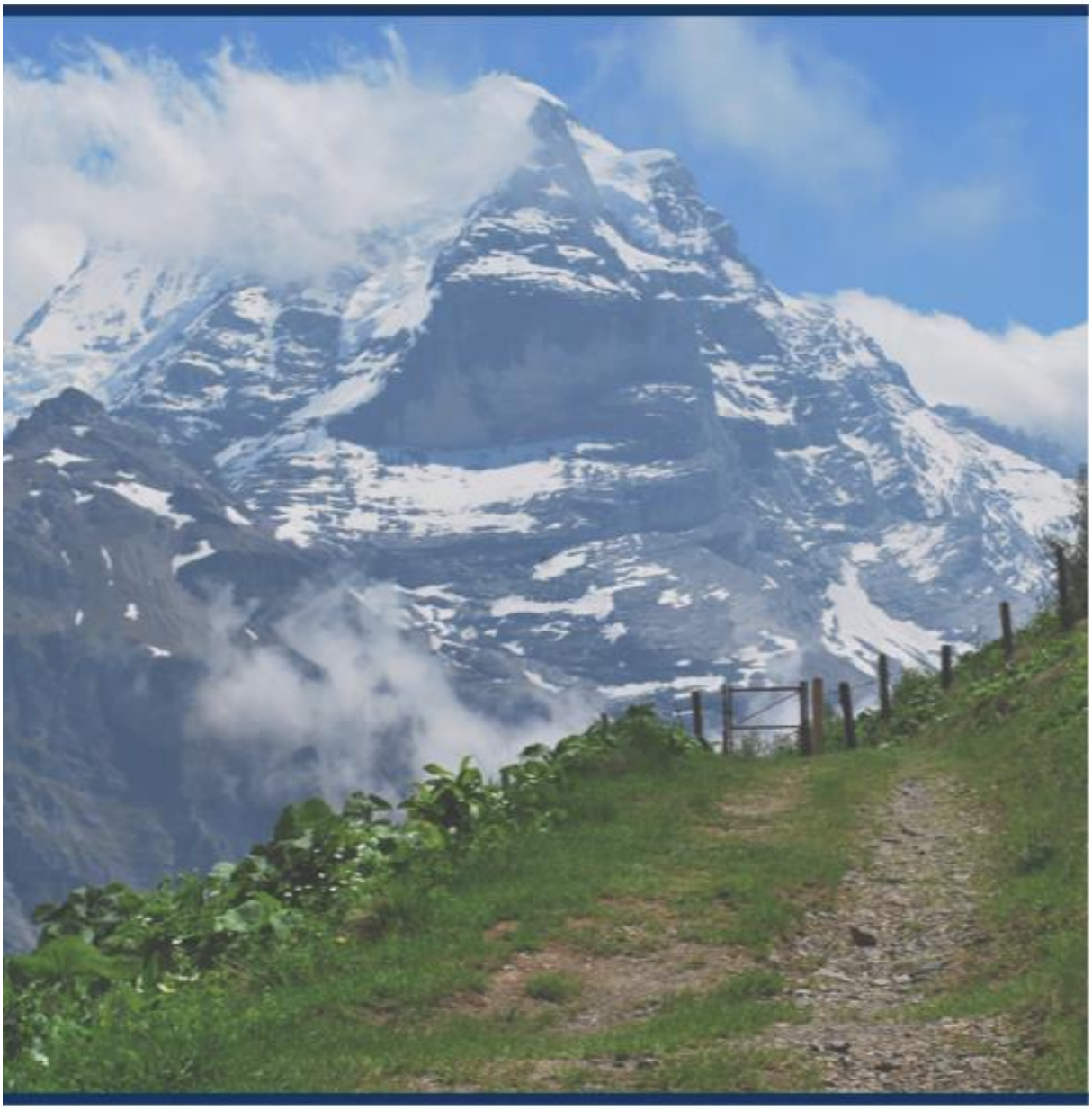

7. Future Directions

JNK2 as a player in the IHH-cyclin D axis

In the above manuscripts, we demonstrated that the JNK1-IHH-Cyclin D axis is a necessary component to induce accelerated liver regeneration after ALPPS surgery. However, as the roles of IHH after sHx is not definitive, neither is the role of JNK2. Although JNK1 is upregulated 1 hour after sHx, it seems unlikely to have the same interacting role with the hedgehog pathway as we have shown in ALPPS, as hedhehog signaling appears to occur with a significant delay (24-48h) after sHx [85] compared to ALPPS (4h). Therefore, JNK2 night play this role in regeneration after sHx (with JNK3 being expressed only in neuronal cells [92,126]) (Fig 14). Likewise, the role of the other hedgehog ligands (SHH, DHH) and their association with JNKs remains uncharacterized after sHx. Therefore, it could be viable that JNK2, rather than JNK1, is interacting with the hedgehog pathway, perhaps through a ligand different than IHH.

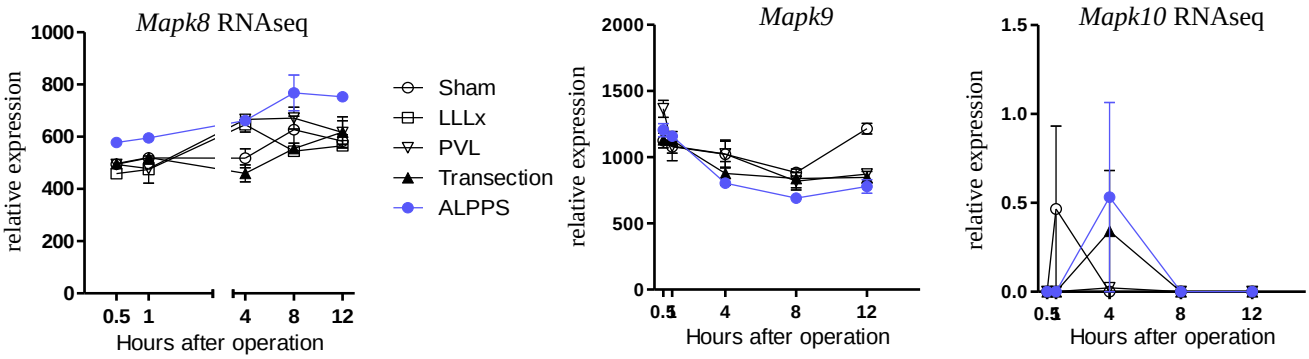

Figure 14. *Mapk8* (JNK1), *Mapk9* (JNK2), *Mapk10* (JNK3) gene expression values from RNA deep sequencing. Although JNK2 seems not be be expressed in ALPPS, whereby JNK1 is highly upregulated, JNK2 could play a compensatory role in regeneration after sHx in interacting with the IHH-CCND1

Plasma factors upstream of the JNK-IHH-cyclin D axis

As described above, we conducted proteomics analysis on plasma samples from mice 30 minutes after ALPPS and control surgeries to connect early circulating factors to the 1h upregulation of JNK1 that mediates the secretion of IHH at 4 hours after operation. Despite the technical challenges of plasma proteomics, ANOVA analysis presented GSTP1 (glutathione s-transeferase pi 1), GPDA (glyceraldehyde-3-phosphate dehydrogenase), and HS90A (heat shock protein 90) as the three most significant plasma proteins present 30 min. after ALPPS compared to PVL and transection (Fig 15). We focused on validating GSTP1 in mouse, known not only for its detoxification properties but also for its phosphorylation

activites on MAPKinases in a catalytic-independent manner [127]. Moreover, GSTP1/2 knockout mice display reduced proliferation and delayed activation of STAT3, JNK, and ERK1/2 signaling after sHx [127]. Validation of GSTP1 upregulation would hence make GSTP1 a promising upstream regulator of JNK1 (upregulated in tissue at 1 hour).

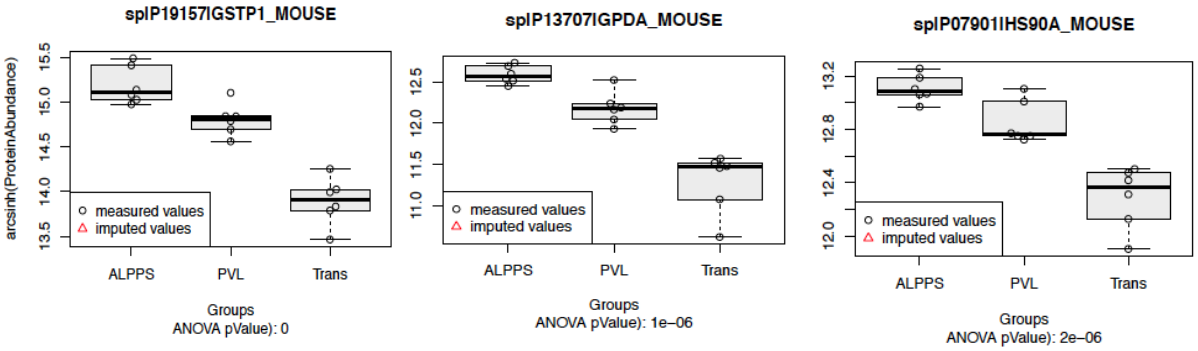

Figure 15. The top 3 dysregulated plasma proteins identified by DIA using MS and ANOVA. GSTP1, GPDA, HS90A.

Indeed, serum GSTP1 (measured by ELISA) was upregulated after ALPPS, however at a time point later than 30 minutes post ALPPS (Fig 16). Therefore, the ELISA measurements could not corroborate the proteomics findings, rendering a regulation of JNK1 through GSTP1 unlikely. Functional evidence (i.e. GSTP1 inhibited by NBDHEX with JNK1-IHH-GLI1-cyclin D assessment) would eventually be required to establish the precise relationship between GSTP1 and JNK1-depedent regeneration after ALPPS.

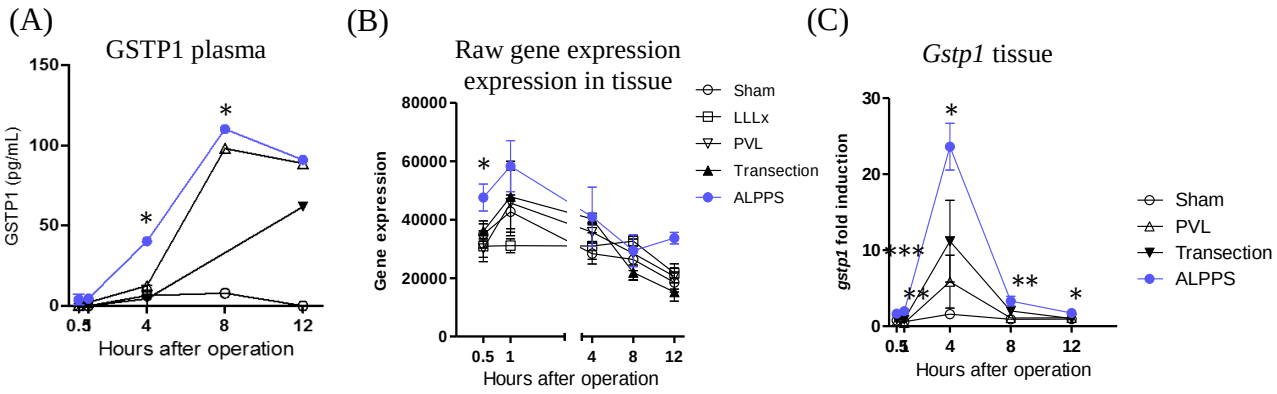

Figure 16. mRNA and protein levels of GSTP1 in mouse suggesting a role of GSTP1 as a plasma factor induced by ALPPS. 0.5 hour time point, student's t-test, PVL compared to ALPPS, (A) p=0.35, (B) p=0.03, (C) p=0.0001.

In an alternative appraoch to shed light onto GSTP1, we measured protein levels in human ALPPS patient plasma (Figure 17). Human plasma was obtained prior to surgery, at laparotomy, and at several time points after both ALPPS stage 1 and 2 surgery. Unfortunately,

only one out of 10 patients had elevated GSTP1 plasma levels. More so, this patient was the only one displaying a decrease in the FLR percentage after stage 1 (i.e a negative regeneration rate after operation). Therefore, we decided not to follow up GSTP1 as a feasible candidate promoting the JNK1-IHH axis. However, our findings do not rule out a role for GSTP1 in ALPPS regeneration and further work may re-integrate GSTP1 as an important player. A wider array (and more complete set) of samples from a well characterized and more homogenous ALPPS patient cohort may be needed to appreciate a regenerative function of GSTP1. Likewise, a more dense time course assessment in mice and man may be of help given that the regenerative kinetics after ALPPS are different in the two species.

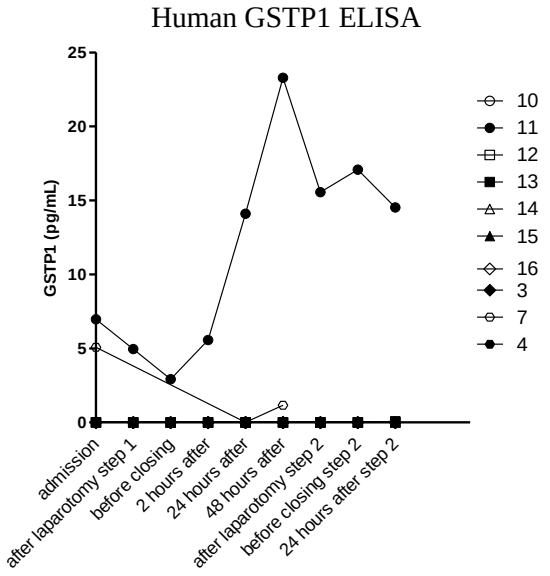

Figure 17. Protein levels of GSTP1 in human ALPPS patient plasma. Patient 11 is the only sample with a decrease in the percentage FLR after stage 1 corresponding with the large increase in GSTP1 protein levels in plasma.

Lastly, as a supplement to our proteomics approach, we conducted plasma protein microarrays (Mouse L308 Array, RayBiotech) on ALPPS, PVL, and transection mouse samples (Fig 18). The plasma protein microarray did reveal unique differences between ALPPS and the control surgeries, particularly the spots for DTK, Frizzled-7, and RANTES seemed to be upregulated. If validated by ELISA or other techniques, these candidates may be investigated through functional approaches in future studies.

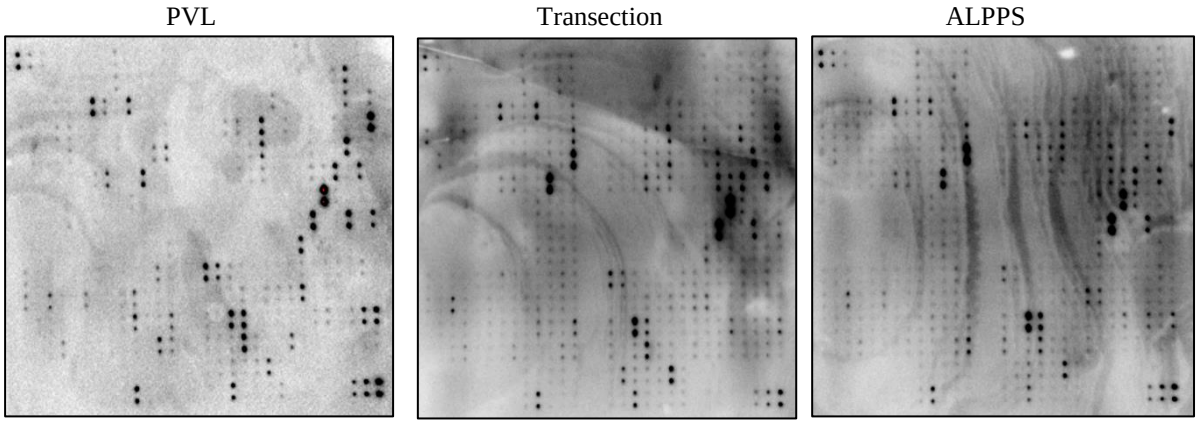

Figure 18. Mouse L308 Array screens 308 mouse proteins with high detection sensitivity.

Characterization of ALPPS processes in mice

The molecular mechanisms in our ALPPS mouse model need to be further characterized to understand the full extent of the processes induced by accelerated regeneration. Firstly, the time course for cell cycle transitions (G0 to G1 to S to M phase) in ALPPS should be explored. Using the genomics data from this project as well as other genomics data accumulated in our lab (for sHx), the time adapted phases should be compared between ALPPS, PVL, and sHx to identify, for example, whether regeneration after ALPPS follows the same basic principles as after sHx, however in a timely condensed way.

Secondly, the JNK1-IHH positive feedback loop needs further investigation to confirm such relation between these two molecules. We have done a few preliminary experiments with neutralizing IHH antibody to see whether IHH inhibition may reduce JNK1 activity after ALPPS; however, our results did not show a direct effect of neutralizing IHH on JNK1 (Fig 19). These experiments need repetition, perhaps with a more direct inhibition of IHH such as through a hepatocyte-specific knockout mouse model or via *siRNA*. Likewise, hepatic stellate cell culture experiments may be helpful for mechanistic studies on the kind of interaction between IHH and JNK1.

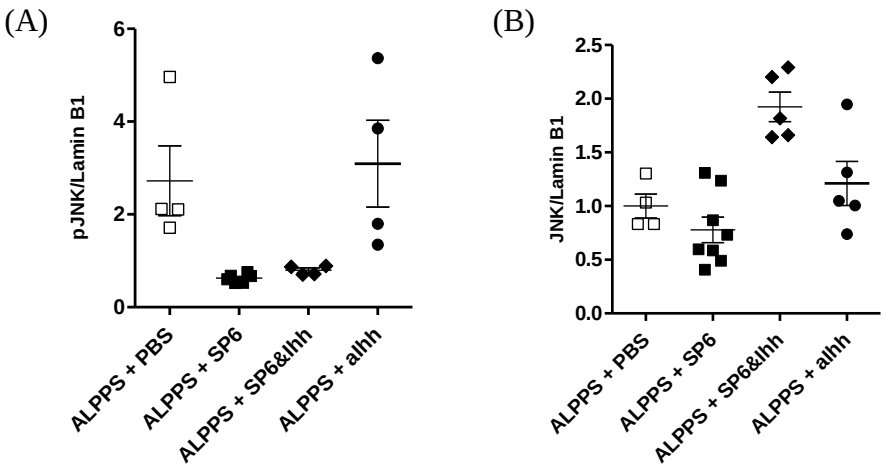

Figure 19. (A) Nuclear pJNK1 and (B) JNK1 fractions in mice that underwent neutralizing IHH antibody (aIHH) before ALPPS surgery.

Lastly, to further corroborate the results of our ALPPS mouse model in clinical settings, we have conducted RNA deep sequencing on human ALPPS tissue (Fig 20). Due to ethical constraints, liver biopsies could only be collected after laparotomy (before ALPPS), and before surgical closure (after complete ALPPS stage 1). We isolated RNA from 5 patient biopsies with similar disease background, positive regenerative rates after ALPPS, and short interval times between stage 1 and stage 2 of ALPPS. From our preliminary analysis, we see a complete gene expression profile shift in biopsies after ALPPS surgery. Our aim is to identify the common pathways and genes dysregulated in ALPPS between these patient biopsies and our published mouse data series (manuscript A), should they exist. Therefore, validation of JNK1 and additional confirmation of IHH is priority. This comparison would solidify the clinical relevance of our ALPPS mouse model. More so, it might promote the view of the JNK1-IHH axis as a possible therapeutic target for patients at risk of liver failure due to incompetent regeneration after surgery.

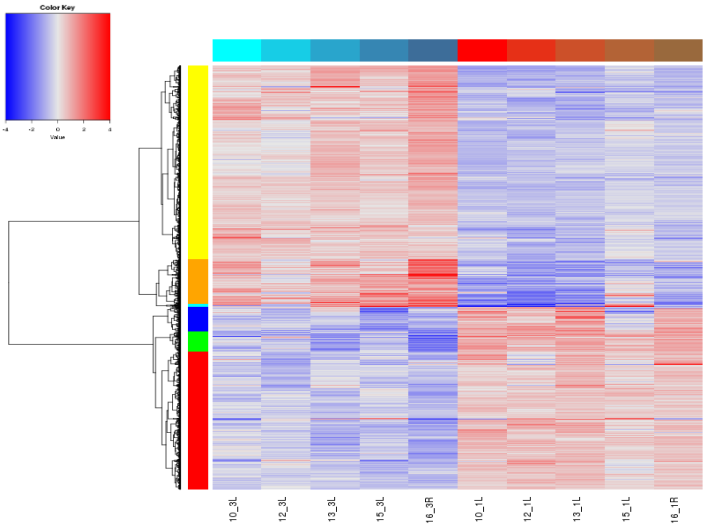

Figure 20. RNA deep sequencing on human ALPPS regenerative liver tissue. '1L' samples denote before surgery, while '3L' samples correspond to after ALPPS stage 1 surgery.

8. Bibliography

1. Muriel P. *Liver Pathophysiology: Therapies and Antioxidants*. Academic Press. 2017.
2. Dufour JF, Clavien PA. *Signaling Pathways in Liver Diseases*. Wiley Blackwell. 2015.
3. Sasse D, Spornitz UM, Maly IP. *Liver Architecture*. Enzyme. 1992; 46:8-32.
4. Glaser SS, Gaudio E, Miller T, Alvaro D, Alpini G. *Cholangiocyte proliferation and liver fibrosis*. Expert Rev Mol Med. 2009; 11:e7.
5. Tabibian JH, Masyuk AI, Masyuk TV, O'Hara SP, LaRusso NF. *Physiology of Cholangiocytes*. Compr Physiol. 2013; 3:10.1002/c120019.
6. Kmiec Z. *Cooperation of Liver Cells in Health and Disease*. Springer. 2001.
7. Apte UM. *Liver Regeneration: Basic Mechanisms, Relevant Models and Clinical Applications*. Academic Press. 2015.
8. Michalopoulos GK. *Liver regeneration*. J Cell Physiol. 2007; 213:286-300.
9. Michalopoulos GK. *Principles of Liver Regeneration and Growth Homeostasis*. Compr Physiol. 2013; 3:485-513.
10. Higgins GM. Anderson RM. *Experimental pathology of the liver, 1: Restoration of the liver of the white rat following partial surgical removal*. Arch Pathol. 1931; 12:186-202.
11. Michalopoulous GK. *Liver Regeneration after Partial Hepatectomy: Critical Analysis of Mechanistic Dilemmas*. Am J Pathol. 2010; 176:2-13.
12. Wu Y, Guo F, Liu J, Xiao X, Huang L, He D. *Triple labeling with three thymidine analogs reveals a well-orchestrated regulation of hepatocyte proliferation during liver regeneration.* Hepatology. 2011; 41:1230-1239.
13. Riehle KJ, Dan YY, Campbell JS, Fausto N. *New concepts in liver regeneration*. J Gastroenterol Hepatol. 2011; 133:203-212.
14. Kang LL, Mars WM, Michalopoulos GK. *Signals and cells involved in regulating liver regeneration*. Cells. 2012; 1:1261-1292.
15. Bissel DM. *Therapy for hepatic fibrosis: revisiting the preclinical models*. Clin Res Hepatol Gastroenterol. 2011; 35:521-525.
16. Fausto N, Laird AD, Webber EM. *Liver regeneration. 2. Role of growth factors and cytokines in hepatic regeneration*. FASEB J. 1995; 33:1098-1109.
17. Zarnegar R, DeFrances MC, Kost DP, Lindroos P, Michalopoulos GK. *Expression of hepatocyte growth factor mRNA in regenerating rat liver after partial hepatectomy*. Biochem Biophys Res Commun. 1991; 177:559-565.
18. Ito N, Kawata S, Tamura S, Kiso S, Tsushima H, Damm D, et al. Heparin-binding *EGF-like growth factor is a potent mitogen for rat hepatocytes*. 1994; 198:25-31.
19. Ding BS, Nolan DJ, Butler JM, James D, Babazadeh AO, Rosenwaks Z, et al. *Inductive angiocrine signals from sinusoidal endothelium are required for liver regeneration*. Nature. 2010; 468:310-315.
20. Paranjpe S, Bowen WC, Mars WM, Orr A, Haynes MM, DeFrances MC, et al. *Combined systemic elimination of MET and epidermal growth factor receptor signaling completely abolishes liver regeneration and leads to liver decompensation*. Hepatology. 2016; 64:1711-1724.
21. Miyaoka Y, Miyajima A. *To divide or not to divide: revisiting liver regeneration*. Cell Div. 2013; 8:10.1186/1747-1028-8-8.
22. Monga SP. *Role and regulation of beta-catenin signaling during physiological liver growth*. Gene Expr. 2014; 16:51-62.
23. Guest RV, Boulter L, Dwyer BJ, Forbes SJ. *Understanding liver regeneration to bring new insights to the mechanisms driving cholangiocarcinoma*. NPJ Reg Med. 2017;

2:10.1038/s41536-017-0018-z.
24. Bell AW, Michalopoulos GK. *Phenobarbital regulates nuclear expression of HNF-alpha in mouse and rat hepatocytes independent of CAR and PXR*. Hepatology. 2006; 44:186-194.
25. Cressman DE, Diamond RH, Taub R. *Rapid activation of the Stat3 transcription complex in liver regeneration*. Hepatology. 1995; 21:1443-1449.
26. Taub R. *Hepatoprotection via the IL-6/Stat3 pathway*. J Clin Invest. 2003; 112:978-980.
27. Forbes SJ, Rosenthal N. *Preparing the ground for tissue regeneration: from mechanism to therapy*. Nat Med. 2014; 20:857-869.
28. Yamada Y, Webber EM, Kirillova I, Peschon JJ, Fausto N. *Analysis of liver regeneration in mice lacking type 1 or type 2 tumor necrosis factor receptor: requirement for type 1 but not type 2 receptor*. Hepatology. 1998; 28:959-970.
29. Wen Y, Feng D, Wu H, Liu W, Li H, Wang F, et al. *Defective inhibition of liver regeneration of osteopontin-deficient mice after partial hepatectomy due to insufficient activation of IL-6/Stat3 pathway*. Int J Biol Sci. 2015; 11:1236-1247.
30. Seki E, Kondo Y, Iimuro Y, Naka T, Son G, Kishimoto T, et al. *Demonstration of cooperative contribution of MET- and EGFR-mediated STAT3 phosphorylation to liver regeneration by exogenous suppressor of cytokine signalings*. J Hepatol. 2008; 48:237-245.
31. Albrecht JH, Hansen LK. *Cyclin D1 promotes mitogen-independent cell cycle progression in hepatocytes*. Cell Growth Differ. 1999; 10:397-404.
32. Li W, Liang X, Kellendonk C, Poli V, Taub R. *STAT3 contributes to the mitogenic response of hepatocytes during liver regeneration*. JBC. 2004; 277:28411-28417.
33. Fausto N, Campbell JS, Riehle KJ. *Liver Regneeration*. Hepatology. 2006; 43:S45-53.
34. Miyaoka Y, Ebato K, Kato H, Arakawa S, Shimizu S, Miyajima A. *Hypertrophy and unconventional cell division of hepatocytes underlie liver regeneration*. Curr Biol. 2012; 22:1166-1175.
35. Wang X, Kiyokawa H, Dennewitz MB, Costa RH. *The Forkhead Box m1b transcription factor is essential for hepatocyte DNA replication and mitosis during mouse liver regeneration.* Proc Natl Acad Sci USA. 2002; 99:16881-16886.
36. Gkretsi V, Apte U, Mars WM, Bowen WC, Luo JH, Yang Y et al. *Liver-specific ablation of integrin-linked kinase in mice results in abnormal histology, enhanced cell proliferation, and hepatomegaly*. Hepatology. 2008; 48:1932-1941.
37. Rana B, Mischoulon D, Xie Y, Bucher NL, Farmer SR. *Cell-extracellular matrix interactions can regulate the switch between growth and differentiation in rat hepatocytes: Reciprocal expression of C/EBP alpha and immediate-early growth response transcription factors*. Mol Cell Biol. 1994; 14:5858-5869.
38. Ichikawa T, Zhang YQ, Kogure K, Hasegawa Y, Takagi H, Mori M et al. *Transforming growth factor beta and activin tonically inhibit DNA synthesis in the rat liver*. Hepatology. 2001; 34:918-925
39. Baghy K, Iozzo RB, Kovalszky I. *Decorin-TGFβ axis in hepatic fibrosis and cirrhosis*. J Histochem Cytochem. 2012; 60:262-268.
40. Buraschi S, Pan N, Tyler-Rubinstein N, Owens RT, Neill T, Iozzo RV. *Decorin antagonizes Met receptor activity and down-regulates beta-catenin and Myc levels*. J Biol Chem. 2010; 285:42075-42085.
41. Liu B, Paranjpe S, Bowen WC, Bell AW, Luo JH, Yu YP et al. *Investigation of the role of glypican 3 in liver regeneration and hepatocyte proliferation*. Am J Pathol. 2009; 175:717-724.
42. Capurro MI, Xu P, Shi W, Li F, Jia A, Filmus J. *Glypican-3 inhibits Hedgehog signaling during development by competing with patched for hedgehog binding.* Dev Cell. 2008; 14:700-711.

43. Sakamoto T, Liu Z, Murase N, Enzure T, Yokomuro S, Poli V, et al. *Mitosis and apoptosis in the liver of interleukin-6-deficient mice after partial hepatectomy*. Hepatology. 1999; 29:403-411.
44. Huang W, Ma K, Zhang J, Qatanani M, Cuvillier J, Liu J et al. *Nuclear receptor-depending bile acid signaling is required for normal liver regeneration*. Science. 2006; 312:233-236.
45. Omenetti A, Yang L, Gainetdinov RR, Guy CD, Choi SS, Chen W et al. *Paracrine modulation of cholangiocyte serotonin synthesis orchestrates biliary remodeling in adult*. Am J Physiol Gastrointest Liver Physiol. 2011; 300:G303-G315.
46. Lesurtel M, Graf R, Aleil B, Walther DJ, Tian Y, Jochum W, et al. *Platelet-derived serotonin mediates liver regeneration*. Science. 2006; 312:104-107.
47. Kron P, Linecker M, Limani P, Schlegel A, Kambakamba P, Lehn JM, et al. *Hypoxia-driven Hif2a coordinates mouse liver regeneration by coupling parenchymal growth to vascular expansion.* Hepatology. 2016; 64:2198-2209.
48. Kachaylo E, Tschuor C, Calo N, Borgeaud N, Ungethum U, Limani P, et al. *PTEN down-regulation promotes β-oxidation to fuel hypertrophic liver growth after hepatectomy in mice*. Hepatology. 2017; 66:908-921.
49. Tsuchida T, Friedman SL. *Mechanisms of hepatic stellate cell activation*. Nat Rev Gastroenterol Hepatol. 2017; 14:397-411.
50. Wells RG, Scwabe RF. *Origin and function of myofibroblasts in the liver*. Semin Liver Dis. 2015; 35:e1.
51. Senoo H, Mezaki Y, Fujiwara M. *The stellate cell system (vitamin A-storing cell system)*. Anat Sci Int. 2017; 92:387-455.
52. Martucci RB, Ziulkoski AL, Fortuna VA, Guaragna RM, Guma FC, Trugo LC, et al. *Beta-carotene storage, conversion to retinoic acid, and induction of the lipocyte phenotype in hepatic stellate cells*. J Cell Biochem. 2004; 15:414-423.
53. Bansal MB. *Hepatic stellate cells: fibrogenic, regenerative or both? Heterogeneity and context are key*. Hepatol Int. 2016; 10:902-908.
54. Bataller R, Brennder DA. *Liver fibrosis*. J Clin Invest. 2005; 2:209-218.
55. Kaur S, Anita K. *Angiogenesis in liver regeneration and fibrosis: 'a double-edged sword'*. Hepatol Int. 2013; 7:959-968.
56. Ramadori G, Neubauer K, Odenthal M, Nakamura T, Knittel T, Schwogler S et al. *The gene of hepatocyte growth factor is expressed in fat-storing cells of rat liver and is downregulated during cell growth and by transforming growth factore-beta*. Biochem Biophys Res Commun. 1992; 183:739-742.
57. Swiderska-Syn M, Syn WK, Xie G, Kruger L, Machado MV, Karaca G. *Myofibroblastic cells function as progenitors to regenerate murine livers after partial hepatectomy*. Gut. 2014; 63:1333-1344.
58. Yin C, Evason KJ, Asahina K, Stainier DYR. *Hepatic stellate cells in liver development, regeneration, and cancer*. J Clin Invest. 2013; 123:1902-1910.
59. Puche JE, Saiman Y, Friedman SL. *Hepatic stellate cells and liver fibrosis*. Compr Physiol. 2013; 3:1473-1492.
60. Zhang DY, Friedman SL. *Fibrosis-dependent mechanisms of hepatocarcinogenesis*. Hepatology. 2012; 56:769-775.
61. Amann T, Bataille F, Spruss T, Muhlbauer M, Gabele E, Scholmerich J, et al. *Activated hepatic stellate cells promote tumorigenicity of hepatocellular carcinoma*. Cancer Sci. 2009; 100:646-653.
62. Makuuchi M, Thai BL, Takayasu K, Takayama T, Kosuge T, Gunven P, et al. *Preoperative portal embolization to increase safety of major hepatectomy for hilar bile duct carcinoma: a preliminary report*. Surgery. 1990; 5:521-527.

63. Clavien PA, Petrowsky H, DeOliveira ML, Graf R. *Strategies for safer liver surgery and partial liver transplantation*. N Engl J Med. 2007; 356:1545-1559.
64. Adam R, Laurent A, Azoulay D, Castaing D, Bismuth H. *Two-stage hepatectomy: A planned strategy to treat irresectable liver tumors*. Ann Surg. 2000; 232:777-785.
65. Clavien PA, Oberkofler CE, Raptis DA, Lehmann K, Rickenbacher A, El-Badry AM. *What is critical for liver surgery and partial liver transplantation: size or quality?* Hepatology. 2010; 52:715-729.
66. de Santibanes E, Clavien PA. *Playing play-doh to prevent postoperative liver failure: the "ALPPS" approach*. Ann Surg. 2012; 255:415-417.
67. Lehmann K, Tschuor C, Rickenbacher A, Jang JH, Oberkofler CE, Tschopp O, et al. *Liver failure after extended hepatectomy in mice is mediated by a p21-dependent barrier to liver regeneration*. Gastroenterology. 2012; 143:1609-1619.
68. Tucker ON, Heaton N. *The 'small for size' liver syndrome*. Curr Opin Crit Care. 2005; 11:150-155.
69. Eshkenazy R, Dreznik Y, Lahat E, Zakai BB, Zendel A, Ariche A. *Small for size liver remnant following resection: prevention and management*. Hepatobiliary Surg Nutr. 2014; 3:303-312.
70. de Santibanes E, Alvarez FA, Ardiles V. *How to avoid postoperative liver failure: a novel method*. World J Surg. 2012; 36:125-128.
71. Schnitzbauer AA, Lang SA, Goessmann H, Nadalin S, Baumgart J, Farkas SA et al. *Right portal vein ligation combined with in situ splitting induces rapid left lateral liver lobe hypertrophy enabling 2-staged extended right hepatic resection in small-for-size settings*. Ann Surg. 2012; 255:405-415.
72. Eshmuminov D, Raptis DA, Linecker M, Wirsching A, Lesurtel M. Clavien PA. *Meta-analysis of associating liver partition with portal vein ligation and portal vein occlusion for two-stage hepatectomy*. Br J Surf. 2016; 103:1768-1782.
73. Linecker M, Kambakamba P, Reiner CS, Linh Nguyen-Kim TD, Stavrou GA, Jenner RM et al. *How much liver needs to be transection in ALPPS? A translational study investigating the concept of less invasiveness*. Surgery. 2017; 161:453-464.
74. Garcia-Perez R, Revilla-Nuin B, Martines CM, Bemabe-Garcia A, Mazo, AB, Paricio PP. *Associated Liver Partition and Portal Vein Ligation (ALPPS) vs Selective Portal Vein Ligation (PVL) for Staged Hepatectomy in a rat model. Similar regenerative response?* PLoS One. 2015; 10:e0144096.
75. Shi H, Yang G, Zheng T, Wang J, Li L, Liang Y, et al. *A preliminary study of ALPPS procedure in a rat model.* Sci Rep. 2015; 5:17567.
76. Schlegel A, Lesurtel M, Melloul E, Limani P, Tschour C, Graf R, et al. *ALPPS: from human to mice highlighting accelerated and novel mechanisms of liver regeneration*. Ann Surg. 2014; 260:839-846.
77. Merchant JL, Saqui-Salces M. *Inhibition of Hedgehog signaling in the gastrointestinal tract: targeting the cancer microenvironment*. Cancer Treat Rev. 2014; 40:12-21.
78. Omenetti A, Choi S, Michelotti G, Diehl AM. *Hedgehog signaling in the liver*. J Hepatol. 2011; 54:366-373.
79. Ingham PW, Piaczek M. *Orchestrating ontogenesis: variations on a theme by sonic hedgehog*. Nat Rev Genet. 2006; 7:840-850.
80. Jenkins D. *Hedgehog signaling: emerging evidence for non-canonical pathways*. Cell Signal. 2009; 9:1023-1034.
81. Briscoe J, Therond PP. *The mechanisms of Hedgehog signaling and its roles in development and disease*. Nat Rev Mol Cell Biol. 2013; 14:416-429.
82. Hooper JE, Scott MP. *Communicating with Hedgehogs*. Nat Rev Cell Biol. 2005; 6:306-317.

83. Yang L, Wang Y, Mao H, Fleig S, Omenetti A, Brown KD et al. *Sonic hedgehog is an autocrine viability factor for myofibroblastic hepatic stellate cells.* J Hepatol. 2008; 48:98-106.
84. Omenetti A, Yang L, Li YX, McCall SJ, Jung Y, Sicklick JK et al. *Hedgehog-mediated mesenchymal-epithelial interactions modulate hepatic response to bile duct ligation*. Lab Invest. 2007; 87:499-514.
85. Ochoa B, Syn WK, Delgado I, Karaca GF, Jung Y, Wang Y, et al. *Hedgehog signaling is critical for normal liver regeneration after partial hepatectomy in mice*. Hepatology. 2010; 51:1712-1723.
86. Bhave VS, Mars W, Donthamsetty S, Zhang X, Tan L, Luo J et al. *Regulation of liver growth by glypican 3, CD81, hedgehog, and Hhex*. Am J Pathol. 2013; 183:153-159.
87. Syn WK, Jung Y, Omenetti A, Abdelmalek M, Guy CD, Yang L, et al. *Hedgehog-mediated epithelial-to-mesenchymal transition and fibrogenic repair in nonalchoholic fatty liver disease*. Gastroenterology. 2009; 137:1478-1488.
88. Sicklick JK, Li YX, Jayaraman A, Kannangai R, Qi Y, Vivekanandan P, et al. *Dysregulation of the Hedgehog pathway in human hepatocarcinogenesis*. Carcinogenesis. 2006; 27:748-757.
89. Philips GM, Chan IS, Swiderska M, Schroder VT, Guy C, Karaca GF et al. *Hedgehog signaling antagonist promotes regression of both liver fibrosis and hepatocellular carcinoma in a murine model of primary liver cancer*. PLoS One. 2011; 6:e23943.
90. Gupta S, Barret T, Whitmarsh AJ, Cavanagh J, Sluss HK, Derijard B, et al. *Selective interaction of JNK protein kinase isoforms with transcription factors*. EMBO J. 1996; 15:2760-2770.
91. Tournier C, Dong C, Turner TK, Jones SN, Flavell RA, Davis RJ. *MKK7 is an essential component of the JNK signal transduction pathway activated by proinflammatory cytokines*. Genes Dev. 2001; 15:1419-1426.
92. Seki E, Brenner DA, Karin M. *A liver full of JNK: signaling in regulation of cell function and disease pathogenesis, and clinical approaches.*.Gastroenterology. 2012; 143:307-320.
93. Bogoyevitch MA, Kobe B. *Uses for JNK: the many and varied substrates of the c-Jun terminal kinases*. Microbial Mol Biol Rev. 2006; 70:1061-1095.
94. Chen N, She QB, Bode AM, Dong Z. *Differential gene expression profiles of JNK1- and JNK2-deficient murine fibroblast cells.* Cancer Res. 2002; 62:1300-1304.
95. Sabapathy K, Hochedlinger K, Nam SY, Bauer A, Karin M, Wagner EF. *Distinct roles for JNK1 and JNK2 in regulating JNK activity and c-Jun-dependent cell proliferation*. Mol Cell. 2004; 15:713-725.
96. Schwabe RF, Bradham CA, Uehara T, Hatano E, Bennet BL, Schoonhoven R et al. *c-Jun-N-terminal kinase drives cyclin D1 expression and proliferation during liver regeneration*. Hepatology. 2003; 37:824-832.
97. Liu H, Lo CR, Czaja MJ. *NF-kappaB inhibition sensitizes hepatocytes to TNF-induced apoptosis through a sustained activation of JNK and c-Jun*. Hepatology. 2002; 35:772-778.
98. Henderson NC, Pollock KJ, Frew J, Mackinnon AC, Flavell RA, Davis RJ, et al. *Critical role of c-jun (NH2) terminal kinase in paracetamol-induced acute liver failure.* Gut. 2007; 56:982-990.
99. Kluwe J, Pradere JP, Gwak GY, Mencin A, De Minicis S, Osterreicher CH et al. *Modulation of hepatic fibrosis by c-Jun-N-terminal kinase inhibition*. Gastroenterology. 2010; 138:347-359.
100. Iansante V, Choy PM, Fung SW, Liu Y, Chai JG, Dyson J, et al. *PARP14 promotes the Warburg effect in hepatocellular carcinoma by inhibiting JNK1-dependent PKM2 phosphorylation and activation*. Nat Commun. 2015; 10:7882.
101. Boege Y, Malehmir M, Healy ME, Betterman K, Lorentzen A, Vucur M et al. *A dual role of*

caspase-8 in triggering and sensing proliferation-associated DNA damage, a key determinant of liver cancer development. Cancer Cell. 2017; 32:342-359.
102. Das M, Garlick DS, Greiner DL, Davis RJ. *The role of JNK in the development of hepatocellular carcinoma*. Genes Dev. 2011; 25:634-645.
103. Tashiro S. *Mechanism of liver regeneration after liver resection and portal vein embolization (ligation) is different?* J Hepatobiliary Pancret Surg. 2009; 16:292-299.
104. Fausto N. *Liver regeneration*. J Hepatol. 2000; 32:19-31.
105. Wuestefeld T, Pesic M, Rudalska R, Dauch D, Longerich T, Kang TW, et al. A *Direct in vivo RNAi screen identifies MKK4 as a key regulator of liver regeneration.* Cell. 2013; 152:389-401.
106. Franco C, Soares R, Pires E, Koci K, Almeida AM, Santos R, et al. *Understanding regeneration through proteomics*. Proteomics. 2013; 13:686-709.
107. Pernemalm M, Lehtio J. *Mass spectrometry-based plasma proteomics: state of the art and future outlook*. Expert Rev Proteomics. 2014; 11:431-448.
108. Anderson NL, Anderson NG. *The human plasma proteome: history, character, and diagnostic prospects*. Mol Cell Proteomics. 2002; 1:845-867.
109. Zaias J, Mineau M, Cray C, Yoon D, Altman NH. *Reference Values for serum proteins of common laboratory rodent strains*. J Am Assoc Lab Anim Sci. 2009; 48:387-390.
110. Rifai N, Gillette MA, Carr SA. *Protein biomarker discovery and validation: the long and uncertain path to clinical utility*. Nat Biotechnol. 2006; 24:971-983.
111. Gillet LC, Navarro P, Tate S, Rost H, Selevsek N, Reiter L, et al. *Targeted data extraction of the MS/MS spectra generated by data-independent acquisition: a new concept for consistent and accurate proteome analysis*. Mol Cell Proteomics. 2012; 11:O111.016717.
112. Venable JD, Dong MQ, Wohlschlegel J, Dillin A, Yates JR. *Automated approach for quantitative analysis of complex peptide mixtures from tandem mass spectra*. Nat Methods 2004; 1:39-45.
113. Panchaud A, Scherl A, Shaffer SA, von Haller PD, Kulasekara HD, Miller SI, et al. *Precursor acquisition independent from ion count: How to dive deeper into the proteomics ocean*. Anal Chem. 2009; 81:6481-6488.
114. Stadelmann WK, Digenis AG, Tobin GR. *Physiology and healing dynamics of chronic cutaneous wounds*. Am J Surg. 1998; 176:26S-38S.
115. Atala A, Irvine DJ, Moses M, Shaunak S. *Wound healing versus regeneration: role of the tissue environment in regenerative medicine*. MRS Bull. 2010; 35:1-22.
116. Roy S, Levesque M. *Limb regeneration in axolotl: is it superhealing?* ScientificWorldJournal. 2006; 6:12-25.
117. Krafts KP. *Tissue repair: the hidden drama*. Organogenesis. 2010; 6:225-233.
118. Bielefeld KA, Amini-Nik S, Alman BA. *Cutaneous wound healing: recruiting developmental pathways for regeneration*. Cell Mol Life Sci. 2013; 70:2059-2081.
119. Asai J, Takenaka H, Kusano KF, Ii M, Luedemann C, Curry C, et al. *Topical sonic hedgehog gene therapy accelerates wound healing in diabetes by enhancing endothelial progenitor cell-mediated microvascular remodeling*. Circulation. 2006; 113:2413-22424.
120. Le H, Kleinerman R, Lerman OZ, Brown D, Galiano R, Gurtner GC, et al. *Hedgehog signaling is essential for normal wound healing*. Wound Repair Regen. 2008; 16:768-773.
121. Gazel A, Banno T, Walsh R, Blumenberg M. *Inhibition of JNK promotes differentiation of epidermal keratinocytes*. Biol Chem. 2006; 281:20530-20541.
122. Deng M, Chen WL, Takatori A, Peng Z, Zhang L, Mongan M, et al. *A role for the mitogen-activated protein kinase kinase kinase 1 in epithelial wound healing*. Mol Biol Cell. 2006; 17:3446-3455.
123. Gonzalez AC, Costa TF, Andrade ZA, Medrado AR. *Wound healing – a literature review*. An

Bras Dermatol. 2016; 91:614-620.
124. Guarda G, Dostert C, Staehli F, Cabalzar K, Castillo R, Tardivel A, et al. *T cells dampen innate immune resposnes through inhibition of NLRP1 and NLRP3 inflammasomes*. Nature. 2009; 460:269-273.
125. Sehran CN, Savill J. *Resolution of inflammation: the beginning programs the end*. Nat Immunol. 2005; 6:1191-1197.
126. Davis RJ. *Signal transduction by the JNK group of MAP kinases*. Cell. 2000; 103:239-252.
127. Pajaud J, Ribault C, Ben Mosbah I, Rauch C, Henderson C, Bellaud P, et al. *Glutathione transferases P1/P2 regulate the timing of signaling pathway activations and cell cycle progression during mouse liver regeneration*. Cell Death Dis. 2015; 6:e1598.

Acknowledgements

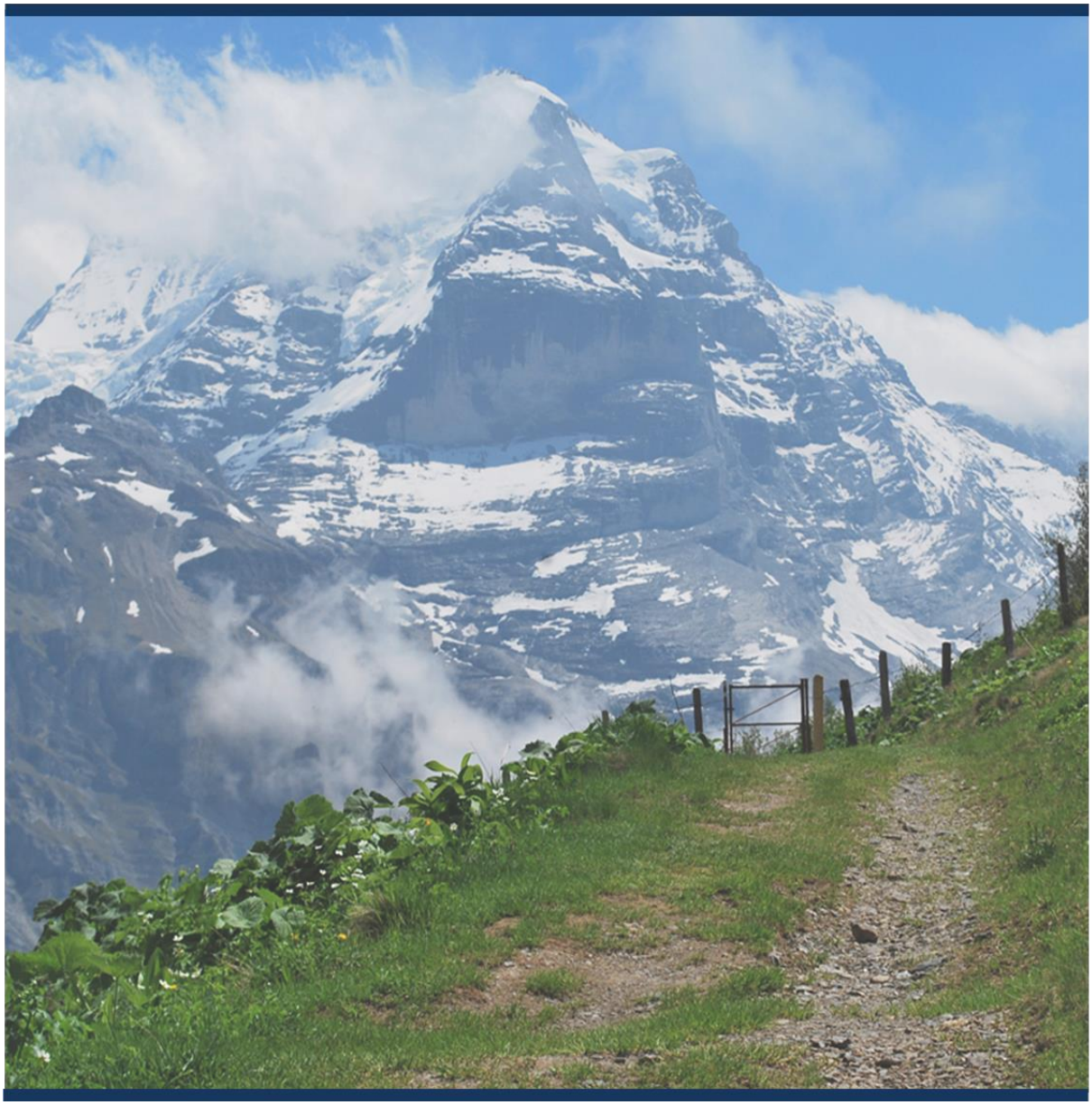

9. Acknowledgements

I wish to express my deepest appreciation to everyone who has supported me on this doctoral journey – emotionally, technically, and scientifically.

I am very thankful for the opportunity to have joined the lab of Prof. Pierre Alain-Clavien and to have worked on the ALPPS project and mouse model. It was an amazing experience to work with such a clinically relevant model and to be part of a team where basic research and innovative medicine are a daily conversation.

I want to thank Rolf Graf for his continuous support, weekly jokes, and good humor that always helped liven the mood in the lab (and no, the mice did not eat my jeans).

I am eternally grateful to Bostjan Humar for his daily support, listening ear, motivations, and biannual hugs. Whether it be luck or true teamwork, these publications, this thesis, and the years of work would not have been possible without him.

My daily work life was always brightened from the laughs and anecdotes of my fellow colleagues in both the pancreas and liver labs, who very quickly learned - '*it's almost always Friday'*. Thank you to Katya and Rong for their continuous support in forms of cheese, chocolates, and pop culture education. If things didn't go our way, there was always '*long hair don't care'*.

I could not have made it through these years without the rest of my Zurich crew – the "English expats"– who made it easy to forget a tough week. They taught me early on how to *work hard to play hard*.

Biggest thanks to my fiancé Michael, who learned my project inside and out (although, he's admitted to just keeping me around as a long term investment for his own liver). I'm so happy to have had you by my side to get me through the long days, tedious months, and happy years.

And lastly, I would never be here today if it wasn't for my parents – their continuous support, love, and sacrifice is unrequitable. This is for you.

Curriculum Vitae

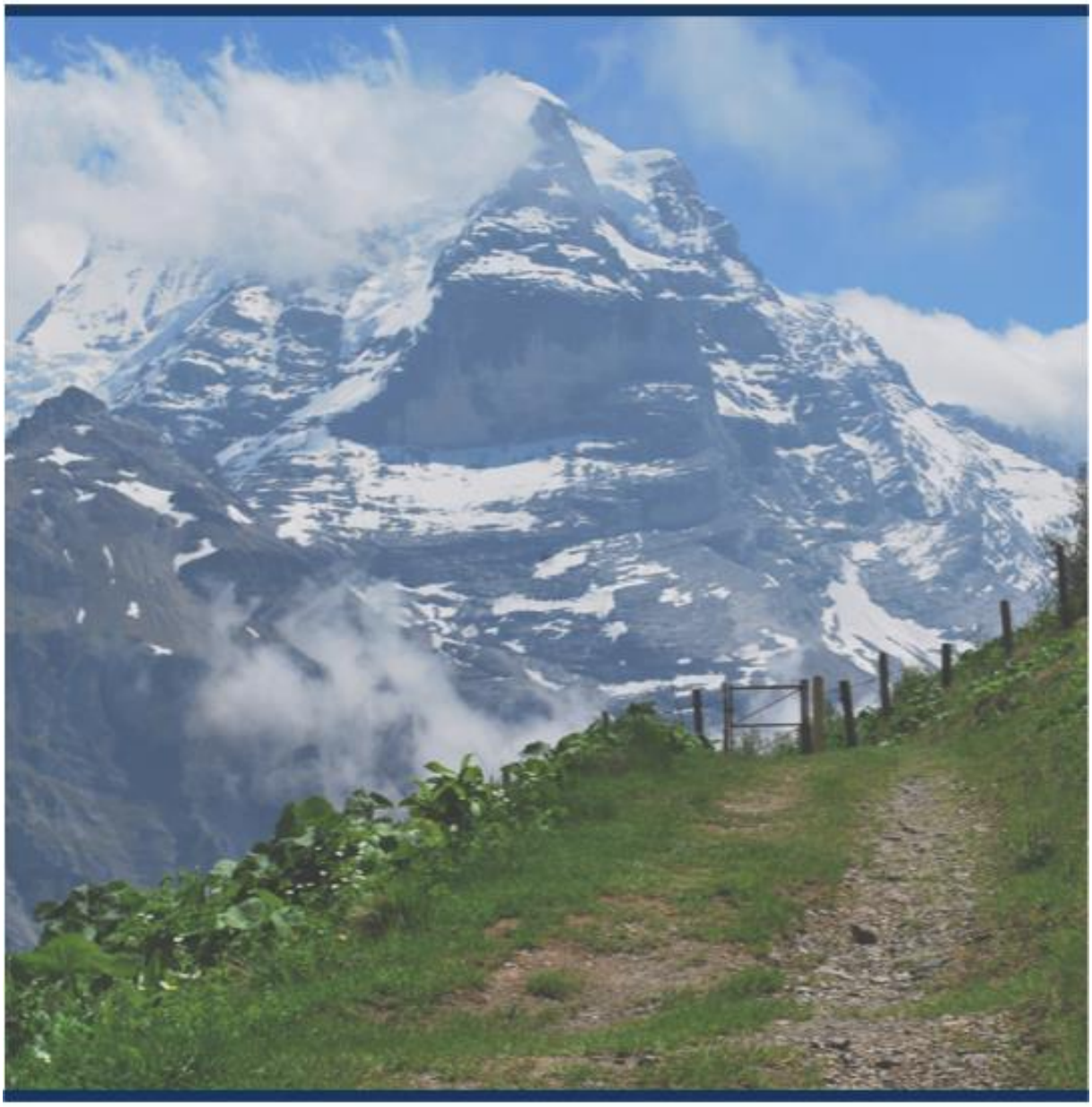

10. Curriculum Vitae

Name: LANGIEWICZ
First Name: Magda
Date of Birth: 27.06.1990
Nationality: Poland

Education

2013-2018	University of Zurich, Switzerland Doctor of Philosophy (PhD), Integrative Molecular Medicine (imMed)
2012-2013	University of California, San Diego USA Masters of Science (M.S), Biology Thesis title: Generation and Characterization of SRSF1 hepatocyte-specific knockout mice.
2008-2012	University of California, San Diego USA Bachelor of Science (B.S.), Molecular Biology
2004-2008	Mission Hills High School, San Marcos, CA USA

Additional training

- LERU Summer School of 2016: Data Stewardship Discovery & Innovation, Leiden University
- Discovering Management, ETH
- Leadership Skills for Doctoral Candidates, UZH
- Scientific Writing, UZH
- Voice Training and Presentation Skills in Sciences and Medicine, UZH
- Good Clinical Practice (GCP) Course I and II, UZH
- Winter School in Personalized Medicine, UZH
- RNA Sequencing – a practical course, FGCZ
- Genomic Medicine, ETH

Awards

2016	Basic research award, Department of Surgery, USZ
2015	Young Investigator Award – Oetliker Prize, Swiss Physiological Society
2011-2012	UCSD Provost Honor Roll
2008-2009	Randy Williams Scholarship Recipient

Leadership

2014-present	Life Science Zurich Young Scientist Network (LSZYSN)
2016-2017	Co-organizer, GRC funded “Bench to Bedside” seminar series
2014-2015	Teacher’s Assistant, Department of Biochemistry, UZH
2012	Teacher’s Assistant, Department of Biology, UCSD

Publications

1. Langiewicz M, Graf R, Humar B, Clavien PA. JNK1 induces Indian hedgehog signaling from stellate cells to accelerate liver regeneration after ligation and transection. Journal of Hepatology. 2018.

2. Linecker M, Frick L, Kron P, Limani P, Kambakamba P, Tschuor C, Langiewicz M, Kachaylo E, Schneider MA, Ungethum U, Calo N, Foti M, Dufour JF, Graf R, Humar B, Clavien PA. Hepatic benefits of exercise can be induced through the AMP analog AICAR. 2017; Submitted.

3. Farnham A, Kurz C, Ozturk MA, Solbiati M, Myllyntaus O, Meekes J, Pham TM, Paz C, Langiewicz M, Andrews S, Kanninen L, Agbemabiese C, Guler AT, Durieux J, Jasim S, Viessman O, Frattini S, Yembergenova D, Thompson M, Marin C, Porte M, Vilmint AG, Curiel RP, Rehncrona C, Malas T, Esposito F, Raap T, Jansen M, Roos M, Hettne K, Schultes EA, Mons B. Early career researchers want open science. Genome Biology. 2017; 18:221.

4. Langiewicz M, Schlegel A, Saponara E, Linecker M, Borger P, Graf R, Humar B, Clavien PA. Hedgehog pathway mediates early acceleration of liver regeneration induced by a novel two-staged hepatectomy in mice. Journal of Hepatology. 2017; 66:560-570.

5. Sen S, Langiewicz M, Jumaa H, Webster NJ. Deletion of serine/arginine-rich splicing factor 3 in hepatocytes predisposes to hepatocellular carcinoma in mice. Hepatology. 2015; 61:171-183.